

DESIGN OF A FULLY DIGITAL MULTI-LEVEL DECISION
FEEDBACK EQUALIZATION CHIP

XIE JIANG

(B.Eng(Hons.), BUPT)

A THESIS SUBMITTED

FOR THE DEGREE OF MASTER OF ENGINEERING

DEPARTMENT OF ELECTRICAL & COMPUTER ENGINEERING

NATIONAL UNIVERSITY OF SINGAPORE

2004

ACKNOWLEDGMENT

I would like to express my deepest appreciation to Prof. Xu Yong Ping for providing the continual guidance and support to me, which were essential in completing this project. I would also like to thank Chan Suet Yin for her contribution to the design of the Feed-Forward Equalizer. My gratitude also reaches out to Bi Lei for his contribution on the architecture investigation before this project. Finally, I appreciate the sponsor of this project – National University of Singapore -- for providing all the necessary funding and the EDA tools.

TABLE OF CONTENTS

Chapter 1 Introduction.....	1
1.1 Overview.....	1
1.2 Objective of the Thesis	2
1.3 Organization of the Thesis	2
Chapter 2 Introduction to MDFE.....	4
2.1 Fixed-delay Tree Search (FDTS/DF).....	4
2.2 RAM Decision Feedback Equalization.....	7
2.2.1 Linear DFE.....	7
2.2.2 RAM-DFE.....	9
2.3 Multi-level Decision Feedback Equalization.....	10
2.4 Implementations of the MDFE	13
Chapter 3 Design and Implementation of FBE.....	15
3.1 Design Considerations for FBE	15
3.2 Simple RAM-FBE (Structure-I)	16
3.3 Look-ahead RAM-FBE (Structure-II)	18
3.4 Improved Look-ahead FBE (Structure III)	20

3.5	Optimized Look-ahead FBE (Structure IV).....	22
3.6	Summary of Structure-I, II, III and IV.....	24
3.7	Behavior Simulation	25
3.8	Functional Verification.....	29
3.8.1	Data Analysis of Group-A	31
3.8.2	Data Analysis of Group-B.....	34
3.9	IC Structure.....	35
3.9.1	SFT_11.....	35
3.9.2	LOOKUP	36
3.9.3	PIPE	37
3.9.4	FEEDBACK	38
3.10	Synthesis and Optimization	39
3.10.1	Design Constraints	40
3.11	Optimization	45
3.12	Static Time Analysis	47
3.12.1	PrimeTime Timing Analysis Flow and Methodology.....	48
3.12.2	Analysis and Reports.	49
	Chapter 4 Implementation of FFE	54
4.1	Introduction to the Feed-forward Equalizer.....	54
4.2	The Transpose Structure	54

4.2.1	Booth Multipliers	55
4.2.2	Addition Implementation	56
4.2.3	Sign Extensions.....	57
4.3	Implementation	58
4.3.1	Functional Verification of FFE	59
4.3.2	Synthesis and Timing Analysis of FFE.....	60
Chapter 5 System Integration of the MDFE Chip.....		64
5.1	System-Level Considerations	64
5.2	Behavior Simulation of the MDFE Chip	66
5.3	System on Chip (SOC) Implementation of the MDFE Chip	69
5.3.1	I/O Pins/Pads in the MDFE Chip.....	69
5.3.2	Constraints for the Synthesis	73
5.3.3	Place and Route (LAYOUT).....	74
5.4	Post–Layout Timing Analysis.....	76
Chapter 6 Conclusion.....		80
REFERENCES		83
APPENDIX.A HDL Codes of the Design.....		87
APPENDIX.B Scripts and Reports.....		98

B.1	Script of the Constraints for Synthesis.....	98
B.2	Script of the Constraints for Pre-layout STA:.....	99
B.3	Script of the Constraints for Post-Layout STA	100
B.4	Area Reports	101
B.5	Dynamic Power Reports	103
B.6	Timing Reports	105

SUMMARY

The design and implementation of a Multi-level Decision Feedback Equalization (MDFE) chip for magnetic recording channel is described. The architecture of the single-chip MDFE incorporates an 8-tap feed-forward equalizer and a 10-tap feedback equalizer. The feed-forward section (FFE) is a linear transposed filter that removes the linear precursor inter-symbol interference (ISI) by a sufficient length to delay the channel response to make it causal. The feedback section (FBE) uses the decision feedback technique to eliminate non-linear postcursor ISI by a look-up table based structure with the past decisions being the addresses, provided that the past decisions are correct. The main idea of MDFE is to eliminate all the ISI and shape the recoding channel with only impulse response plus some noise components remain.

The design is targeted at a 0.35 μ m CMOS technology. The minimum clock rate of the chip is projected to be 150MHz with minimal sacrifice in the core area and the dynamic power consumption. The final design shows that at post-layout level, the MDFE chip can operate at a clock rate of 170MHz in *TYPICAL* condition, 230MHz in *BEST* case, and 125MHz in *WORST* case. The speed can be further improved by removing the bottleneck at the FFE, which only runs up to 185 MHz as opposed to 200 MHz for the FBE. The chip, which is composed of 73,386 gates and 54 I/O pads, has the chip area of 4.4mm², and consumes dynamic power of 143.03mW under a 3.3-V supply.

LIST OF TABLES

Table.2-1 Comparison of MDFE architectures.....	14
Table.3-1 Data path delay of Structure-I	18
Table.3-2 Data path delay of Structure-II	20
Table.3-3 Core Area and Speed of Structure-III & II	21
Table.3-4 Comparison between Structure-IV & III	23
Table.3-5 Comparison between Structure-IV & III	23
Table.3-6 Summary of Structure-I, II, III & IV	24
Table.3-7 Performance summary of FBE (Structure-IV)	53
Table.4-1 Signal Description of FFE	59
Table.4-2 Performance of FFE	63
Table.5-1 Signal Description of the MDFE chip	65
Table.5-2 Data analysis for the MDFE chip	68
Table.5-3 I/O Ports and Pads Description of the MDFE chip.	72
Table.5-4 Performance of the MDFE chip at post-layout level.....	79
Table.6-1 Published DFE/MDFE filters/detectors.....	81

LIST OF FIGURES

Figure.2-1	Fixed-delay tree search (FDTS/DF) detector.....	4
Figure.2-2	FDTS/DF search algorithm.....	5
Figure.2-3	Principle of FDTS/DF detection	6
Figure.2-4	Block diagram of the linear DFE.....	7
Figure.2-5	Block diagram of RAM-DFE.....	9
Figure.2-6	Digital communication channel with MDFE.....	11
Figure.3-1	System diagram of FFE and FBE	15
Figure.3-2	Block diagram of FBE (Structure-I)	17
Figure.3-3	Segmentation of complicated combination logic.....	18
Figure.3-4	Block diagram of FBE (Structure-II).....	19
Figure.3-5	Block diagram of FBE (Structure III).....	21
Figure.3-7	Block diagram of FBE (Structure IV).....	22
Figure.3-8	Operation diagram of FBE.....	26
Figure.3-9	Clock waveform of FBE (Structure-IV)	28
Figure.3-10	FBE functional simulation data (for Group-A)	30
Figure.3-11	FBE functional simulation data (for Group-B).....	33
Figure.3-12	Schematic view of FBE	35
Figure.3-13	I/O description of module SFT_11	36
Figure.3-14	Schematic view of the module LOOKUP	37
Figure.3-15	Schematic view of the module PIPE	38

Figure.3-16	Schematic view of the module FEEDBACK	39
Figure.3-17	Logic synthesis flow chart.....	40
Figure.3-18	Waveform of input delay	43
Figure.3-19	Waveform of output delay	44
Figure.3-20	User flow of PrimeTime	48
Figure.3-21	Histogram of path timing analysis.....	52
Figure.4-1	FIR filter architecture used for FFE.....	55
Figure.4-2	Block diagram of the feed-forward equalizer (FFE).....	58
Figure.4-3	Functional simulation for FFE.....	60
Figure.4-4	Leaf diagram of critical path in FFE.....	62
Figure.5-1	Block diagram of the MDFE chip.....	65
Figure.5-2	Functional verification of the MDFE chip.....	67
Figure.5-3	Schematic view of the combined system (full ports).....	70
Figure.5-4	Schematic view of the combined system (partial ports)	71
Figure.5-5	Diagram of the I/O pads of the chip.....	73
Figure.5-6	Flow chart of the layout process	74
Figure.5-7	Layout view of the MDFE chip	75
Figure.5-8	Time waveform of the critical path (Pre-Layout level)	77
Figure.5-9	Time waveform of the critical path (Post-Layout level).....	77

Chapter 1 Introduction

1.1 Overview

As the magnetic recording industry strives toward high recording densities, the design of equalizers becomes one of the most crucial issues. Inter symbol interference (ISI) is severe at high recording densities and causes degradation in the detection performance because of the difficulty to achieve accurate equalization or because of the excessive noise enhancement. Conventional read-back processing involves the use of run-length limited (RLL) [1][2] codes with peak detection and some read-back equalization. At recording densities in the range of 2-2.5, this turns out to be highly inadequate. Several more sophisticated detection schemes which give improved detection performance at high recording densities are now being pursued.

These schemes can be broadly classified into two categories: one is based on the principle of partial-response signaling coupled with the maximum-likelihood sequence detection (PRML) and the other is based on the principle of decision feedback equalization (DFE). Class-IV PRML [3][4], and extended PRML [5][6] are examples of the first category. Fixed-delay tree search with decision feedback (FDTS/DF) [7], adaptive RAM-DFE [8][14] and multilevel DFE (MDFE) [9] are examples of the second category.

The main idea of decision feedback is to cancel all the precursor and postcursor ISI of the channel impulse response using a 2-tap filter. The feed-forward section (FFE) is a linear filter that removes the linear precursor ISI by averaging and distributing the energy to the postcursor ISI. The feedback equalizer (FBE) is a technique used to eliminate non-linear postcursor ISI by the decision-feedback, provided that the past decisions are correct, so that the output only consists of the impulse response plus some noise components.

1.2 Objective of the Thesis

The objective of this thesis is to design and implement an integrated multilevel decision feedback equalization chip for magnetic recording channel. The MDFE chip consists of a feed-forward and a feedback equalizer. The two sections could either run together as a whole system or be tested independently. This design aims to attain a minimum clock rate of **150MHz** (typical-case) using 0.35 μ m CMOS technology with minimal sacrifice in the core area and the dynamic power consumption.

1.3 Organization of the Thesis

The thesis is organized as follows. Chapter 2 introduces some background knowledge about FDTS/DF, RAM-DFE and MDFE. Chapter 3 deals with the design and implementation of the feedback equalizer (FBE). Several different architectures are

first investigated and compared, from which the final architecture of FBE is decided. The functional simulation and static time analysis results are presented. Chapter 4 mainly concerns the implementation of the feed-forward equalizer (FFE). Chapter 5 presents the integration of FBE and FFE. The overall design is verified and further synthesized to physical level. The post-layout analysis is carried out and the result is presented. Finally, Chapter 6 concludes this research. Some future work is also suggested.

Chapter 2 Introduction to MDFE

2.1 Fixed-delay Tree Search (FDTS/DF)

Fixed delay tree search with decision feedback (FDTS/DF) detector [7][10] is an architecture which has been explored extensively in the magnetic recording channels. Figure.2-1 shows the architecture of FDTS/DF with search depth (τ) equal to 1. The feed-forward equalizer (FFE) and feedback equalizer (FBE) are both adaptive, according to the raw channel read-back impulse response.

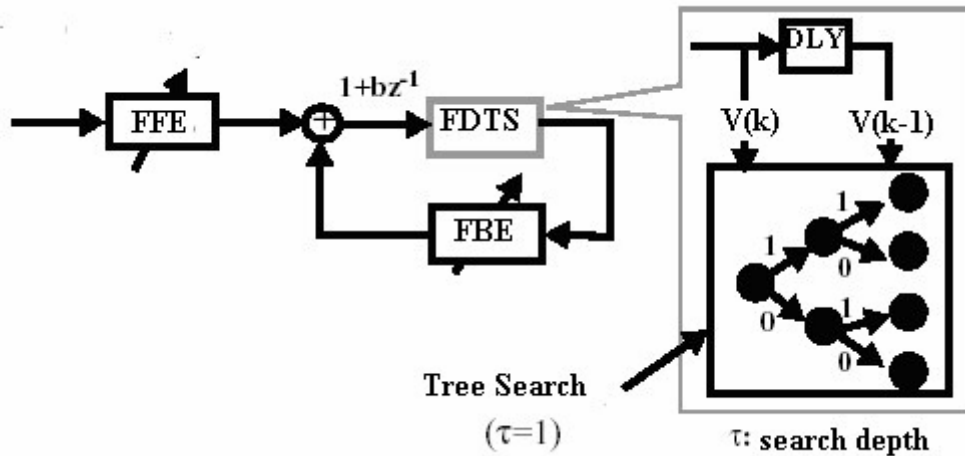


Figure.2-1 Fixed-delay tree search (FDTS/DF) detector

The core is a tree-search detector, which computes the accumulated path metrics for each paths, compares them and selects the path direction at the data cursor. The state diagram of $\tau = 1$ tree search is shown on Figure.2-2: M_k is the accumulated path metrics for path k , defined as:

$$M_k = \sum_{j=1}^{\tau} (y_j - \bar{y}_{j,k})^2 \quad (2.1)$$

where y_j is the received read-back samples, and $\bar{y}_{j,k}$ is the ideal read-back samples if path k is selected. Instead of selecting exact one out of the four possible paths, FDTS/DF algorithm only selects the upper-half or lower-half which the detection should proceed at the data cursor, and the decoding window moves along to the next data cursor. Complete analysis can be found in [10][11]. When the search depth is equal to zero, the decision only depends on the current sample, which corresponds to the well-known decision feedback equalization (DFE).

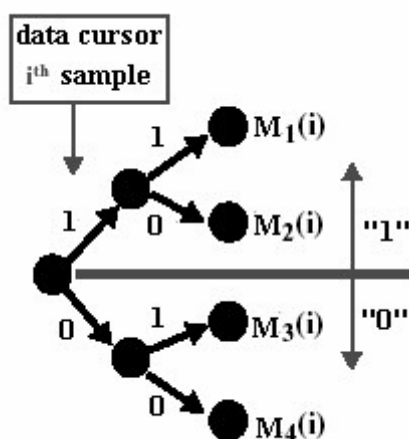


Figure.2-2 FDTS/DF search algorithm

In FDTS/DF, FFE and FBE are designed to remove the precursor ISI and postcursor ISI of the channel impulse response, as shown in Figure.2-3. In digital communication channels where the response of the channel to a symbol to be transmitted is much longer than the symbol itself, a common source of signal distortion is inter-symbol interference (ISI). This means that the responses of the transmitted symbols overlap each other in time. The resulting superposition of signals causes shifts in the location of signal peaks and variances in signal amplitude. When signal distortion is too large, erroneous detections are made at the output. Therefore, as transmission rates increase,

symbols are packed more closely together, increasing ISI and the likelihood of erroneous detections. But if the effects of ISI can somehow be reduced, the achievable transmission rate for a given error probability can be increased.

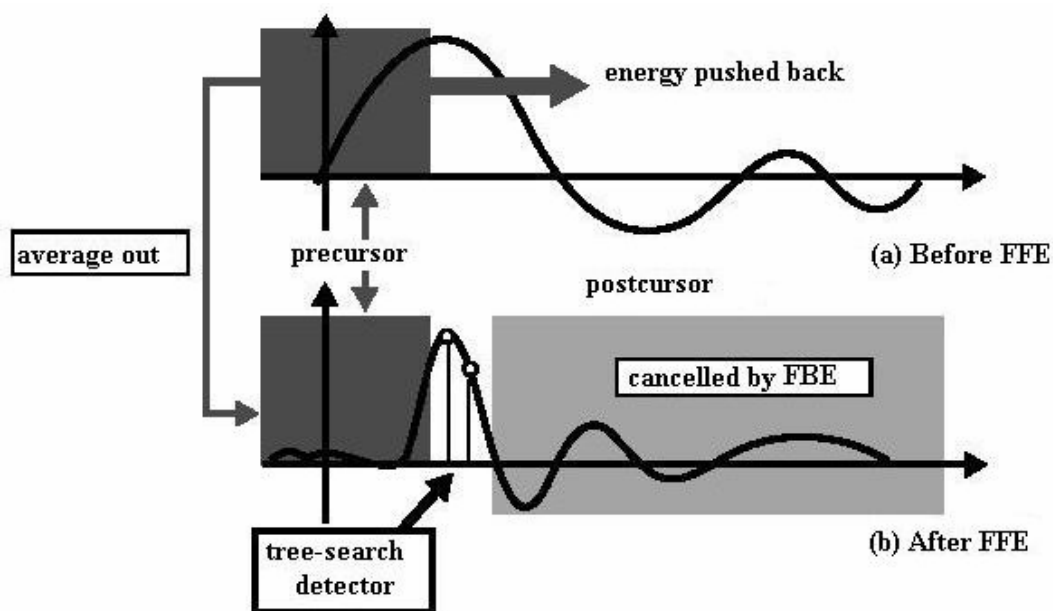


Figure.2-3 Principle of FDTS/DF detection

FFE and DFE coefficients are usually adaptive according to the MMSE algorithm, to maximize the detector performance. However, the filter coefficients can be also analytically decided given the known input signal spectrum. Linear models for the optimization of $\tau = 1$ tree-search detector and the relative definitions could denote the statistical expectation. Therefore, we can determine the optimal FFE and FBE filter coefficients without using adaptive algorithms, given that the channel impulse response, input sequence power spectrum, and noise power spectrum are known.

2.2 RAM Decision Feedback Equalization

Decision Feedback Equalization (DFE) [12] is another technique used to eliminate all ISI so that the output consists only of the impulse response, plus some noise component. The magnetic recording channel at high density exhibits significant non-linear inter-symbol interference, which degrades the performance of linear equalization techniques. The RAM-DFE is proposed as a solution to this problem, in which a digital random access memory (RAM) is used in the feedback path of a feedback equalizer (FBE). It is capable of canceling the non-linear post-cursor inter-symbol interference (ISI).

2.2.1 Linear DFE

The linear DFE shown in Figure.2-4 uses an FIR filter in its decision feedback section and is capable of eliminating linear ISI only.

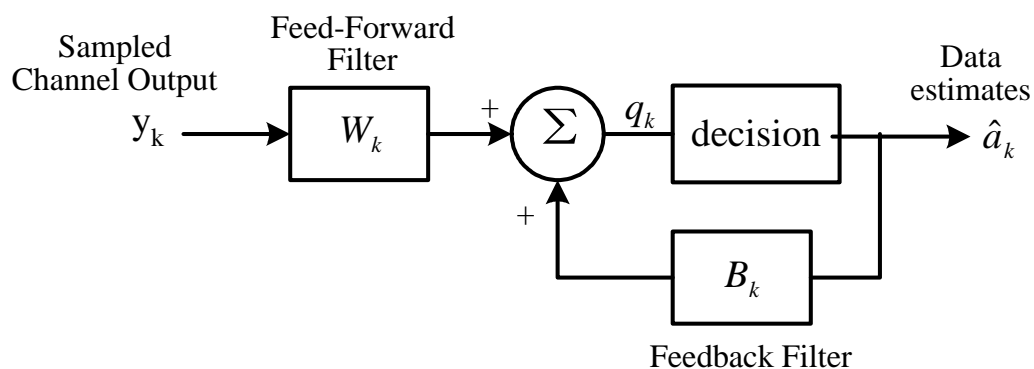


Figure.2-4 Block diagram of the linear DFE

The linear DFE is described by (with L feed-forward coefficients and M feedback coefficients is described by:

$$q_k = \sum_{l=0}^{L-1} w_l y_{k+1} + \sum_{m=1}^M b_m \hat{a}_{k-m} \quad (2.2)$$

$$= \mathbf{w}' y_{k+L-1:k} + \mathbf{b}' \hat{\mathbf{a}}_{k-1:k-M} \quad (2.3)$$

with $y_{k+L-1:k} = [y_{k+L-1} \dots y_k]'$ as the vector of channel outputs, and \mathbf{w} and \mathbf{b} as the corresponding coefficient vectors of the linear DFE, $w = [w_0, \dots, w_{L-1}]'$ and $b = [b_1, \dots, b_M]'$. For notational convenience, we assume the feed-forward section to be noncausal (realized with L units of delay). A good setting for the coefficient vectors in the linear DFE minimizes the mean square error $E[\varepsilon_k^2]$, where

$$\varepsilon_k = a_k - q_k \quad (2.4)$$

The corresponding settings for the linear DFE are well known to be computed as $[w' b'] = p' R^{-1}$, where $p' = E\{[y'_{k+L-1:k} a'_{k-1:k-M}] a_k\}$ is the cross-correlation vector between the current estimated data symbol a_k and the vector of combined channel outputs and previous decisions; and

$$R = E\{[y'_{k+L-1:k} a'_{k-1:k-M}] [y'_{k+L-1:k} a'_{k-1:k-M}]\} \quad (2.5)$$

is the autocorrelation matrix of the combined channel outputs and previous decisions.

Assuming correct output decisions, the minimum mean-square error (MMSE) is

$$\sigma_{mmse}^2 = E\{a_k^2\} - p' R^{-1} p \quad (2.6)$$

2.2.2 RAM-DFE

The RAM-DFE is shown in Figure.2-5, with linear feedback replaced by a lookup table. We define the RAM-DFE parameters using a new notation. If M past decision bits are arranged in a vector and used as a lookup table address, then we can interpret the content of the addressed location as the corresponding table output.

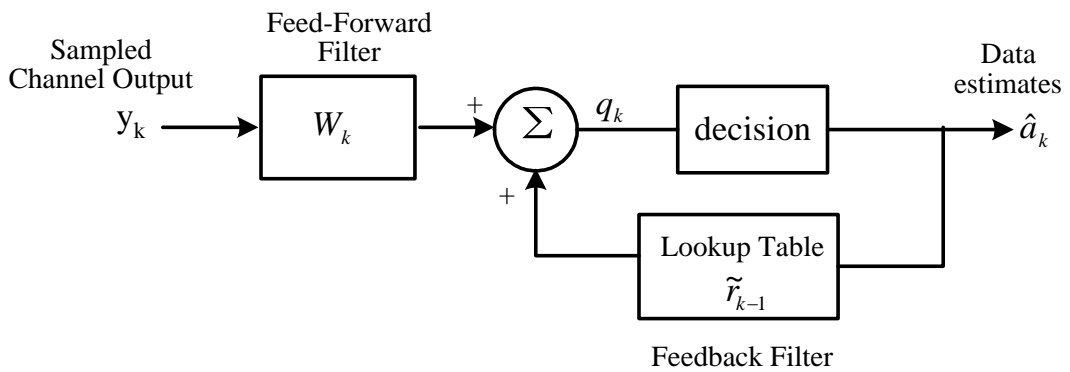


Figure.2-5 Block diagram of RAM-DFE

Let us denote an index for the address vector as \tilde{i}_{k-1} , where can write

$$0 \leq \tilde{i}_{k-1} = \sum_{m=0}^{M-1} \frac{1}{2} (a_{k-1-m} + 1) 2^m \leq 2^M - 1 \quad (2.7)$$

If we further define a 2^M -dimensional vector

$$s(\tilde{i}_{k-1}) = [s_0(\tilde{i}_{k-1}) s_1(\tilde{i}_{k-1}) \dots s_{2^M-1}(\tilde{i}_{k-1})]' \quad (2.8)$$

then we can write the RAM output as

$$r(\tilde{i}_{k-1}) = \tilde{b}' s(\tilde{i}_{k-1}) \quad (2.9)$$

where $\tilde{\mathbf{b}} = [\tilde{b}_0 \dots \tilde{b}_{2^M-1}]'$ is a vector with the contents of the corresponding ram locations. Since the feedback path is linear in the 2^M newly defined inputs, the analysis is then the same as the linear DFE with $\hat{a}_{k-1:k-M}$ replaced by $s(\tilde{i}_{k-1})$, and \mathbf{b} replaced by $\tilde{\mathbf{b}}$. The MMSE for the RAM-DFE is quadratic in the parameters $[w' \tilde{\mathbf{b}}']$ and has a unique global MMSE, because the autocorrelation matrix is nonsingular. The 2^M elements of $\tilde{\mathbf{b}}$ are then the contents of the lookup table.

The MMSE for both the linear DFE and the RAM-DFE can be computed and compared. The quantities $\tilde{\rho}$ and \tilde{R} are not trivially computed in terms of the given finite-state machine model for the channel. We show how to compute these quantities in term of $f(i_k)$. The DFE output SNR in either case is computed as

$$SNR = \frac{E(a_k^2) - \sigma_{mmse}^2}{\sigma_{mmse}^2} \quad (2.10)$$

In summary, RAM-DFE can very closely achieve the MMSE solution for the measured read signal. Furthermore, by using signed-LMS, all explicit multiplications may be eliminated from the adaptation procedure, making the RAM-DFE well suited to high-speed applications such as magnetic recording.

2.3 Multi-level Decision Feedback Equalization

A simplified version of FDTS/DF [13] is called Multi-Level Decision Feedback Equalization (MDFE) [9][15] because it is architecturally identical to DFE. The only

difference is that the algorithm for determining the coefficients of the forward and backward equalizers is changed so that the output becomes multi-level. A digital communication channel incorporating MDFE is shown in Figure2-6.

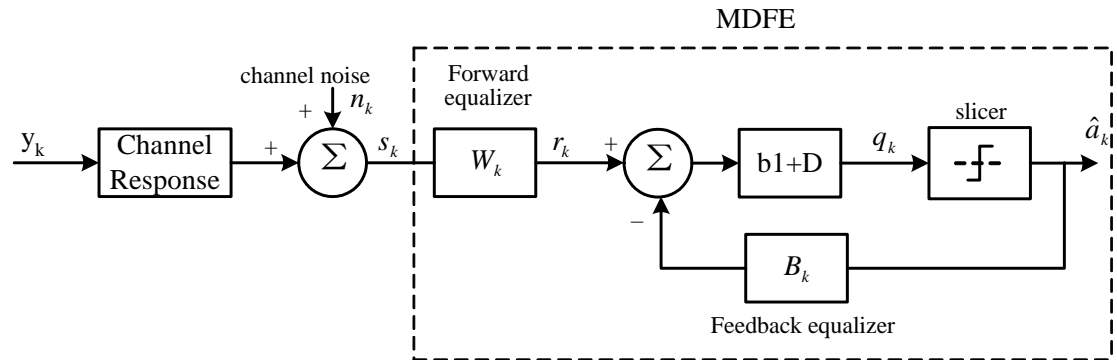


Figure.2-6 Digital Communication Channel with MDFE

In this channel, a digital data stream, y_k , consisting of positive and negative impulses, enters the channel response block. The channel response block includes the response of the transmission media, plus that of filters that are used to shape the signal before and after its transmission. White noise is then factored in with the addition of the n_k term. After sampling, the transformed signal, s_k , enters the MDFE through a linear transversal filter - the forward FIR filter with coefficients W_k . This filter is of sufficient length to delay the response to make it causal. It is designed to remove pre-cursor ISI from the response - the ISI due to future symbols.

The output of the forward filter, r_k , is summed with the output of the feedback section. The B_k coefficients of the feedback section, or backward filter, are chosen

to match the combined response of the channel block and the forward filter to a unit impulse. In other words, when the output of the backward filter is subtracted from r_k , all of the channel responses except for the unit impulse response of a single y_k input are removed.

The coefficients in MDFE are determined in the same way as in DFE. One difference is the error signal, ($\varepsilon_k = q_k - \hat{q}_k$), due to the changed target, \hat{q}_k , and actual, q_k , outputs in MDFE. Also, the b_1 term is removed from its normal position in the backward filter and is now calculated by a separate algorithm for its use in the linear discriminant. Its equation is:

$$b_{1,k+1} = b_{1,k} - 2\mu_{b_1}(\hat{a}_{k+1} + \hat{a}_{k-1} + 2b_{1,k}\hat{a}_k)\varepsilon_k \quad (2.11)$$

where μ_{b_1} is the rate of adaptation for $b_{1,k}$.

Because the error signal, ε_k , now uses a future detected symbol, \hat{a}_{k+1} , a delay must be added to the coefficient update equations for the forward and backward equalizers. The update equation for the forward equalizer coefficients, $W_k = [w_{0,k}, w_{1,k}, \dots, w_{M,k}]$, becomes:

$$W_{k+1} = W_k + 2\mu_w S_{k-1} \varepsilon_{k-1} \quad (2.12)$$

The update equation for the backward equalizer coefficients, $B_k^1 = [b_{2,k}, \dots, b_{N,k}]$, becomes:

$$B_{k+1}^1 = B_k^1 + 2\mu_b \hat{A}_{k-1} \varepsilon_{k-1} \quad (2.13)$$

Once the values for b_1 , W_k , and B_k^1 are calculated, W_k and B_k^1 must be multiplied through by the linear discriminant, $(b_1 + D)$, to obtain the actual coefficients to be loaded into the equalizers. Thus, the target response of MDFE is multiplied by $(b_1 + D)$, yielding:

$$\hat{q}_k = b_1 \hat{a}_{k+1} + (1 + b_1^2) \hat{a}_k + b_1 \hat{a}_{k-1} \quad (2.14)$$

MDFE provides superior performance to the other disk data detection methods, such as peak detection and Partial Response (PR) Equalization, while offering a simple, low-cost, low-power implementation. Thus, MDFE is a promise solution for the increasing disk drive storage density.

2.4 Implementations of the MDFE

The most significant differences between analog and digital implementation are the non-idealities such as offset and nonlinearity that are associated with analog circuits. Table.2-1 briefly compares the three architectures. If offset proves to be a surmountable problem, the mostly analog MDFE will be the smallest of the three implementations. It is reasonable to assume, with the design of the counters in the

mostly digital MDFE, the comparators will be the speed-limiting factor for all three implementations. In this case the most efficient in terms of size and power will be the mostly analog MDFE. For a completely digital implementation, the transposed FFE and the RAM-DFE are worthy of consideration.

Table.2-1 Comparison of MDFE architectures

Architecture	Programming Coefficients	Estimated Area	Design Challenge
Analog	Hard, ADC-DAC	Smallest	Integrator DC gain,offset
Digital	Easy	Medium	Fast digital circuits
Mixed-Signal	Easy	Largest	Fast digital circuits, DAC

Chapter 3 Design and Implementation of FBE

3.1 Design Considerations for FBE

The block diagram of MDFE to be implemented is given in Figure 3-1. As described before, the feed-forward section (FFE) is a linear filter that shapes the read-channel pulse response, and the feedback section (FBE) is used to eliminate the non-linear post-cursor ISI, provided that the past decisions are correct. An impulse response plus some noise components will therefore be obtained at the output.

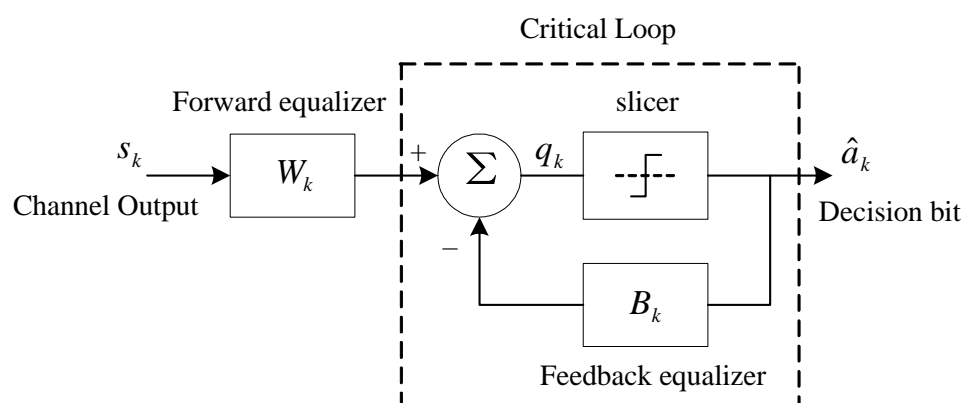


Figure.3-1 System Diagram of FFE and FBE

being the addresses. A key specification for the FBE is the speed. When the current decision is available, the feedback coefficient must be ready before next clock arrives. Thus, the operation of the FBE must be completed within one clock cycle. This imposed some difficulties on the FBE design. In this chapter, a number of

architectures for FBE are investigated and compared, from which the final architecture is chosen. The number of taps and coefficients are determined from the system-level simulation done elsewhere. The full digital implementation is a prerequisite for this work. This design aims to attain a minimum clock rate of 150 MHz with minimal sacrifice in the core area and the dynamic power consumption.

3.2 Simple RAM-FBE (Structure-I)

A simple structure of the RAM-FBE, as shown in Figure.3-2, is first investigated. It is composed of a 12-tap D-Flip-Flop chain together with two SRAMs as the two look-up tables. Each SRAM has the size of $2^6 \times 8$ bits. To achieve the goal of performing a broad range of recording densities, minimizing the noise enhancement and a good post-cursor ISI cancellation, the length of FBE must be long enough. The choice of 12-tap FBE is based on the work done in [17] where it showed that the satisfactory performance can be achieved the minimum number of feedback taps of 12.

All the feedback coefficients are pre-calculated and loaded into the look-up tables (LUT) through a series interface prior to the read operation of the channel. At the rising clock edge of time k , for example, the past decisions stored in the D-Flip-Flop chain are used to address the look-up tables. Two outputs from the lookup tables, $data_A$ and $data_B$ are summed to produce the final feedback value FB_k . This feedback data is then added to the 8-bit output data, FE_k , from the FFE. The slice

takes the sum as its input and produces the current decision-bit a_k , which is based on the sign of the summation.

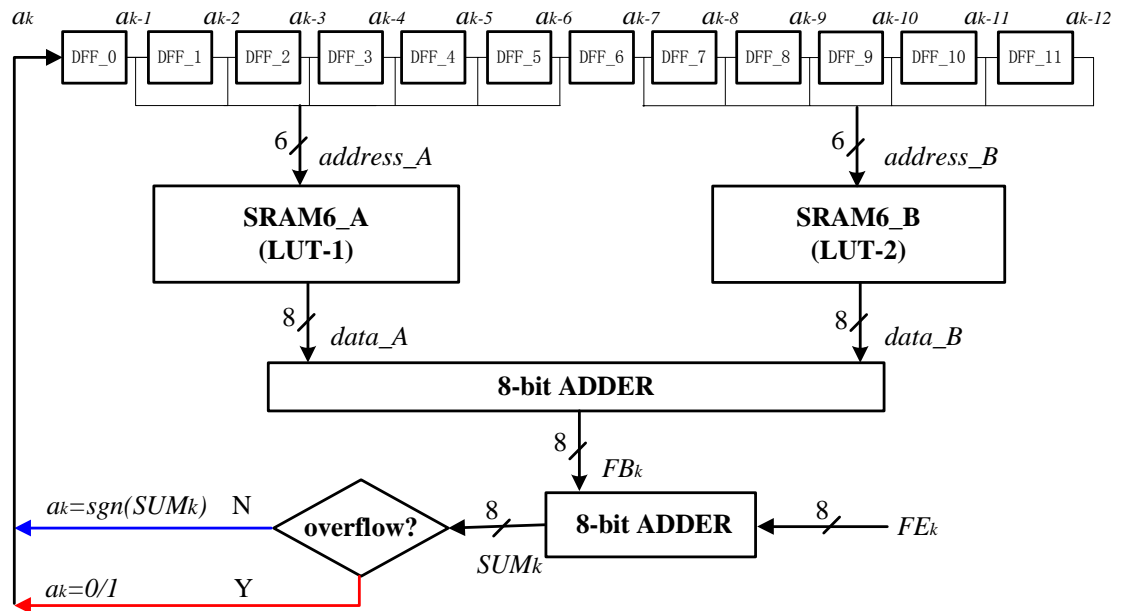


Figure.3-2 Block diagram of FBE (Structure-I)

Though this structure is quite simple to be implemented, it has a disadvantage of its long critical path. For each data path which may start from $a_{k-1}, a_{k-2}, \dots, a_{k-12}$, it will go through a $2^6 \times 8$ bits SRAM and two 8-bit adder together with some combination logic gates, and then go back to the D-Flip-Flop chain.

Table.3-1 gives the path delay report after optimization. The highest clock rate that can be achieved for this structure is only about 75 MHz, far below the spec of **150MHz**. The critical path in this structure is 13.07ns, which is mainly caused by the SRAMs and the adders.

Table.3-1 Data path delay of Structure-I

	Path Through	Path Delay
a_{k-1} to data_A	SRAM6_A	4.91 ns
data_A to FB_k	8-bit adder	3.78 ns
FB_k to SUM_k	8-bit adder	3.82 ns
SUM_k to a_k	logic gates	0.56 ns

3.3 Look-ahead RAM-FBE (Structure-II)

To reduce the delay caused by the SRAM and adders as in the Structure I, the pipeline technique can be employed. In the synchronous logic design, shorting the path delay of the combination logic between the sequential logic is the most effective way to increase the system speed. As shown in Figure.3-3, the large combinational logic block can be segmented into several small ones that are divided by flip-flops. This is so called PIPELINE principle [18].

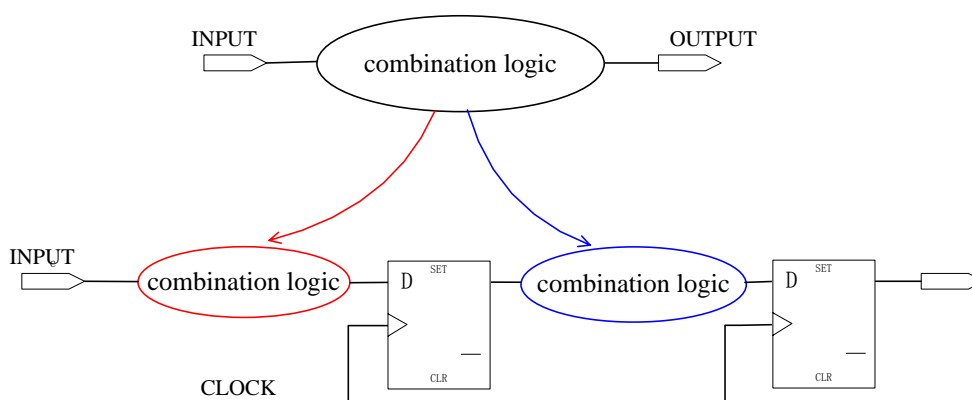


Figure.3-3 Segmentation of complicated combination logic

According to this method, a new design is explored with the pipeline insertion and the Look-Ahead operation. As shown in Figure.3-4, Structure-II has 2 combinational

logic stages. This design is composed of an 11-tap D-Flip-Flop chain where the first bit is taken as the look-ahead bit compared to Structure-I. Therefore, the first 6-bit SRAMs in Structure-I is split into two 5-bit SRAMs which store the coefficients for the current decision of “1” and “0”, respectively. Thus, in this structure, three lookup tables are needed. Two sets of coefficients are pre-calculated and later selected by the multiplexer that is controlled by the current decision bit.

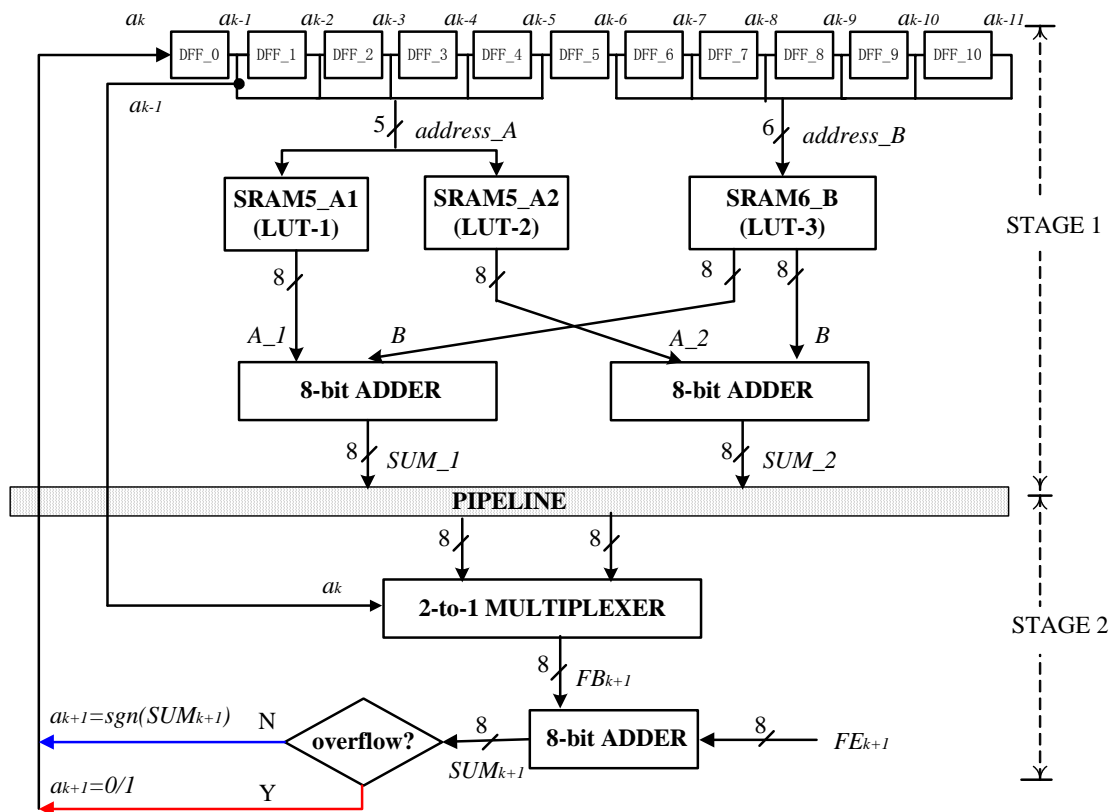


Figure.3-4 Block diagram of FBE (Structure-II)

Table.3-2 is the path delay report for Structure-II. The critical path (in stage-1) is reduced to 7.99ns and the speed is increased to 125MHz. This is attributed to the removal of one adder and some logic gates from the whole data path. However, it still

could not reach **150MHz** for the bottleneck is still concern with the delay by SRAM.

Table.3-2 Data path delay of Structure-II

	Path	Path Through	Path Delay
Stage-1	a_{k-1} to SUM_1	SRAM5_A1 & 1 8-bit adder	7.99 ns
Stage-2	FB_k to a_k	1 8-bit adder & logic gates	3.76 ns

3.4 Improved Look-ahead FBE (Structure III)

Though the system speed has been increased by the improvements made in Structure-II, the size of each lookup table is rather big ($2^5 \times 8$ or $2^6 \times 8$). As the time taken by the FBE to generate the output to some extent is affected by the read access time of the SRAM, large size will possibly cause more delays and large silicon area. Therefore, we will split the big lookup table in to small ones [16].

Structure-III, as shown in Figure.3-5, is an improved version of Structure-II with a special focus on the chip area. This structure also has two pipeline stages and one 11-tap D-Flip-Flop chain, but it uses several small SRAMs ($2^2 \times 8$ or $2^3 \times 8$) to reduce the core area and the dynamic power. In this structure, 5 lookup tables are employed.

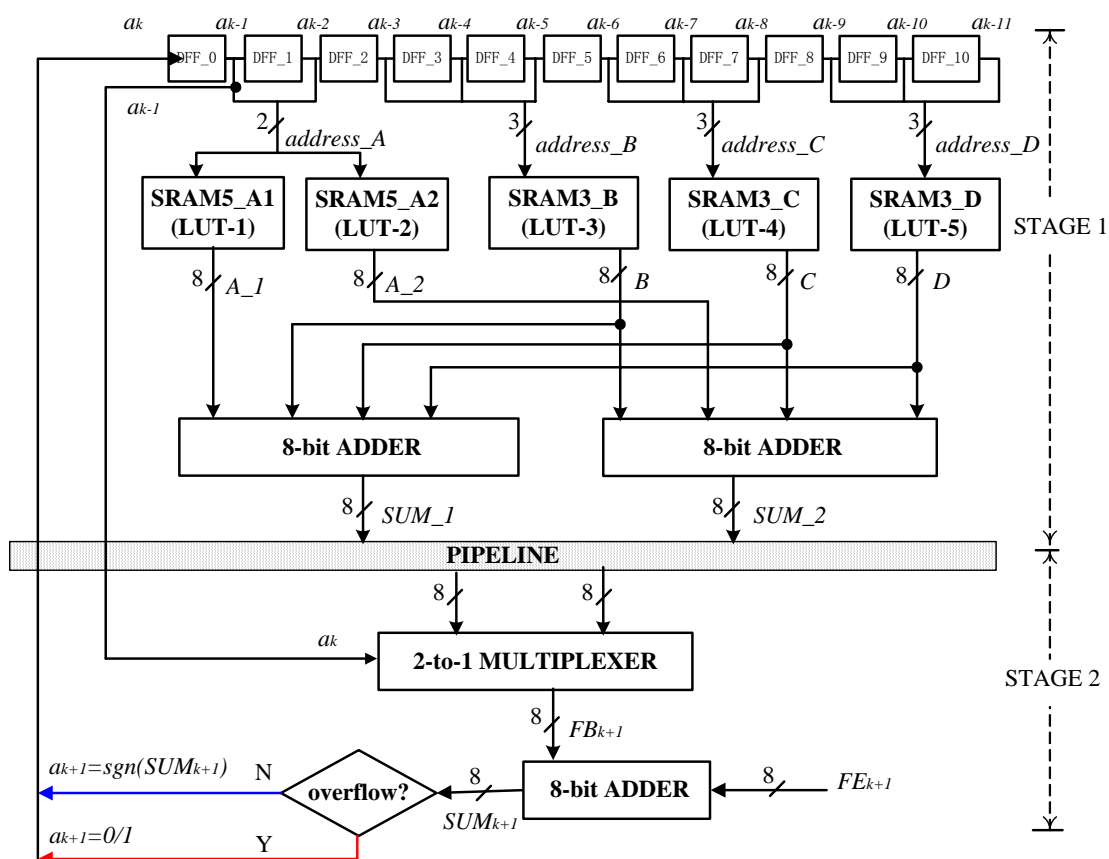


Figure.3-5 Block diagram of FBE (Structure III)

Synthesis and simulation results show that there is a significant improvement on the chip area in Structure II, while maintaining the same speed. The critical path is still in Stage-1. Table.3-3 shows the performance comparison between Structure II and III. The speed of the FBE needs to be further improved.

Table.3-3 Core Area and Speed of Structure-III & II

	Critical Path	Clock Rate	Core Area
Structure-II	7.99 ns	125 MHz	0.82 mm ²
Structure-III	7.70 ns	130 MHz	0.26 mm ²

3.5 Optimized Look-ahead FBE (Structure IV)

It has been found that the bottleneck for the speed in the previous structure is due to the SRAM and the adder in Stage-1. Thus, the SRAMs can be further split to small sizes and more pipelines can be employed. This leads to the Structure IV as shown in Figure.3-7.

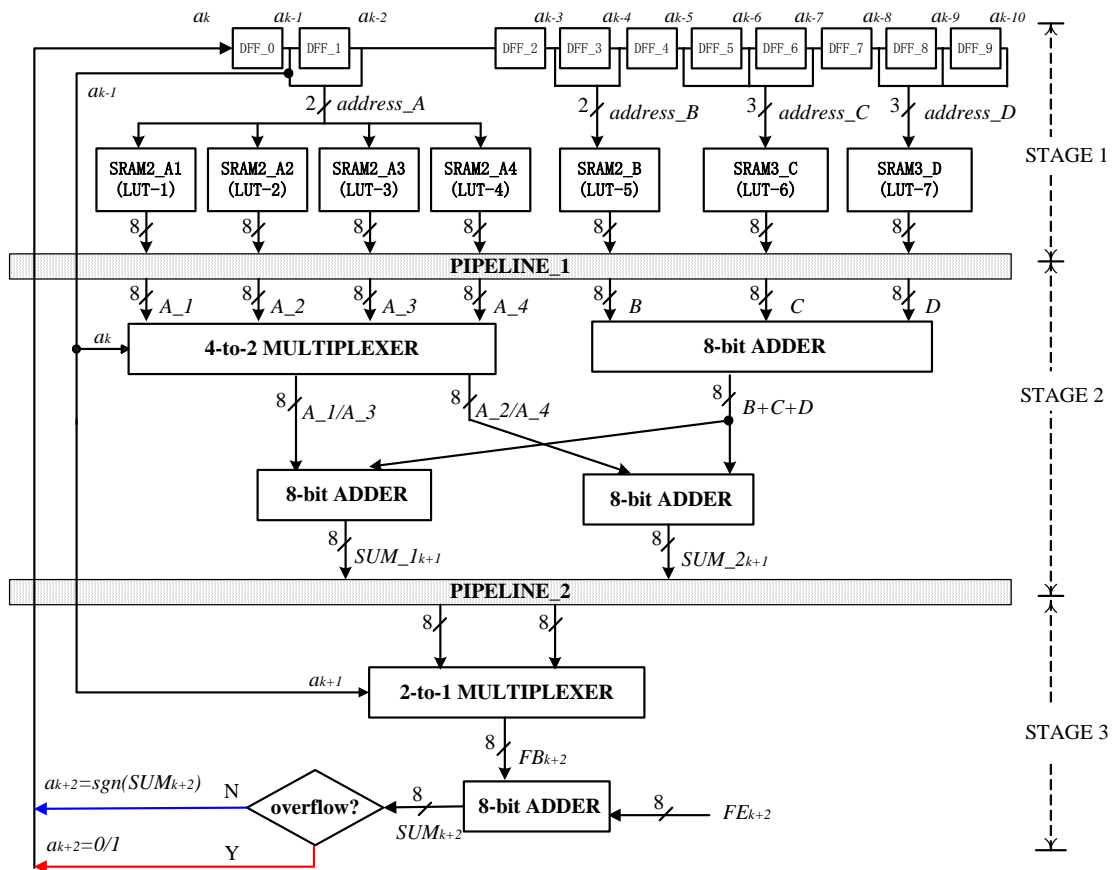


Figure.3-7 Block diagram of FBE (Structure IV)

Structure IV has three pipeline stages and one 10-tap D-Flip-Flop chain. It looks ahead for 2 bits, instead of just one as in the two previous structures. The first two 2-bit SRAM, which is in structure-III, are split into four 2-bit SRAMs which store the coefficients for the current decision of “1” and “0” and the next decision of “1” and

“0” respectively. Thus, in this structure, seven lookup tables are needed. Four sets of coefficients are pre-calculated and later selected by the multiplexer that is controlled by the current decision bit and the next decision in different pipeline stages.

The three pipeline stages relax the timing constraint, while the 2-bit look ahead avoids the problem of latency introduced by the pipeline stages. In this structure, although seven lookup tables are needed, the size of each lookup table or RAM, which is $2^2 \times 8$ or $2^3 \times 8$, is still quite small.

Table.3-4 shows the path delay report of Structure IV. As the 2 pipeline stages in Structure-II and III are split into 3 stages, here the critical path is no longer in Stage-1 but in Stage-2 only caused by the adders. It can be seen that evaluation the critical path is reduced to **4.60ns** and the speed of **200MHz** is attained.

Table.3-4 Comparison between Structure-IV & III

	Path	Path Through	Path Delay
Stage-1	a_{k-12} to D	SRAM3_D	3.91 ns
Stage-2	D to SUM_1	2 8-bit adders	4.60 ns
Stage-3	FB_k to a_k	1 8-bit adder & logic gates	3.47 ns

Table.3-5 shows the comparison with the Structure III. The chip area is 0.33 mm^2 , only slightly larger than that of Structure-III (0.26 mm^2).

Table.3-5 Comparison between Structure-IV & III

	Critical Path	Speed	Core Area
Structure-III	7.70 ns	130 MHz	0.26 mm ²
Structure-IV	4.60 ns	200 MHz	0.33 mm ²

3.6 Summary of Structure-I, II, III and IV

The performances of the four structures are summarized in Table.3-6. Structure-I is a direct implementation based on the operation of the MDFE. Although it is simple, it has the worst performance. The speed improvement of both Structure-II and Structure-III are benefited from the pipeline technique. Structure-III has the smallest core area which is achieved by replacing the big SRAMs with small ones. However, both of them are limited at the frequency of no more than 130MHz. Structure IV shows superior speed performance to the other three structures with slightly larger core area and high power consumption than those of Structure III. Its speed performance is attributed to its 3 pipeline and the use of small SRAMs. The Structure IV is finally chosen for the implementation of FBE.

Table.3-6 Summary of Structure-I, II, III & IV

Structure	I	II	III	IV
Taps	12	11	11	10
Pipeline Stages	No pipeline	2	2	3
SRAM	$2^6 \times 8$ bits ($\times 2$)	$2^5 \times 8$ bits ($\times 2$) $2^6 \times 8$ bits ($\times 1$)	$2^2 \times 8$ bits ($\times 2$) $2^3 \times 8$ bits ($\times 3$)	$2^2 \times 8$ bits ($\times 5$) $2^3 \times 8$ bits ($\times 2$)
Clock Rate (MHz)	75	125	130	200
Core Area (mm ²)	/	0.82	0.26	0.33
Dynamic Power (mW)	/	1091.7	18.39	43.86

3.7 Behavior Simulation

Behavior simulation is quite necessary when the system-level design is done. There are several ways to create an imaginary simulation model of a system. The behavioral simulation gives out the verification that if a logical system works correctly. The simulation tool used here is Verilog-XL3.0 [24][25] by CADENCE. In the next subsections, the verification result and the data analysis of FBE and the whole system will be given.

As was described before, all the feedback coefficients are pre-calculated and loaded (written) into the lookup tables prior to the read operation of the channel. One of the simulation results is shown in Figure 3-8. In stage-1, the outputs ($A_1, A_2, A_3, A_4, B, C, D$) of the SRAMs are determined by the previous decisions captured in the DFF chain ($a_{k-1}, a_{k-2}, a_{k-3}, a_{k-4}, a_{k-5}, a_{k-6}, a_{k-7}, a_{k-8}, a_{k-9}, a_{k-10}$). SUM_1 and SUM_2 are the outputs generated in stage-2. $FB, SUM, over-pos, over-neg,$ and a_k are outputs generated in stage-3. CLK is the system clock, and FE is an external signal from the feed-forward equalizer.

As shown in Figure 3-7, with the look-ahead, the FBE is allowed to complete its operation in three clock cycles, thus the timing constraints on the critical path is relaxed.

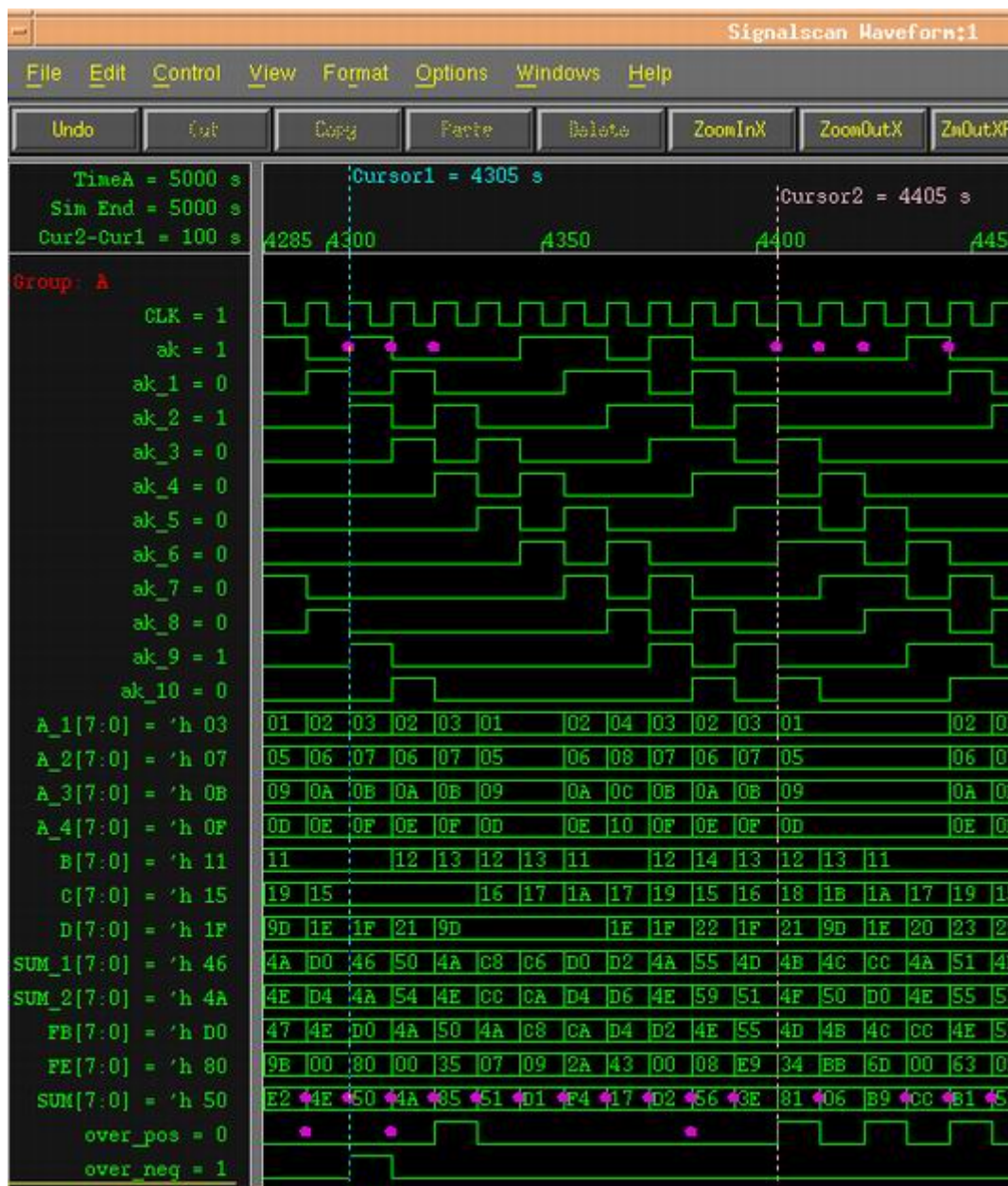


Figure.3-8 Operation diagram of FBE

At the first rising clock edge, the previous decisions stored in the shift register are used to address the look-up table, or the SRAM. The shift register is simply implemented as a chain of 10 D-flip-flops with asynchronous reset and responds to input data at the rising clock edge. The six earliest decision bits, $\{a_{k-5}, a_{k-6}, a_{k-7}\}$ and

$\{a_{k-8}, a_{k-9}, a_{k-10}\}$ are used to address SRAM_C and SRAM_D, respectively. The two second recent decision bits, $\{a_{k-3}, a_{k-4}\}$, are used to address SRAM_B and the two most recent decision bits, $\{a_{k-1}, a_{k-2}\}$, address four look-up tables, SRAM2_A1(for the case of $a_k=0, a_{k+1}=0$), SRAM2_A2(for the case of $a_k=0, a_{k+1}=1$), SRAM2_A3(for the case of $a_k=1, a_{k+1}=0$), and SRAM2_A4(for the case of $a_k=1, a_{k+1}=1$).

At the second rising clock edge, 4 possible values of FB are summed up by the previous 7 output data from the 7 look-up tables. At the same time, the current decision bit a_k is clocked into the first bit in the shift register, and this value is used as the select signal for the 4 to 2 multiplexer to choose the corresponding SUM_1 and SUM_2 from the 4 sum values. The computation of the 2nd stage outputs are shown in the following 2 equations.

$$\begin{cases} SUM_1_{k+1} | (a_k = 0, a_{k+1} = 0) = A_1 + B + C + D \\ SUM_2_{k+1} | (a_k = 0, a_{k+1} = 1) = A_2 + B + C + D \end{cases} \quad (3.1)$$

or,

$$\begin{cases} SUM_1_{k+1} | (a_k = 1, a_{k+1} = 0) = A_3 + B + C + D \\ SUM_2_{k+1} | (a_k = 1, a_{k+1} = 1) = A_4 + B + C + D \end{cases} \quad (3.2)$$

At the third rising clock edge, the current decision bit a_{k+1} is clocked into the first bit in the shift register. This value is used as the select signal for the 2 to 1 multiplexer to choose the corresponding FB_{k+2} from the two pre-calculated feedback values like following:

$$\begin{cases} FB_{k+2} | (a_{k+1} = 0) = SUM_1_{k+1} \\ FB_{k+2} | (a_{k+1} = 1) = SUM_2_{k+1} \end{cases} \quad (3.3)$$

The final feedback value FB_{k+2} will then be summed with the 8-bit input from the feed-forward filter. FE_{k+2} at the main adder to produce a_{k+2} , which is based on the sign of the summation. The computation of the 3rd stage outputs are:

$$SUM_{k+2} = FE_{k+2} + FB_{k+2} \quad (3.4)$$

In the case of no overflow:

$$a_{k+2} = \text{sgn}(SUM_{k+2}) \quad (3.5)$$

In the case of positive or negative overflow:

$$\begin{cases} a_{k+2} = 0; (\text{pos} - \text{overflow}) \\ a_{k+2} = 1; (\text{neg} - \text{overflow}) \end{cases} \quad (3.6)$$

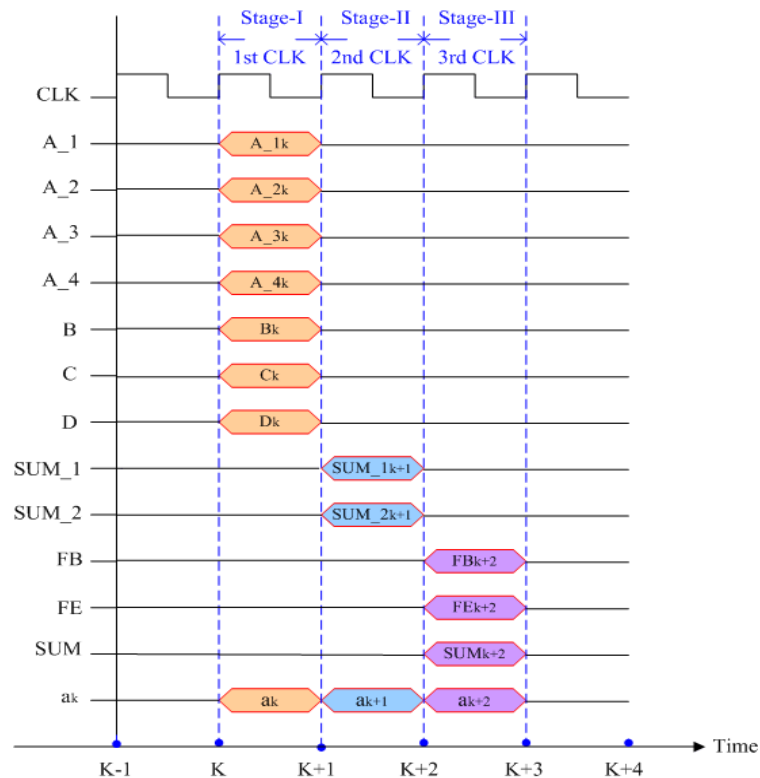


Figure.3-9 Clock waveform of FBE (Structure-IV)

The above operation is illustrated in Figure.3-9, in which it shows that the operation of the FBE is completed in three clock cycles.

3.8 Functional Verification

To do the functional verification, hundreds of vectors are fed into FBE as the simulated input data FE (8-bit). Therefore, the outputs of FBE could be verified, such as FB , SUM , and a_k . Figure.3-10 and Figure.3-11 shows the behavioral simulation result of FBE by vectors. Each data line presents for the variables in FBE system and they are listed by time. From the data, we could have an analysis that if this system is running just as correctly as predicted.

As the system is a feedback loop and the only factors which could influence the whole operation are a_k and FE , especially a_k , the analysis could be taken out by **Typical Cases**. Totally such kinds of cases are 6 and they could be classified by 2 groups. Group-A includes 4 cases which mainly concern with the operation with different a_k/a_{k+1} , for a_k is to verify the logic in stage-2 and a_{k+1} is to verify the logic in Stage-3. Group-B includes the other 2 cases which concern with the data overflow. For these two cases, a_k/a_{k+1} are not relevant.

- ◆ Typical Case.1: $a_k = 0, a_{k+1} = 0$;
- ◆ Typical Case.2: $a_k = 1, a_{k+1} = 0$;
- ◆ Typical Case.3: $a_k = 0, a_{k+1} = 1$;
- ◆ Typical Case.4: $a_k = 1, a_{k+1} = 1$;
- ◆ Typical Case.5: positive overflow;
- ◆ Typical Case.6: negative overflow;

Figure.3-10 and Figure.3-11 have exactly the same simulation data, and the only difference is they have different markers to show the case analysis of Group-A and Group-B respectively.

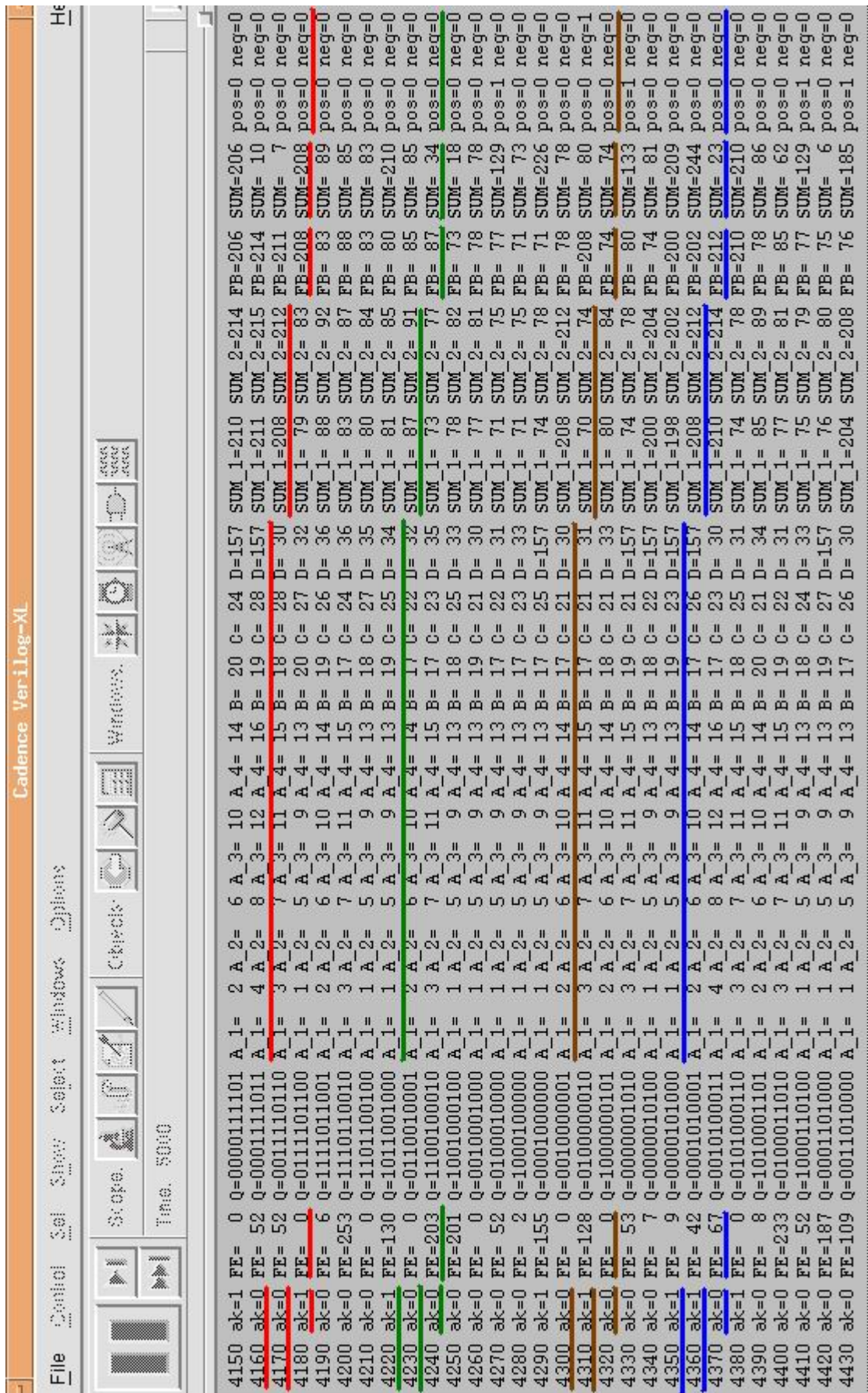


Figure.3-10 FBE functional simulation data (for Group-A)

3.8.1 Data Analysis of Group-A

◆ **Typical Case.1: $a_k = 0, a_{k+1} = 0$;**

At time $k = 4160$,

$$A_1=4, A_2=8, A_3=12, A_4= 16, B= 19, C=28, D=157$$

At time $k+1 = 4170, a_k=0$, according to (3.1),

$$\begin{aligned} SUM_1_{k+1} / (a_k=0, a_{k+1}=0) &= 4+19+28+157 = 208 \\ SUM_2_{k+1} / (a_k=0, a_{k+1}=1) &= 8+19+28+157 = 212 \end{aligned}$$

At time $k+2 = 4180, a_{k+1}=0$, according to (3.3),

$$FB_{k+2} / (a_{k+1}=0) = SUM_1_{k+1} = 208$$

In the meanwhile, $FE_{k+2} = 0$, according to (3.4),

$$SUM_{k+2} = 208+0 = 208$$

There is no data overflow, so according to (3.5),

$$a_{k+2} = \text{sgn} (SUM_{k+2}) = 1$$

◆ **Typical Case.2 $a_k = 1, a_{k+1} = 0$;**

At time $k = 4220$,

$$A_1=1, A_2=5, A_3=9, A_4= 13, B= 19, C=25, D=34$$

At time $k+1 = 4230, a_k=1$, according to (3.2),

$$\begin{aligned} SUM_1_{k+1} / (a_k=1, a_{k+1}=0) &= 9+19+25+34 = 87 \\ SUM_2_{k+1} / (a_k=1, a_{k+1}=1) &= 13+19+25+34 = 91 \end{aligned}$$

At time $k+2 = 4240, a_{k+1}=0$, according to (3.3),

$$FB_{k+2} / (a_{k+1}=0) = SUM_1_{k+1} = 87$$

In the meanwhile, $FE_{k+2} = 203$, according to (3.4),

$$SUM_{k+2} = 203+87 = 34$$

There is no data overflow, so according to (3.5),

$$a_{k+2} = \text{sgn} (SUM_{k+2}) = 0$$

◆ **Typical Case.3** $a_k = 0, a_{k+1} = 1$;

At time $k = 4300$,

$$A_1=2, A_2=6, A_3=10, A_4=14, B=17, C=21, D=30$$

At time $k+1 = 4310, a_k=0$, according to (3.1),

$$\begin{aligned} SUM_1|_{k+1} / (a_k=0, a_{k+1}=0) &= 2+17+21+30 = 70 \\ SUM_2|_{k+1} / (a_k=0, a_{k+1}=1) &= 6+17+21+30 = 74 \end{aligned}$$

At time $k+2 = 4320, a_{k+1}=1$, according to (3.3),

$$FB_{k+2} / (a_{k+1}=1) = SUM_2|_{k+1} = 74$$

In the meanwhile, $FE_{k+2} = 0$, according to (3.4),

$$SUM_{k+2} = 0+74 = 74$$

There is no data overflow, so according to (3.5),

$$a_{k+2} = \text{sgn}(SUM_{k+2}) = 0$$

◆ **Typical Case.4** $a_k = 1, a_{k+1} = 1$;

At time $k = 4350$,

$$A_1=1, A_2=5, A_3=9, A_4=13, B=19, C=23, D=157$$

At time $k+1 = 4360, a_k=1$, according to (3.2),

$$\begin{aligned} SUM_1|_{k+1} / (a_k=1, a_{k+1}=0) &= 9+19+23+157 = 208 \\ SUM_2|_{k+1} / (a_k=1, a_{k+1}=1) &= 13+19+23+157 = 212 \end{aligned}$$

At time $k+2 = 4370, a_{k+1}=1$, according to (3.3),

$$FB_{k+2} / (a_{k+1}=1) = SUM_2|_{k+1} = 212$$

In the meanwhile, $FE_{k+2} = 67$, according to (3.4),

$$SUM_{k+2} = 67+212 = 279$$

There is no data overflow, so according to (3.5),

$$a_{k+2} = \text{sgn}(SUM_{k+2}) = 0$$

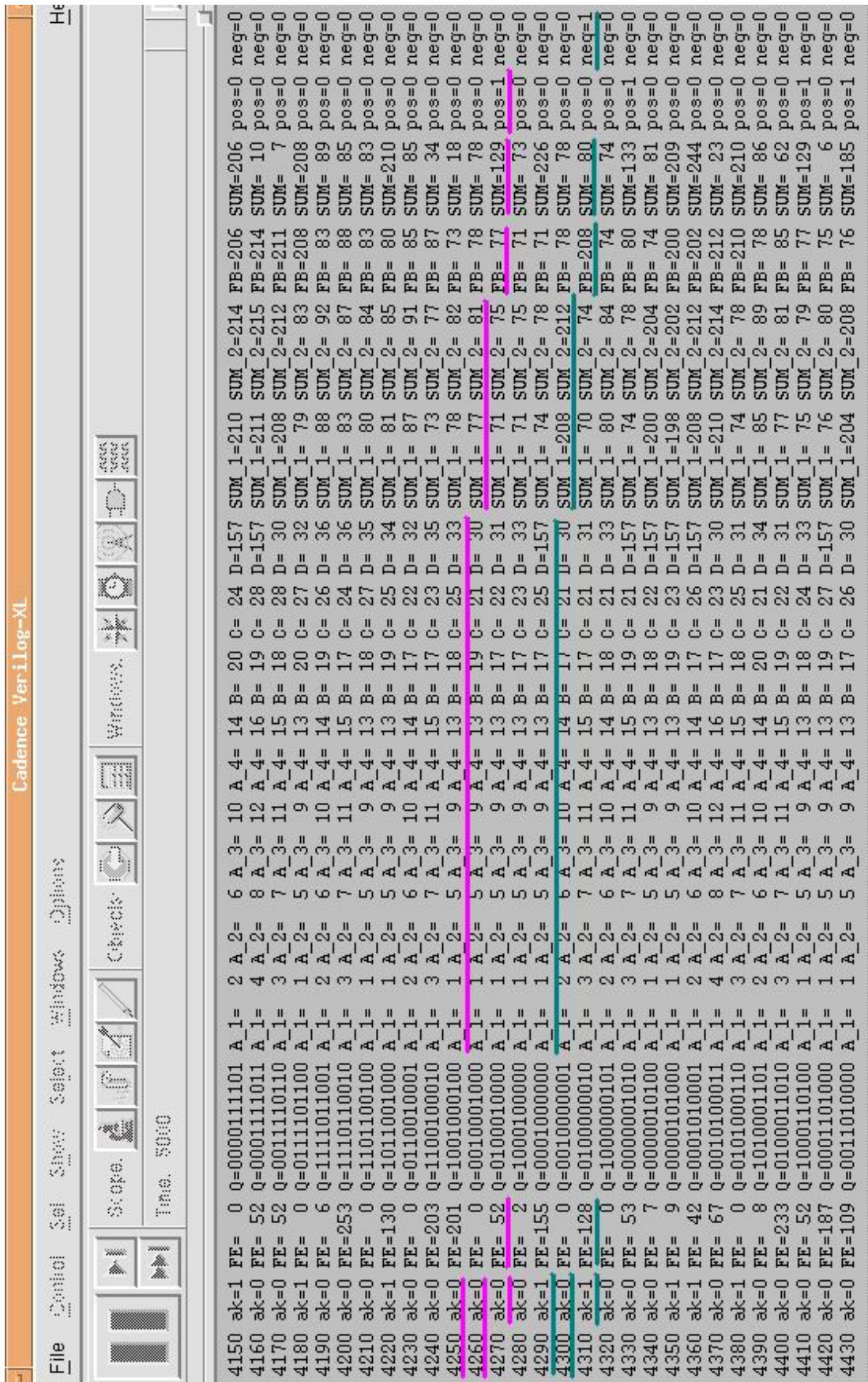


Figure.3-11 FBE functional simulation data (for Group-B)

3.8.2 Data Analysis of Group-B

◆ Typical Case.5 *Positive Overflow;*

At time $k = 4250$, $A_1=1$, $A_2=5$, $A_3=9$, $A_4= 13$, $B= 18$, $C=25$, $D=33$

At time $k+1 = 4260$, $a_k=0$, according to (3.1),

$$SUM_1_{k+1} | (a_k=0, a_{k+1}=0) = 1+18+25+33 = 77$$

$$SUM_2_{k+1} | (a_k=0, a_{k+1}=1) = 5+18+25+33 = 81$$

At time $k+2 = 4270$, $a_{k+1}=0$, according to (3.3),

$$FB_{k+2}/(a_{k+1}=0) = SUM_1_{k+1}= 77$$

In the meanwhile, $FE_{k+2} = 52$, according to (3.4),

$$SUM_{k+2}= 52+77 = 129$$

There is a positive overflow (**pos=1**), so according to (3.6),

$$a_{k+1} = 0;$$

◆ Typical Case.6 *Negative Overflow;*

At time $k = 4290$, $A_1=1$, $A_2=5$, $A_3=9$, $A_4= 13$, $B= 17$, $C=25$, $D=157$

At time $k+1 = 4300$, $a_k=1$, according to (3.2),

$$SUM_1_{k+1} | (a_k=1, a_{k+1}=0) = 9+17+25+157 = 208$$

$$SUM_2_{k+1} | (a_k=1, a_{k+1}=1) = 13+17+25+157 = 212$$

At time $k+2 = 4310$, $a_{k+1}=0$, according to (3.3),

$$FB_{k+2}/(a_{k+1}=0) = SUM_1_{k+1}= 208$$

In the meanwhile, $FE_{k+2} = 128$, according to (3.4),

$$SUM_{k+2}= 128+208 = 80$$

There is a negative overflow (**neg=1**), so according to (3.6),

$$a_{k+1} = 1;$$

From the analysis with the 6 typical cases, we could get conclusion that it is a good functional simulation with correct logic verification.

3.9 IC Structure

The schematic view of the synthesized FBE is shown in Figure.3-12. The entire FBE structure is composed by 4 functional sub-modules, namely, SFT_11, LOCKUP, PIPE and FEEDBACK.

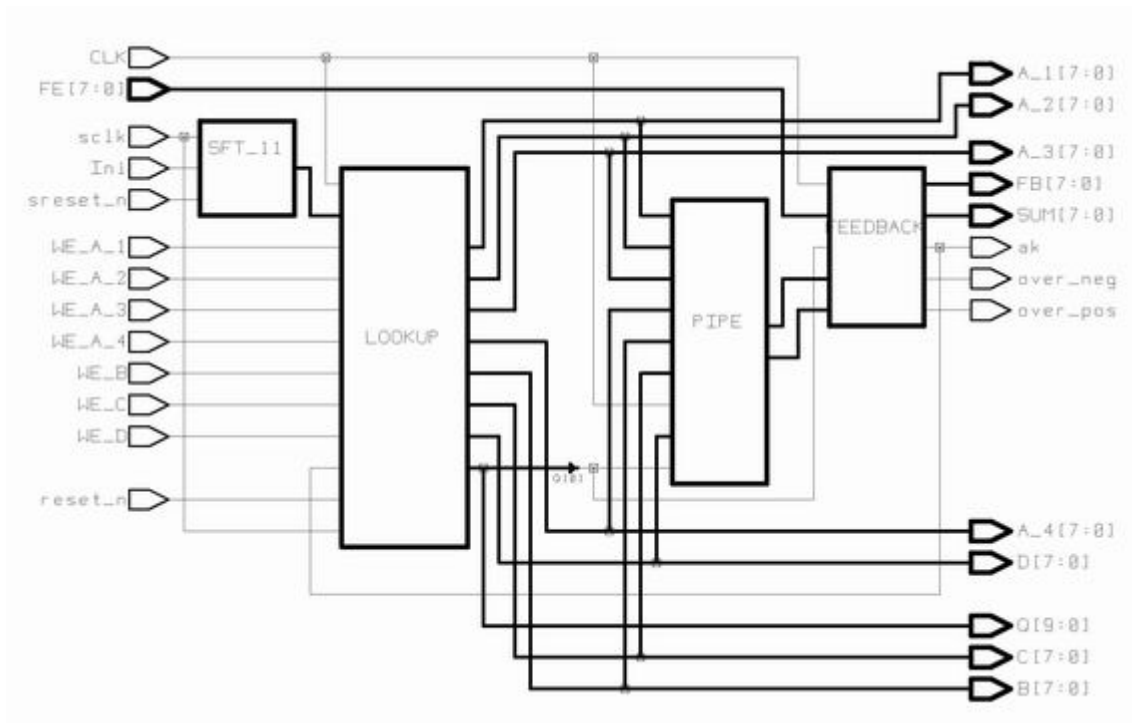


Figure.3-12 Schematic View of FBE

3.9.1 SFT_11

This module is a “Series-to-Parallel Converter” which is required for SRAM’s initialization. In the earlier description, the largest SRAM in the FBE is $2^3 \times 8$, which means that its address width is 3 bits and the data width is 8 bits. Therefore, an 11-bit

parallel data is needed to initialize the SRAM with the pre-determined lookup table values. In other words, 11 I/O pads are needed for this purpose. To reduce the number of pads, a series data input is chosen.

Figure.3-13 shows the port declaration of this module. “*Ini*” is the series input port and “*Initial_Data*” is the 11-bits parallel output port. There are 11 D-flip-flops in it to achieve the function as a “Series-to-Parallel Converter”.

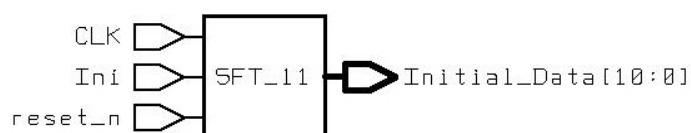


Figure.3-13 I/O description of module SFT_11

3.9.2 LOOKUP

This module contains 7 SRAM’s and 10 D-flip-flops which is just corresponding to the “Stage-1” section in Figure.3-9. Input a_k is the current decision bit generated by the critical loop itself, and the output Q is a 10-bit wide parallel data which present for the latest 10 decision bits latched in the D-flip-flop chains. In other words, it is Q that addresses SRAM2_A_1, SRAM2_A_2, SRAM2_A_3, SRAM2_A_4, SRAM2_B, SRAM3_C and SRAM3_D at the same time. Therefore, the outputs A_1 , A_2 , A_3 , A_4 , B , C , and D are the output data from those SRAMs at the current clock. The other input ports WE_A_1 , WE_A_2 , WE_A_3 , WE_A_4 , WE_B , WE_C , WE_D , and *Initial_Data* are used for SRAM initialization, and the port “*Initial_Data*” comes

from module SFT_11 and act as the address line for all SRAMs. Figure.3-14 gives the detailed schematic illustration of this module according to Figure.3-7.

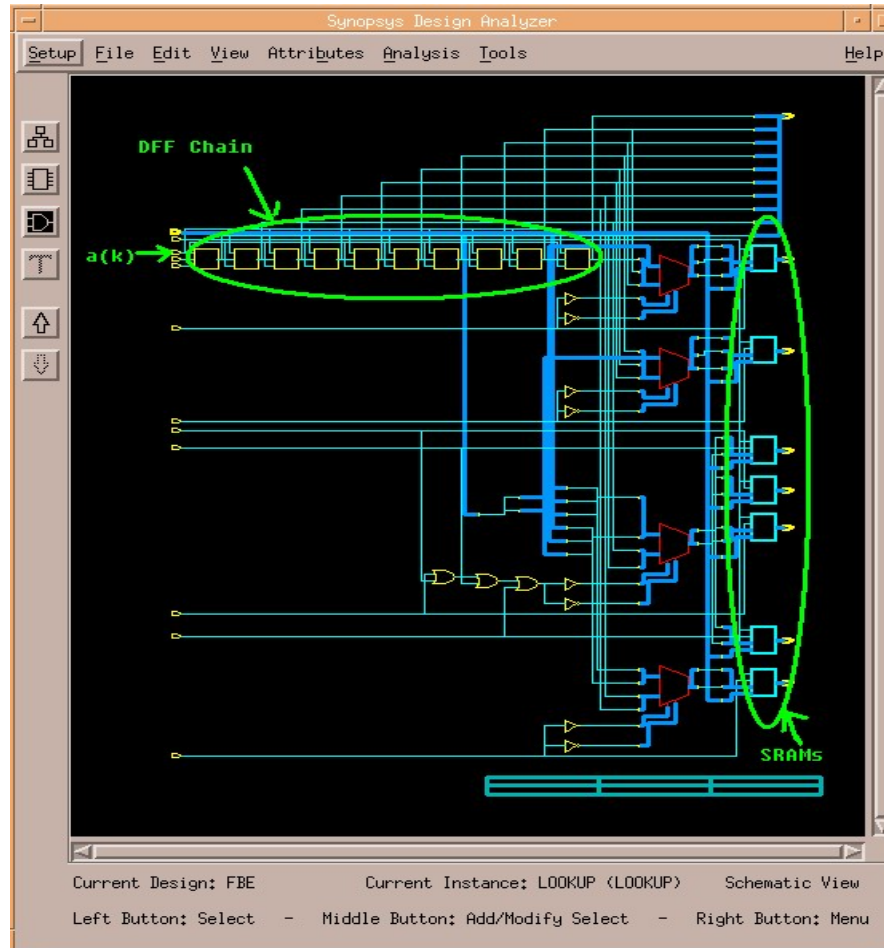


Figure.3-14 Schematic View of the Module LOOKUP

3.9.3 PIPE

This module is corresponding to the “Stage-2” section in Figure.3-9. At the 2nd clock, the output data from module LOOKUP arrives at module PIPE. At the same time, Q_0 represents a_k which is the lowest bit of Q and used as the selection bit for PIPE. The internal multiplexer will make the choice as to which data should be added up. The

summation result appears at the output ports, SUM_1 and SUM_2 . The detailed schematic view of PIPE block with reference to Figure 3-7 is given in Figure.3-15.

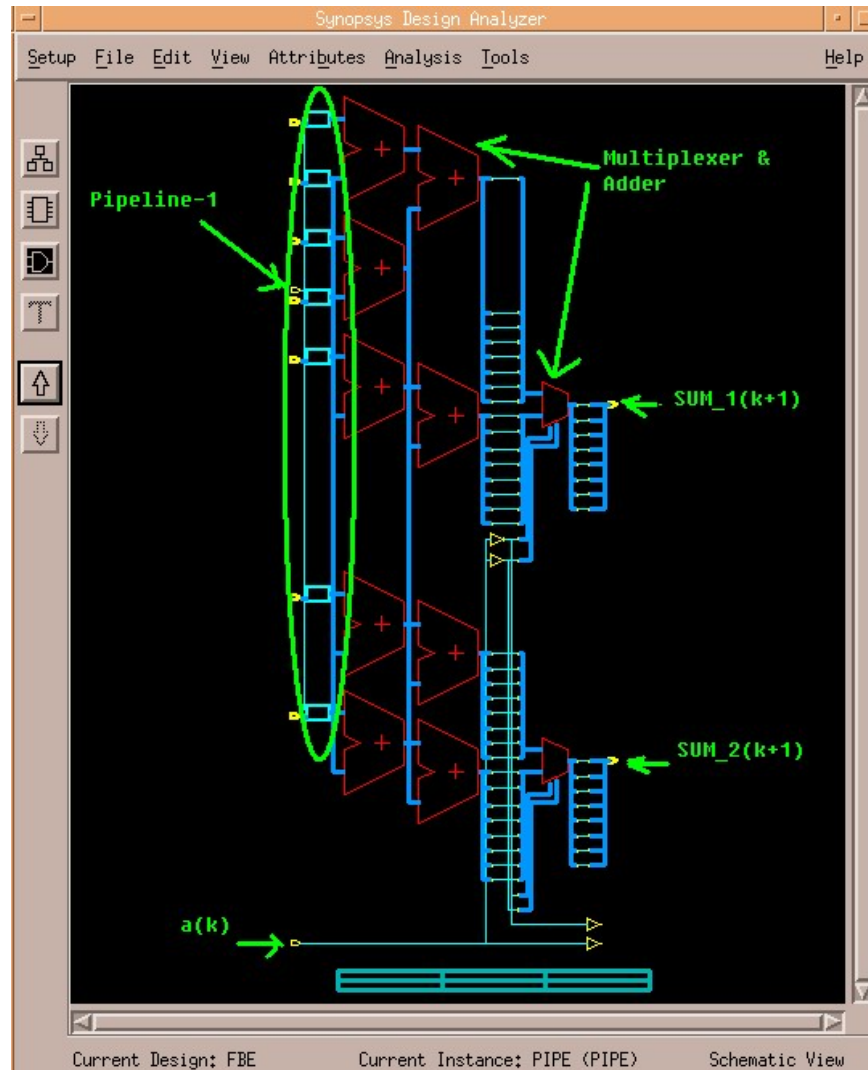


Figure.3-15 Schematic View of the Module PIPE

3.9.4 FEEDBACK

The module “feedback” is the last stage, or “Stage-3” section in Figure.3-9. At this stage, all of the former look up table value will be summed up and the output (FB) is an 8-bit wide parallel data. Similar to module PIPE, $Q0$ still acts as the selection bit

for the 2-to-1 multiplexer. The only difference is that at this stage $Q0$ represents a_{k+1} . The output from this stage, FB , will be summed with the data from the feed-forward equalizer, FFE. If there is no overflow, the decision bit a_{k+2} will then be generated. This decision bit is the final output of the entire MDFE. The detailed schematic view of the FEEDBACK block is referenced to Figure.3-16.

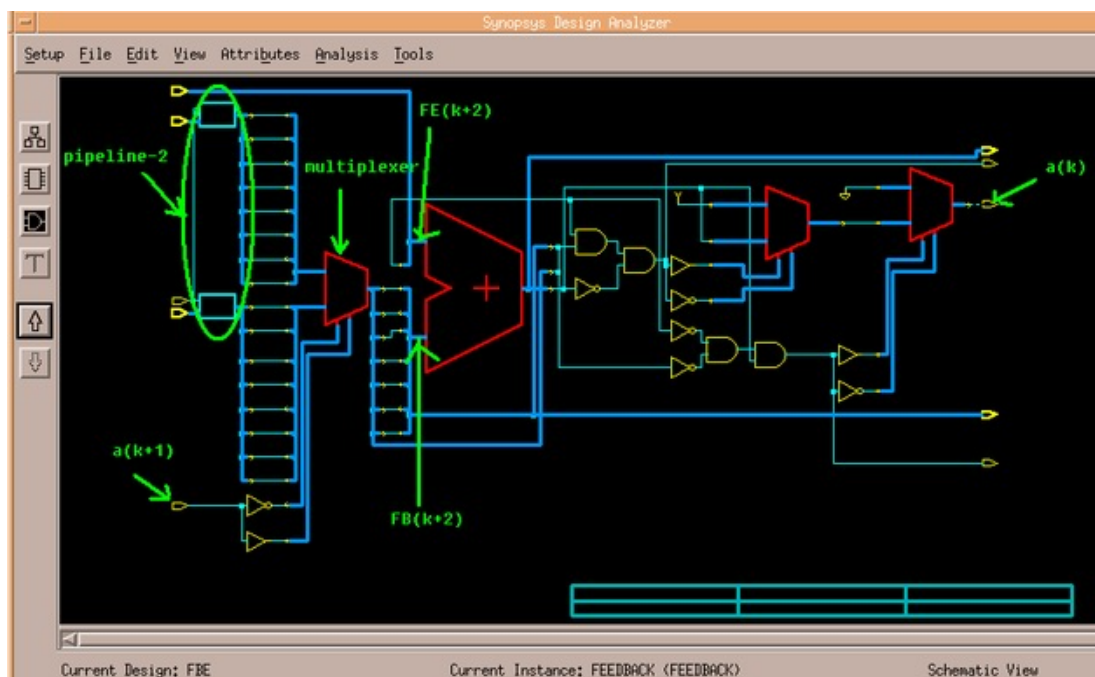


Figure.3-16 Schematic View of the Module FEEDBACK

3.10 Synthesis and Optimization

To transform the RTL codes into logic gates, an intermediate stage is needed as synthesis. The synthesis tool used is Design Analyzer [26] supplied by Synopsys. Design Compiler synthesizes a circuit with the targeted technology. Design Compiler

also optimizes logic designs for speed, area, and other factors. This optimization is performed for hierarchical combinational or sequential circuit design descriptions.

Figure 3-17 shows the flowchart of the logic synthesis process.

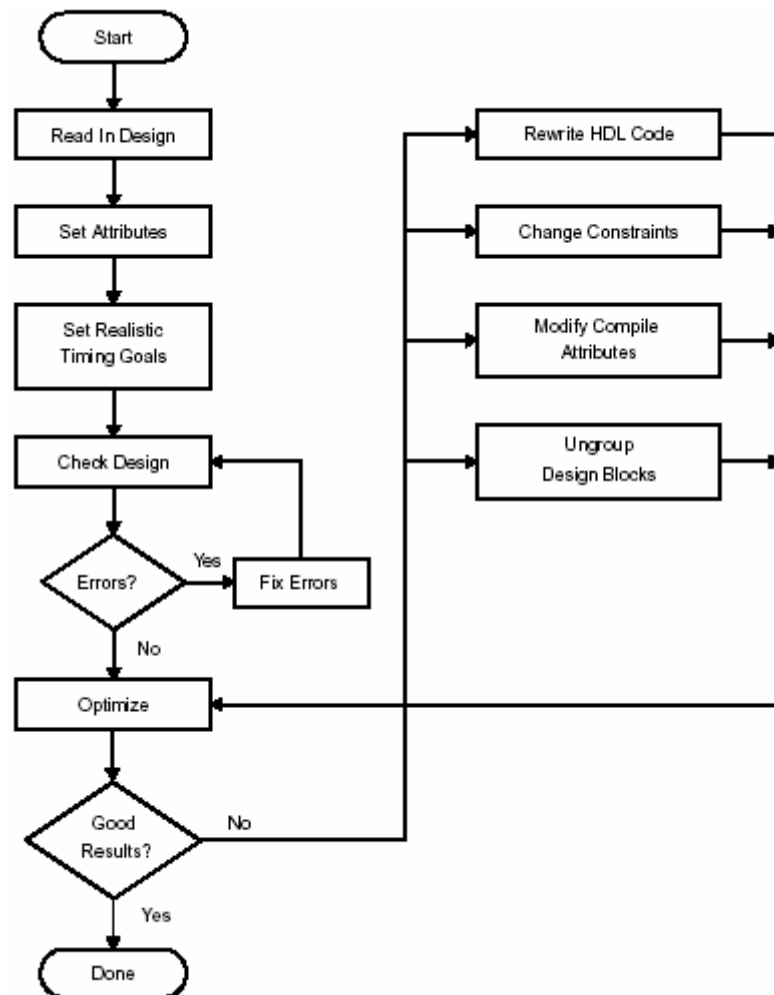


Figure.3-17 Logic Synthesis Flow Chart

3.10.1 Design Constraints

Design constraints [27] define the environmental attributes, timing, etc. and set the optimization goals for Design Analyzer to work at. The constraints used for this design are described below.

Synthesis Constraints for FBE:

• Clock Period:	5 ns
• Clock Uncertainty:	0.3 ns
• Input Delay (max):	2 ns
• Output Delay:	0
• Operating Conditions:	Typical (Library: csx_HRDLIB)
• Wire Load Model:	10k
• Output Load:	2 pf

a). **Clock** ----- Synchronous design is constrained by specifying the system clocks.

This is done by the “create_clock” command in the script. There are two Synchronous clock inputs, CLK and sclk, in this design. CLK is for the critical loop and sclk is for the SRAM’s initialization. In order to obtain an operating frequency of 200MHz (which is over the spec of 150MHz), here both of them are defined as **5ns**. However, these two values can be set differently for these two clocks. In addition to the clock period, the clock skew also needs to be specified. “set_clock_uncertainty” command sets clock skew attributes on clock objects or flip-flop clock pins. This command sets the clock skew values for all flip-flops and latches in the transitive fan-out of the specified clocks, ports, or pins. In this design, both clock skews are set to **0.3ns** according to the datasheet of AMS 0.35 μ m technology.

b). **Operating Condition** ----- In most technologies, variations in operating conditions, such as temperature, supply voltage and the manufacturing process, can strongly affect circuit performance (speed). Most technology libraries have predefined sets of operating conditions, timing ranges, and wire load models. The Design

Compiler timing analyzer uses this library information when performing a static delay analysis. To ensure that acceptable performance levels are maintained over a range of operating conditions, optimization is carried out within the specified operation conditions.

In this design, the operating condition is set as “**TYPICAL**” case, which means that the supply voltage is 3.3V, the process (scaling factor to account for variations in the semiconductor manufacturing process) is as default as 1.00, the temperature is 25.00 °C, and the interconnect model (tree_type for driving pins and network loads) is also as default as the balanced case. Apart from the typical case, the simulations are also done for different corners, such as **WORST** case and **BEST** case, and the report could be found in Table.3-5 at the end of this chapter.

c). **Wire Load Mode** ----- Design Compiler uses wire load models to estimate the resistance, capacitance, and area of nets before floor planning or layout. The wire load models, provided by the technology library, define a fanout-to-length relationship, and the “fanout” is the total number of pins on the net excluding the driver pin. If Design Compiler encounters a fanout count greater than the largest fanout_length pair, it uses the **slope** value to extrapolate the wire length. In AMS’s technology library csx_HRDLIB.db, 10k, 30k and 100k are three types of wire load model,

Normally Design Compiler will automatically pick the correct wire load model based on area. According to this design (core area = 0.33 mm²) which was mentioned before,

model **10k** is then be chosen as the max wire load model.

e). **Input Delay** ----- The “set_input_delay” command sets input path delays and input ports relative to a path edge. Input delays are used to model the external delays arriving at the input ports of the constrained module. These delays are defined relative to a real or virtual clock and are specified to the right of the active clock edge. For this design with the clock period of 5ns, the input delay is typically no more than **2ns** for all the input ports.

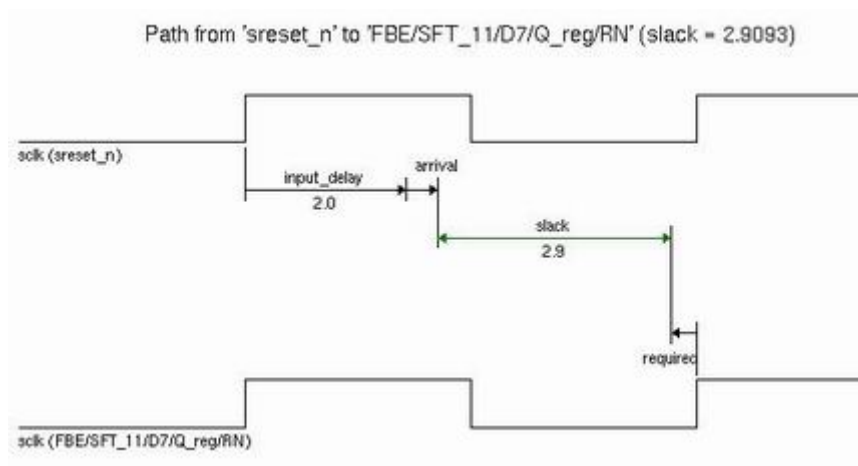


Figure.3-18 Waveform of Input Delay

Figure.3-18 shows that for the path that starts from the point “sreset_n” and end at the point “FBE/SFT_11/D7/Q_reg/RN”, the clock (sclk) period is 5ns and the input delay is 2.0ns. Data arrives within the required time and the slack is 2.9ns.

f) **Output Delay** ----- Output delays are used to model the external delays leaving the output ports of the constrained module. Output delays must be defined relative to a

real or virtual clock to be considered a path constraint. Output delays are defined to the left of the active clock edge; this delay corresponds to the time before the next rising edge. In this design, the output ports are not driving any other subsequent blocks but are mainly for test purpose, so it is unnecessary to set output delay value. (The default value is **zero**)

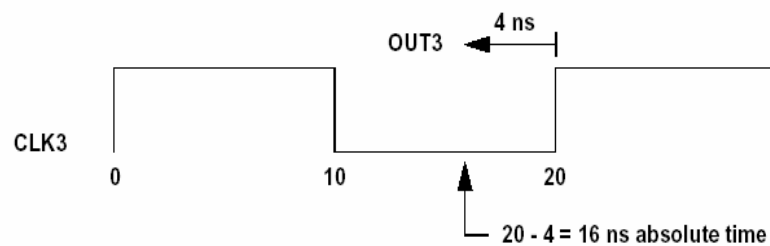


Figure.3-19 Waveform of Output Delay

In order to make it clear, Figure.3-19 shows an example of the output delay waveform. The clock period is 20ns, and the output delay is 4ns, so the absolute time should be no more than 16ns.

g) **Output Load** ----- The “set_load” command places a load on a port or a net. The units of this load must be consistent with the technology library. This value is used for timing optimizations, not for maximum fanout optimizations. Since during the test, the output ports drive the test instrument. With reference to our existing test instrument (Logic Analyzer) whose input capacitance is 2pF, the output load value here is set to **2pF**.

3.11 Optimization

Optimization (compiling) [28] is the step in the synthesis process that attempts to implement a combination of library cells that meets the functional, speed, and area requirements of the design. Optimization transforms a design into a technology-specific circuit based on the attributes and constraints placed on the design.

There are several ways to achieve the same logic but use the different instances or different structure. If the design is mainly concerned with the SPEED, more complicated instances, such as parallel structures, could be used instead of simple ones. If the design is mainly concerned with the CHIP AREA, simpler instances should be taken though the speed may be degraded.

To account for the inaccuracy of the modeling and other unpredicted effects and ensure that the specifications are met, the system is sometime over constrained. Over constraint is to constrain the design more than it is required by the specifications. The disadvantage of this method is that under the over constraint condition, the area of the design may be larger than what it is required and more resources are used. Thus a trade-off is needed.

Once all of the initial steps are completed the optimization can be executed. Different options allow further control of this process. In hierarchically structured systems, the

option "boundary optimization" is of importance. Activating this option allows the optimization to take place across module boundaries and permits the inversion of port signals.

Another parameter controlling the relative amount of CPU time spent during the mapping phase is the "map effort". By specifying '-map_effort low', it takes the least time to compile but could only run a test to check the logic. Low is not recommended if the design must meet timing or area goals. On the other hand, using the option '-map_effort high' can produce better designs. The mapping process proceeds until it has tried all strategies. However, high forces the tool to exhaust all possible strategies for the optimization, so it takes significantly longer time to compile. Normally, "-map_effort medium" is used as the default setting because Design Compiler tries to find a good mapping but does not use some CPU-intensive strategies. Medium is appropriate for getting a quick idea of how large a circuit will be, and it is used for most cases, also in this design.

When the optimization is done, the design will be synthesized to the gate level and mapped into a gate-level netlist.

3.12 Static Time Analysis

Static timing analysis is an exhaustive method of analyzing, debugging, and validating design performance. First, a design is analyzed and then all possible paths are timed (without enumerating individual paths) and checked against the requirements. The advantages of using this method are fast operation and identification of critical paths. For some tools such as PrimeTime [29] the disadvantages of using this method are that false paths are often identified as being in violation and static-timing analysis is typically restricted to the synchronous portions of a design.

The EDA tool used for static time analysis in this project is Primetime, a stand-alone, full-chip, gate-level static timing analyzer from synopsys. PrimeTime performs timing analysis at the gate level and provides a comprehensive set of modeling technologies for representing non-synthesized blocks for analysis. This technology includes three elements which are stamp modeling language, model extraction, and quick timing models. It provides functions to support both top-down and bottom-up design methodologies. The PrimeTime is a static timing analyzer, which means that it does not activate the circuit with many input vectors and measure the delay. Instead, it uses a library which contains timing information about these standard cells, identifies all the paths in the design, and finds out the critical path (maximum worst case delay from input to output). In this sense, it is "static".

3.12.1 PrimeTime Timing Analysis Flow and Methodology

As was shown in Figure.3-20, the PrimeTime user flow follows these general steps:

- ◆ Read and link the designs and libraries;
- ◆ Specify the attributes, environment, constraints, and timing exceptions, including wire load models or annotated delays or parasitics; port drive and capacitance; clocks; latches; uncertainty; input and output delay; and false and multicycle paths;
- ◆ Perform analysis and create reports;
- ◆ (Optional) Budget the design or characterize the context and write a script for Design Compiler, and perform mode analysis and case analysis.

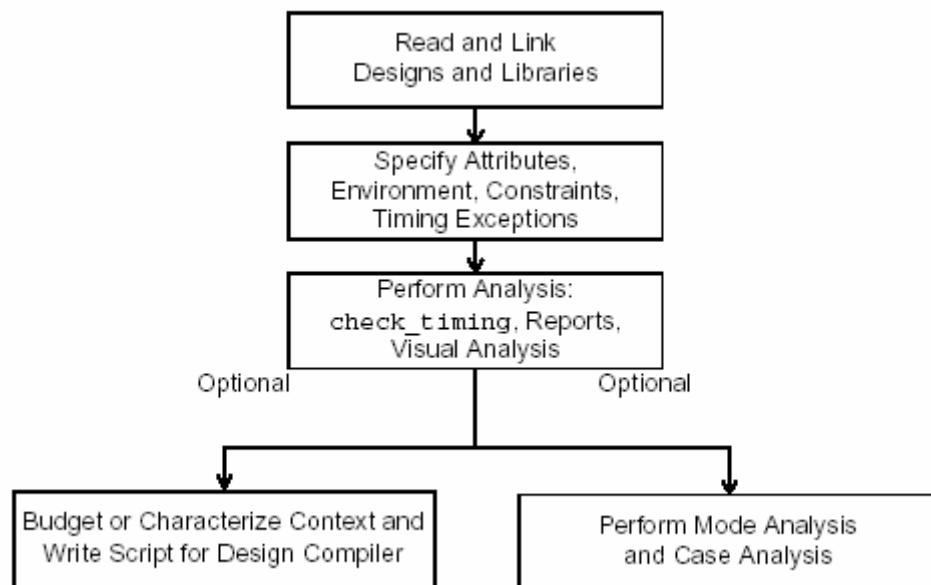


Figure.3-20 User flow of Primetime

3.12.2 Analysis and Reports.

Followed by the steps above, the static timing analysis was carried out. the results will be discussed and analyzed in this section.

(a). Design Information

Design information reports show information about objects and assertions within a design. It provides a summary of the current design attributes, including

- ◆ Analysis type
- ◆ Operating conditions
- ◆ Wire load models
- ◆ Design rules

In this design, the summary of the design information of **FBE** is reported as below.

```
report_design -nosplit
*****
Report : design
Design : FBE
Version: 2001.08-SP1
Date   : Mon May 17 16:43:52 2004
*****

Design Attribute          Value
-----
Operating Conditions:
  analysis_type           single
  operating_condition_max_name TYPICAL
  process_max             1
  temperature_max         25
  voltage_max             3.3
  tree_type_max           balanced_case

Wire Load:                (use report_wire_load for more information)
  wire_load_mode          enclosed
  wire_load_model_max     10k
  wire_load_model_library_max csx_HRDLIB
  wire_load_selection_type_max user-specified
  wire_load_selection_group_max sub_micron
  wire_load_min_block_size 0

Design Rules:
  max_capacitance        ---
  min_capacitance        ---
  max_fanout              ---
  max_transition          ---
  max_area                ---

Timing Ranges:
  fastest_factor          ---
  slowest_factor          ---

1
pt_shell>
```

(b). *Timing Checks Coverage*

The default report is a summary of checks by type. The report shows for each type of check (setup, for example) the number and the percentage of checks that meet constraints, violate constraints, and are untested. Static timing is considered exhaustive—all paths are checked, and so forth. However, if the assertions are incomplete or if paths are disabled (using false paths, disabled arcs, case analysis, and so forth), some timing checks are not tested.

```

|report_analysis_coverage
|*****
Report : analysis_coverage
Design : FBE
Version: 2000.11-SP1
Date   : Wed Oct 29 17:40:40 2003
|*****

```

Type of Check	Total	Met	Violated	Untested
setup	1245	669 (54%)	0 (0%)	576 (46%)
hold	1533	668 (44%)	0 (0%)	865 (56%)
recovery	309	21 (7%)	0 (0%)	288 (93%)
removal	21	0 (0%)	0 (0%)	21 (100%)
min_pulse_width	1071	762 (71%)	0 (0%)	309 (29%)
All Checks	4179	2120 (51%)	0 (0%)	2059 (49%)

```

1
primetime>

```

From the above report of coverage, we could get that there is no violated case in setup or hold time. There are also some untested paths for there may be some disabled arcs.

(c). *Constraint Violations*

It is a summary of the constraint violations in the design, including the amount by which a constraint is violated or met and the design object that is the worst violator. PrimeTime can report on the maximum area of a design and certain timing constraints. It can also verify whether the netlist meets specific pin limits.

```

*****
Report : constraint
Design : FBE
Version: 2000.11-SP1
Date   : Tue Oct 28 20:17:21 2003
*****

```

Group (max_delay/setup)	Cost	Weight	Weighted Cost
CLK	0.00	1.00	0.00
sclk	0.00	1.00	0.00

max_delay/setup			0.00

Group (min_delay/hold)	Cost	Weight	Weighted Cost
CLK	0.00	1.00	0.00
sclk	0.00	1.00	0.00

min_delay/hold			0.00

Constraint	Cost

max_delay/setup	0.00
min_delay/hold	0.00
recovery	0.00
sequential_clock_pulse_width	0.00
max_capacitance	0.00
max_transition	0.00

1

If there are violations been found, the value of Cost will not be zero. The above report shows that there is no any violation of the constraint in this design.

(d). Path-Based Timing

A path timing report provides detailed timing information about any number of requested paths. It reports the longest maximum path in the design for each path group. Typically, use this to measure paths for setup timing.

- ◆ Gate levels in the logic path
- ◆ Incremental delay value of each gate level
- ◆ Sum of the total path delays
- ◆ Amount of slack in the path
- ◆ Source and destination clock name, latency, and uncertainty

This report shows the path with the worst slack for each path group based on maximum delay. The clock period here is 5ns. In Figure.3-21, the “max_path” report

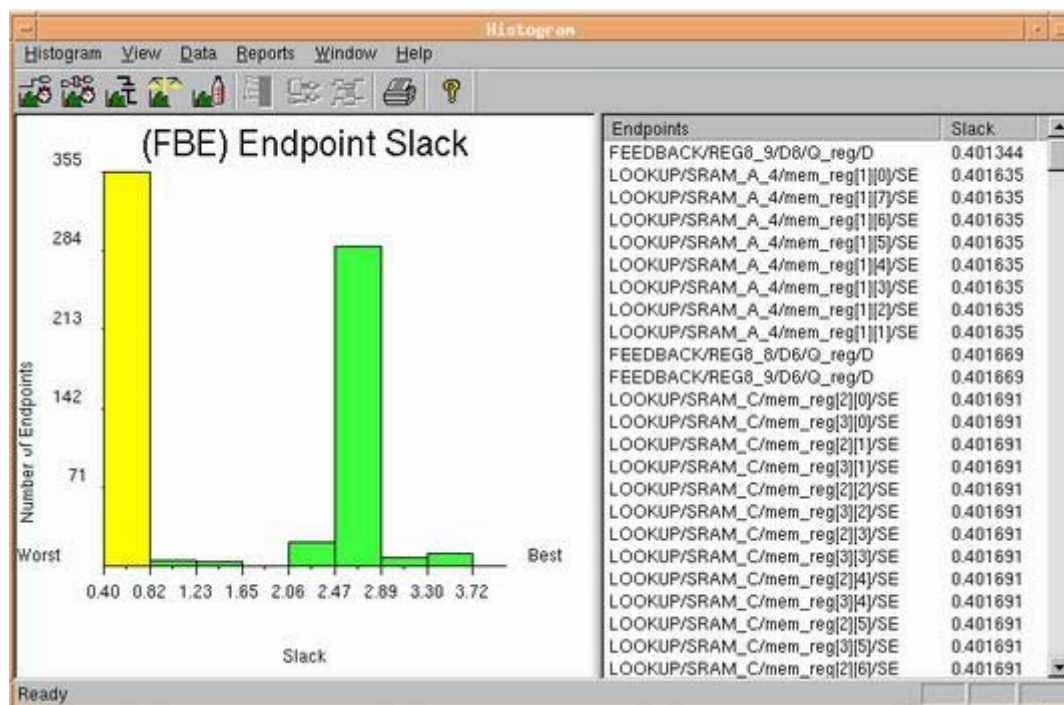


Figure.3-21 Histogram of path timing analysis

is shown as histogram. It reports all the max paths in FBE and lists them in groups.

The longest path (**critical path**) can be extracted from this report as follows:

Startpoint: PIPE / REG8_5 / D4 / Q_reg

Endpoint: FEEDBACK / REG8_9 / D8 / Q_reg

Slack: 0.40 ns (MET)

From the reports obtained during the static timing analysis, there is no coverage or constraint violations, and a MET slack of 0.40 means that the design fulfills the timing constraints (clock period is 5ns, clock rate is 200MHz). So the optimization to the design is successfully fulfilled the spec of 150MHz. The performance of FBE is listed in Table.3-7, and the detailed reports of timing, area, and dynamic power are in Appendix.B.4, B.5, and B.6.

Table.3-7 Performance summary of FBE (Structure-IV)

	FBE
Supply Voltage (V)	3.3
CMOS Technology (μm)	0.35
Speed in BEST case (MHz)	270
Speed in TYPICAL case (MHz)	200
Speed in WORST case (MHz)	130
Core Area (mm^2)	0.33
Dynamic Power (mW)	43.86

Chapter 4 Implementation of FFE

4.1 Introduction to the Feed-forward Equalizer

The feed-forward equalizer (FFE) is implemented as a fully digital 8-tap programmable FIR filter. The FIR is realized using the transposed form architecture. The multipliers are of parallel array type that uses radix-4 modified Booth encoding [19] and a carry save partial product reduction scheme. The accumulation of filter terms is performed in carry save format at each tap, with a pipelined carry propagate adder merging the carry and sum vectors after the last stage. To account for programmable coefficients, an 8×8 -bit SRAM is implemented to store the 8-tap coefficients. The speed of the filter is defined as the rate at which input samples can be processed. To increase the speed, it is necessary to reduce the critical path delay between input and output.

4.2 The Transpose Structure

Application of the transposition theorem [20] results in the transpose direct form structure as shown in Fig.4.1 in which input is fed to all of the coefficient multipliers in parallel and the results are accumulated over N sample periods, where N is the filter order. This structure retains the regularity of the linear accumulation direct form structure but has a delay equal to $T_m + T_a$, T_m is the multiplier delay and T_a is the

adder delay. Therefore, it is independent of the filter length.

One of the primary disadvantages of this structure is that the registers occur in the accumulation path and therefore must have the length of the internal word length of the filter rather than the possibly shorter input word length. This gives rise to the heavy loading on the clock buses. Another disadvantage is the large loading on the input data broadcast bus since all multipliers are fed in parallel. These are relatively minor problems, however, which may be partially reduced by appropriate buffering and by distributing the network in a tree-like structure.

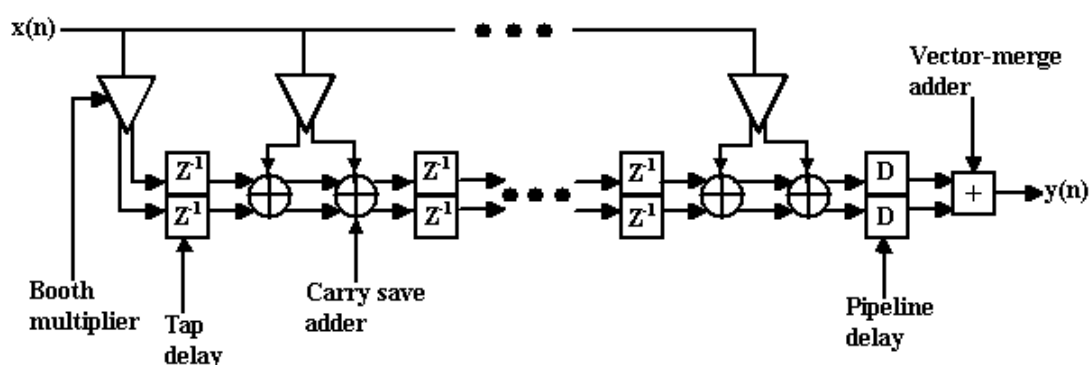


Figure.4-1 FIR filter architecture used for FFE

4.2.1 Booth Multipliers

The primary limitation in the achievable throughput in the transpose direct form structure is the multiplier delay. To speed up the multiplication delay, the multipliers used are parallel array multipliers that use radix-4 modified Booth encoding [19] and a carry save partial product reduction scheme.

The modified Booth algorithm is based on encoding the 2's complement operand (i.e. multiplier) in order to reduce the number of partial products to be added. This makes the multiplier faster and uses less hardware (area). For example, the radix-4 modified Booth algorithm is based on partitioning the multiplier into overlapping groups of 3-b, and each group is decoded to generate the correct partial product. A detailed explanation of the Booth algorithm can be found in [19]

4.2.2 Addition Implementation

The next limiting factor in the achievable throughput is due to the classic problem of carry propagation. The simple carry ripple adder circuit is limited by its ripple path delay which is proportional to the word length of the adder. To avoid the long critical path of the carry ripple adder, the adders in each tap position are converted to carry save adders.

A so-called vector-merge adder (VMA) [23] has to be used in the final stage to add the final sum and carry as shown in Figure.4-1. The VMA is really just a carry propagate adder. Since only one carry propagate adder is required, it is possible to use one of the more complex fast adder techniques without an excessive impact on the total area. A pipelined carry ripple adder is employed here for the VMA.

There are a few drawbacks to the carry save scheme, however, with the most

important of these being the negative impact of doubling the number of registers required within the filter core. This increase in area is a price that must be paid in order to achieve a high throughput which is the goal of this work.

4.2.3 Sign Extensions

With increasing parallelism, the amount of shifts between the partial products and intermediate sums to be added tends to increase. When obeying the rules of 2's complement arithmetic the sign bits of the numbers to be added have to be extended up to the most significant bit of the expected sum. This leads to a multiple and redundant addition of the most significant bits in each row of adders which further on leads to additional full adders per row. This slows down the circuit's speed and increases the layout area.

Hence, a modified 2's complement number representation is derived [21], this scheme is equal to a subsection of the algorithm already derived by Baogh-Wooley [22]. The modified 2's complement number representation together with algorithms for the simplified addition of 2's complement numbers [21] can eliminate the need of the common sign bit extension in additions so that all adder cells of the multiplier have the same load. This leads to an optimal transistor sizing and to an appropriate area reduction.

4.3 Implementation

The FFE implements two blocks as shown in Figure.4-2:

- Front-end
- Back-end

The front consists of an 11-bit shift-left register to shift the data in serially and an 8×8 -bit register-based dual-port SRAM to store the 8-tap coefficients. The back consists of the transposed-formed FIR filter described in the previous section. Table.4-1 is the description of the signals presented in Figure.4-2.

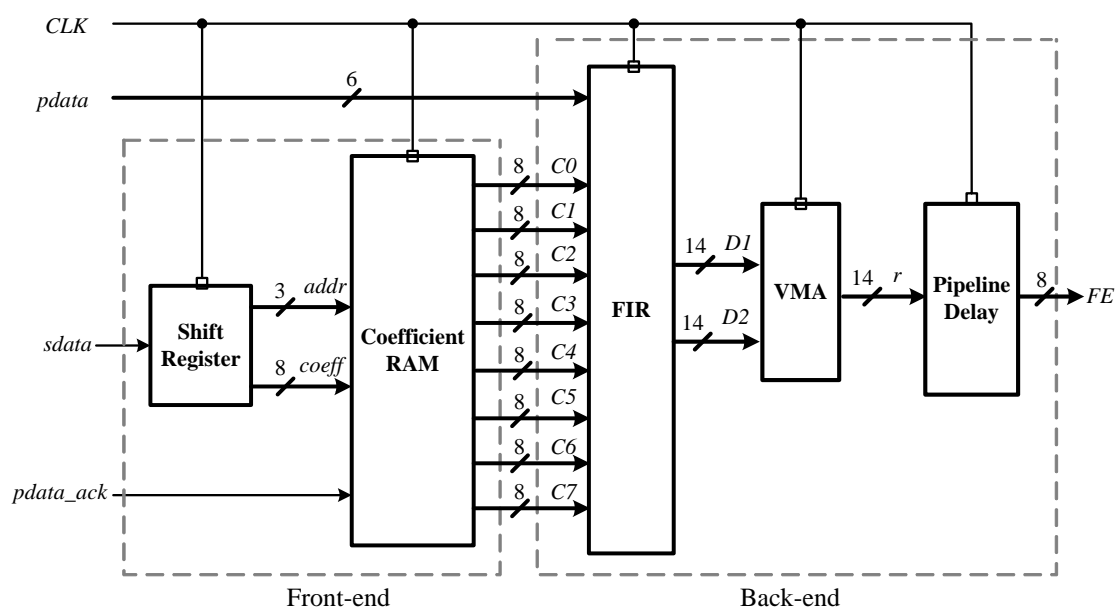


Figure.4-2 Block diagram of the Feed-forward Equalizer (FFE)

Table.4-1 Signal Description of FFE

Signal	width	I/O attribute	Description
CLK	/	Input	System clock
pdata_ack	1 bit	Input	Valid input data acknowledgement
pdata	6 bits	Input	Input data for FFE
sdata	1 bit	Input	Initialization data for the look-up-tables in FFE
addr	3 bits	Inter-connection	Address for the lookup table
coeff	8 bits	Inter-connection	Coefficient for the lookup table
C0	8 bits	Inter-connection	Coefficient for the 1 st tap
C1	8 bits	Inter-connection	Coefficient for the 2 nd tap
C2	8 bits	Inter-connection	Coefficient for the 3 rd tap
C3	8 bits	Inter-connection	Coefficient for the 4 th tap
C4	8 bits	Inter-connection	Coefficient for the 5 th tap
C5	8 bits	Inter-connection	Coefficient for the 6 th tap
C6	8 bits	Inter-connection	Coefficient for the 7 th tap
C7	8 bits	Inter-connection	Coefficient for the 8 th tap
D1	14 bits	Inter-connection	Data generated by the FIR
D2	14 bits	Inter-connection	Data generated by the FIR
r	14 bits	Inter-connection	Output from VMA
FE	8 bits	Output	Equalized output from FFE

4.3.1 Functional Verification of FFE

Figure.4-3 gives out the functional simulation result of FFE. From the data presented, we could get that there is totally 10 clock cycles to complete a full operation from input to output.

Before time **k = 4080**, $ack=0$;

There is no valid input data

At time **k = 4080**, $ack=1$;

With the first valid input data *pdata* (6-bit); No valid coefficient out yet.

At time $k+1 = 4090$, $ack=1$;

Coefficient C_0, C_1, \dots, C_7 is offered by the front end and sent to the back-end

At time $k+9 = 4170$ (after 8 taps), $ack=1$;

FIR gives the first output r (14-bit)

At time $k+10 = 4180$ (after a pipeline delay), $ack=1$;

FE (8-bit) is got, which is the first 8 bits of r .

```

4040 pdata= x ack=0 c0= x c1= x c2= x c3= x c4= x c5= x c6= x c7= x r= x FE= x
4050 pdata= x ack=0 c0= x c1= x c2= x c3= x c4= x c5= x c6= x c7= x r= x FE= x
4060 pdata= x ack=0 c0= x c1= x c2= x c3= x c4= x c5= x c6= x c7= x r= x FE= x
4070 pdata= x ack=0 c0= x c1= x c2= x c3= x c4= x c5= x c6= x c7= x r= x FE= x
4080 pdata=11 ack=1 c0= x c1= x c2= x c3= x c4= x c5= x c6= x c7= x r= x FE= x
4090 pdata=38 ack=1 c0=223 c1= 80 c2=179 c3=186 c4= 10 c5=127 c6=250 c7= 98 r= x FE= x
4100 pdata=37 ack=1 c0=223 c1= 80 c2=179 c3=186 c4= 10 c5=127 c6=250 c7= 98 r= x FE= x
4110 pdata= 0 ack=1 c0=223 c1= 80 c2=179 c3=186 c4= 10 c5=127 c6=250 c7= 98 r= x FE= x
4120 pdata=26 ack=1 c0=223 c1= 80 c2=179 c3=186 c4= 10 c5=127 c6=250 c7= 98 r= x FE= x
4130 pdata= 1 ack=1 c0=223 c1= 80 c2=179 c3=186 c4= 10 c5=127 c6=250 c7= 98 r= x FE= x
4140 pdata= 0 ack=1 c0=223 c1= 80 c2=179 c3=186 c4= 10 c5=127 c6=250 c7= 98 r= x FE= x
4150 pdata=26 ack=1 c0=223 c1= 80 c2=179 c3=186 c4= 10 c5=127 c6=250 c7= 98 r= x FE= x
4160 pdata=26 ack=1 c0=223 c1= 80 c2=179 c3=186 c4= 10 c5=127 c6=250 c7= 98 r= x FE= x
4170 pdata= 0 ack=1 c0=223 c1= 80 c2=179 c3=186 c4= 10 c5=127 c6=250 c7= 98 r= 1419 FE= x
4180 pdata= 3 ack=1 c0=223 c1= 80 c2=179 c3=186 c4= 10 c5=127 c6=250 c7= 98 r=13030 FE= 22
4190 pdata=63 ack=1 c0=223 c1= 80 c2=179 c3=186 c4= 10 c5=127 c6=250 c7= 98 r=12901 FE=203
4200 pdata= 0 ack=1 c0=223 c1= 80 c2=179 c3=186 c4= 10 c5=127 c6=250 c7= 98 r= 0 FE=201
4210 pdata=26 ack=1 c0=223 c1= 80 c2=179 c3=186 c4= 10 c5=127 c6=250 c7= 98 r= 3354 FE= 0
4220 pdata= 0 ack=1 c0=223 c1= 80 c2=179 c3=186 c4= 10 c5=127 c6=250 c7= 98 r= 129 FE= 52
4230 pdata=38 ack=1 c0=223 c1= 80 c2=179 c3=186 c4= 10 c5=127 c6=250 c7= 98 r= 0 FE= 2
4240 pdata=37 ack=1 c0=223 c1= 80 c2=179 c3=186 c4= 10 c5=127 c6=250 c7= 98 r= 3354 FE= 0
4250 pdata= 0 ack=1 c0=223 c1= 80 c2=179 c3=186 c4= 10 c5=127 c6=250 c7= 98 r= 3354 FE= 52
4260 pdata=26 ack=1 c0=223 c1= 80 c2=179 c3=186 c4= 10 c5=127 c6=250 c7= 98 r= 0 FE= 52
4270 pdata= 1 ack=1 c0=223 c1= 80 c2=179 c3=186 c4= 10 c5=127 c6=250 c7= 98 r= 387 FE= 0
4280 pdata= 0 ack=1 c0=223 c1= 80 c2=179 c3=186 c4= 10 c5=127 c6=250 c7= 98 r=16255 FE= 6
4290 pdata=26 ack=1 c0=223 c1= 80 c2=179 c3=186 c4= 10 c5=127 c6=250 c7= 98 r= 0 FE=253
4300 pdata=26 ack=1 c0=223 c1= 80 c2=179 c3=186 c4= 10 c5=127 c6=250 c7= 98 r= 3354 FE= 0

```

Figure.4-3 Functional simulation for FFE

4.3.2 Synthesis and Timing Analysis of FFE

The feed-forward equalizer (FFE) is also implemented as a digital, static CMOS

design, using 0.35 μ m, 3-layer metal process provided by AMS. As was introduced in Chapter 3, the constraints set for FFE are described below. All constraints are the same as those of FBE to achieve the same performance.

Synthesis Constraints for FFE:

• Clock Period:	5.0 ns
• Clock Uncertainty:	0.3 ns
• Input Delay (max):	2 ns
• Output Delay:	0
• Operating Conditions:	Typical (Library: csx_HRDLIB)
• Wire Load Model:	10k
• Output Load:	2 pf

But, according to the timing report, there are some violated paths which could not fulfill the timing constraints. The critical path is reported as below:

```
*****
Report : timing
Design : FFE
*****
Startpoint: front_end/RAM/h0_reg[1]
Endpoint:   back_end/tap0/q_S_reg[7]
Path Type:  max
```

Point	Incr	Path
clock CLK (rise edge)	5.00	5.00
clock network delay (ideal)	0.00	5.00
clock uncertainty	-0.30	4.70
back_end/tap0/q_S_reg[7]/C (DF8)	0.00	4.70 r
library setup time	-0.13	4.57
data required time		4.57
<hr/>		
data required time		4.57
data arrival time		-4.93
<hr/>		
slack (VIOLATED)		-0.35

To get the more detailed analysis of the critical path, a leaf diagram [29] is presented in Figure.4-4. The path delay caused by the front-end is 13.73% of 5.0ns, which is about 0.7ns. The rest of the path delay is caused by the back-end, which is about 4.3ns. The booth multiplier section takes the most partition. Thus the bottleneck is mainly caused by the booth multiplier.

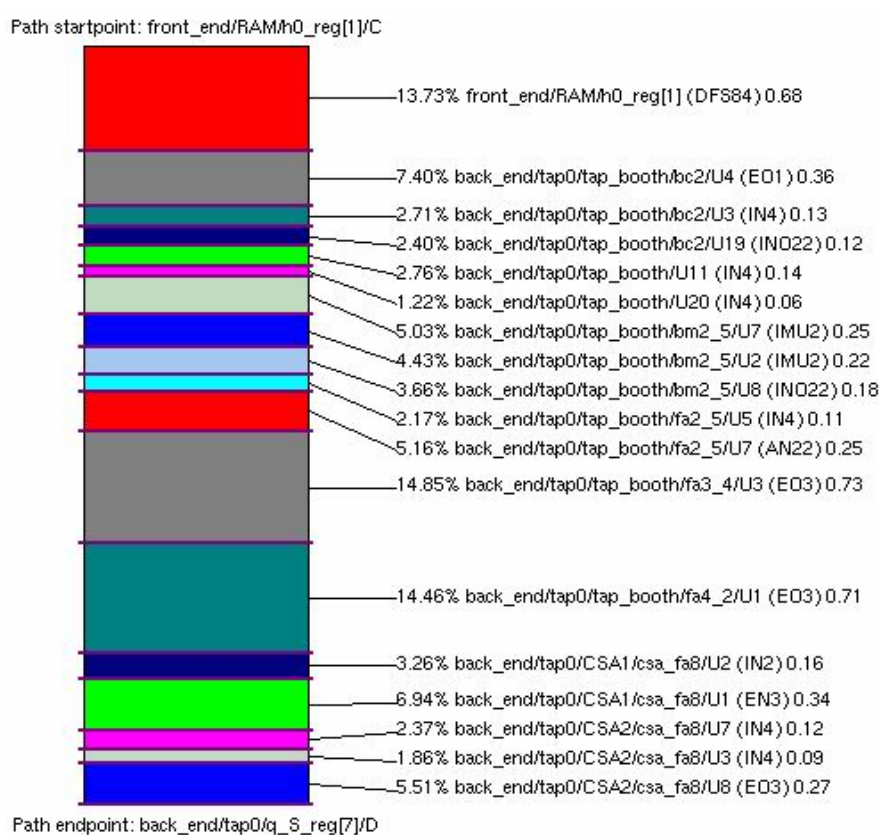


Figure.4-4 Leaf diagram of critical path in FFE

For the slack is only 0.35ns violated, we could first try a looser constraint with a new clock period without modifying the design structure:

• New Clock Period: 5.4 ns

The new timing report is got as below. In this case (clock period = 5.4ns), the slack is MET, so the clock rate could achieve **185MHz**, which is fulfill the spec (150MHz).

```

*****
Report : timing
Design : FFE
*****
Startpoint: front_end/RAM/h0_reg[1]
Endpoint:   back_end/tap0/q_S_reg[7]
Path Type:  max

Point                                          Incr      Path
-----
clock CLK (rise edge)                       5.40      5.40
clock network delay (ideal)                 0.00      5.40
clock uncertainty                           -0.30     5.10
back_end/tap0/q_S_reg[7]/C (DF8)           0.00      5.10 r
library setup time                         -0.13     4.97
data required time                          4.97
-----
data required time                          4.97
data arrival time                          -4.93
-----
slack (MET)                                 0.05

```

The performance is listed in Table.4-2. For this design the clock rate could reach 185MHz. The detailed reports of timing, area, and dynamic power are in Appendix.B.4, B5, and B6.

Table.4-2 Performance of FFE

	FFE
Supply Voltage (V)	3.3
CMOS Technology (μm)	0.35
Speed in BEST case (MHz)	250
Speed in TYPICAL case (MHz)	185
Speed in WORST case (MHz)	125
Core Area (mm^2)	0.68
Dynamic Power (mW)	45.20

Chapter 5 System Integration of the MDFE Chip

After the FBE and FFE are successfully synthesized and verified, this chapter will mainly deal with the system integration of the entire MDFE chip. In the following sections, the system-level design, functional verification, and the IC layout implementation will be presented.

5.1 System-Level Considerations

Apart from the direct integration of FFE and FBE blocks, the MDFE chip should provide an interface for the initialization data (filter coefficients) to be loaded prior to the operation of the equalizer. To reduce the pin counts, a series interface is chosen. Some test points may need to be inserted to test the functions of individual blocks. The block diagram of the MDFE chip is shown in Figure.5-1. The system is operated under a system clock, CLK . According to the specifications, the input data to the FFE (also the input of MDFE chip) is 6-bit and the output of the FFE is an 8-bit parallel data that is fed to the FBE. SUM allows the observation of the summation result of FFE and FBE so that the functionality can be validated. a_k is the final output of the slicer, which is the sign bit of SUM . The 2-to-1 multiplexer inserted between the FFE and FBE enables the test of these two individual blocks. Table.5-1 is the detailed description of the signals in the system.

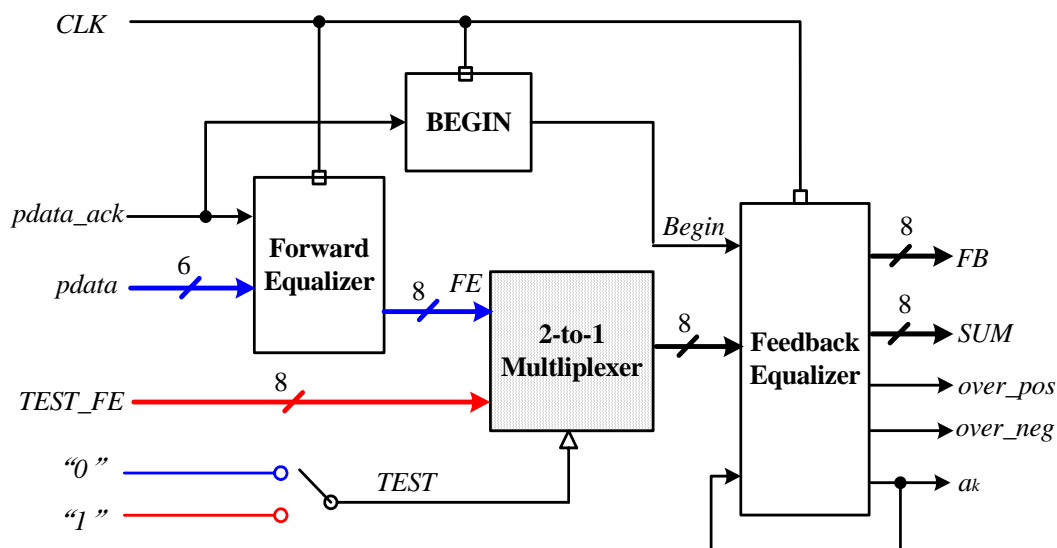


Figure.5-1 Block diagram of the MDFE chip

Table.5-1 Signal Description of the MDFE chip

Signal	width	I/O attribute	Description
CLK	/	Input	System clock
pdata_ack	1 bit	Input	Valid input data acknowledgement
pdata	6 bits	Input	Input data for FFE
sdata	1 bit	Input	Initialization data for the look-up-tables in FFE
Ini	1 bit	Input	Initialization data for the look-up-tables in FBE
Begin	1 bit	Inter-connection	Valid data detection for FBE
FE	8 bits	Inter-connection	Output data from FFE / input data to FBE
FB	8 bits	Output	Output data from FBE
SUM	8 bits	Output	Summation of FE and FB
over_pos	1 bit	Output	Positive overflow detection
over_neg	1 bit	Output	Negative overflow detection
ak	1 bit	Output	Decision bit, output from the slicer

As described in Chapter 4, the output of the FFE will only be ready after 10 clock cycles from the time when FFE starts receiving valid input data. Therefore, section

FBE must know when it is the correct time to receive the data. The BEGIN block is inserted to coordinate this between the FFE and FBE. The input signal, *pdata_ack*, acknowledges the first valid data bit of FFE. After 10 clock cycles, the signal “*Begin*” is sent to FBE to stop its null cycling and begin to receive the valid input data.

5.2 Behavior Simulation of the MDFE Chip

To do the behavior simulation, hundreds of vectors are fed into FFE as the simulated input data (6-bit). Therefore, the coordination of the combined system could be verified through the output data such as *pdata_ack*, *FE*, *Begin*, and a_k .

Figure.5-2 gives out the direct logic relationship of the three sections in the combined system. The variables in the data list are defined as below:

- *Integer number*: system time
- *Y(pdata)*: 6-bits parallel input signal to FFE
- *ack(pdata_ack)*: valid-data detect signal in FFE / input signal to BEGIN
- *FE*: output signal from FFE / input signal to FBE
- *begin*: output signal from BEGIN / valid data detect signal in FBE
- *ak*: output signal from the slicer
- *Q*: 10-bit parallel signals of the D-flip-flop chain in FBE
- *A_1,A_2,A_3,A_4,B,C,D*: output signal from FBE
- *X1(SUM_1),X2(SUM_2)*: output signal from FBE
- *FB*: output signal from FBE
- *X(SUM)*: Summation of FB and FE
- *pos(over_pos)*: positive overflow detect signal
- *neg(over_neg)*: negative overflow detect signal

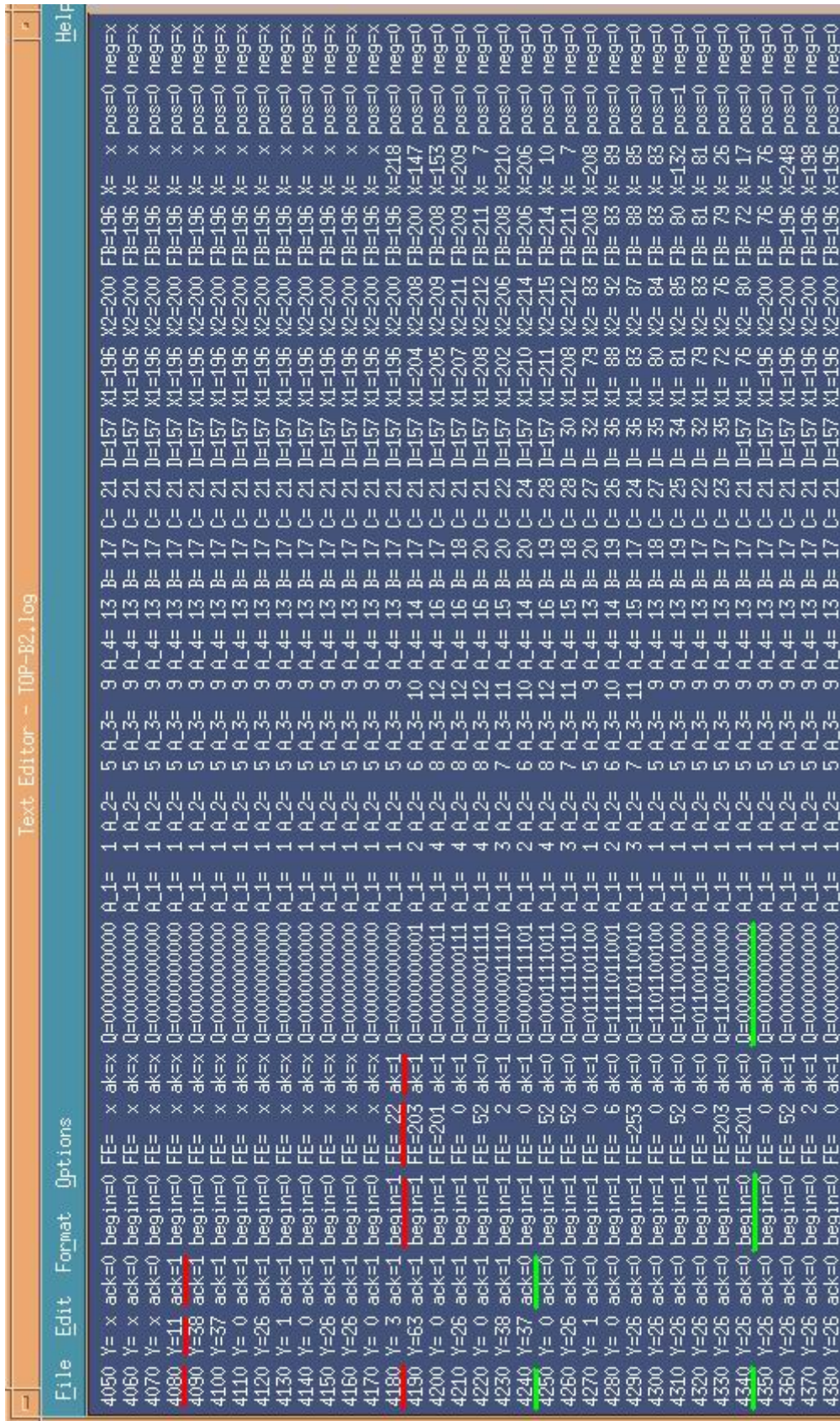


Figure.5-2 Functional verification of the MDFE chip

Table.5-2 is the data analysis for the typical cases in the functional verification according to the data listed in Figure.5-2.

Table.5-2 Data analysis for the MDFE chip

Time	ack	pdata	FE	Begin	ak	FBE
Before 4080	0	no valid data	no valid data	0	no valid data	NULL
4080	1	valid data	no valid data	0	no valid data	NULL
4180	1	valid data	valid data	1	valid data	in normal operation (run by Begin=1)
4240	0	no valid data	valid data	1	valid data	in normal operation
4340	0	no valid data	no valid data	0	no valid data	NULL (reset by Begin=0)
After 4340	0	no valid data	no valid data	0	no valid data	NULL

From the verification result in Figure.5-2 and the data analysis in Table.5-2, it can be seen that the block BEGIN works correctly in coordinating FFE and FBE. If there is no valid input data for FFE, FBE will wait in null cycling. When the valid input arrives, FBE will start to run in normal operation mode. For the same reason, when the operation is interrupted when there is no valid input data any more, FBE will stop receiving data from FFE and reset itself.

As the respective function of FFE or FBE was described before, here the data analysis is only concern with the coordination of the combined system.

5.3 System on Chip (SOC) Implementation of the MDFE Chip

For VLSI design, all the designs needed to be converted into transistor level in order to be fabricated on silicon. In this project, the Standard Cell approach is used to synthesize the design to layout. The generation of the whole layout can be easily done by the automatic layout tool – Silicon Ensemble (SE)-CADENCE [30]. With the help of the tool, it is only required to set the parameters for placement of the components and the routing of the wires, the rest will be taken care by SE to optimize the placement and routing of the design.

5.3.1 I/O Pins/Pads in the MDFE Chip

The detailed schematic illustrations of the signal ports and the interconnection of the MDFE system are shown in Figure.5-3 and Figure.5-4. Figure.5-3 is the overall system block diagram with all the I/O ports except those for testing, which is depicted in Figure.5-4.

As shown in Figure.5-3, there are totally 22 input pins and 110 output pins. If added with the pins of the testing port *TEST* and *TEST_FE*, which are 9, there will be $22+110+9=141$ I/O pins all together and that is too many for the chip.

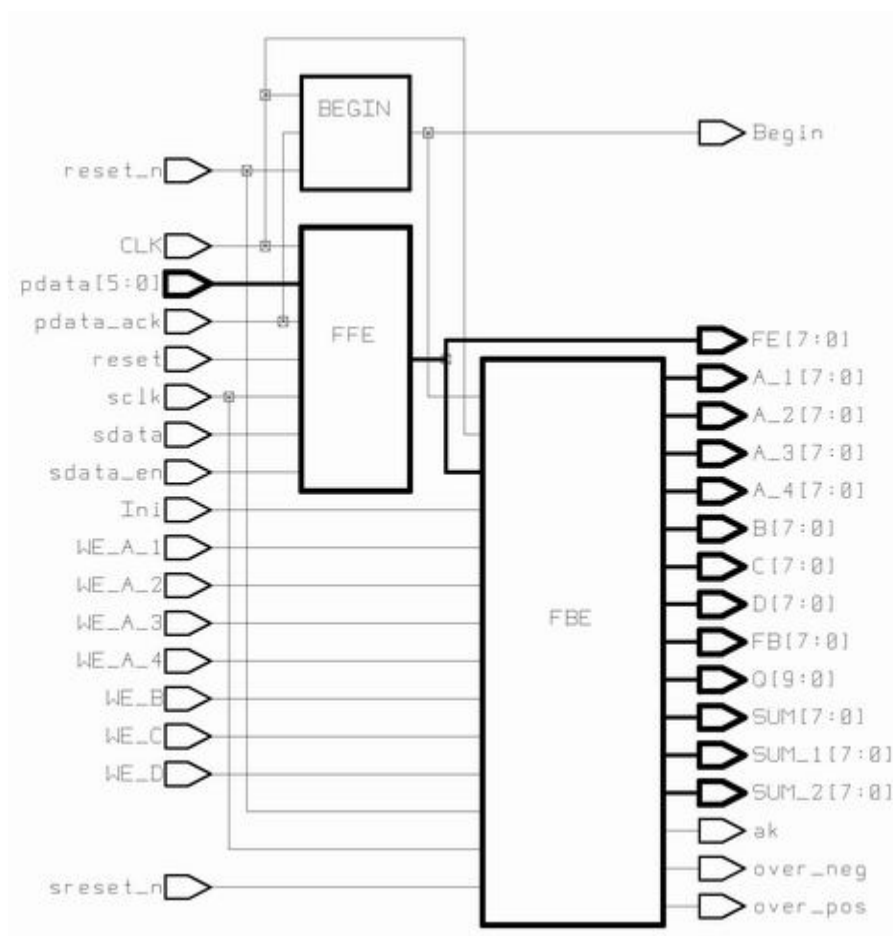


Figure.5-3 Schematic View of the combined system (full ports)

For the input ports are all compulsory in the functional operation, we could only reduce the optional output ports. As in Figure.5-4, ports FE, FB, a_k , $over_pos$ and $over_neg$ are kept and others are removed. As a result, there are 52 I/O pads left. Figure.5-5 shows the intended layout diagram of the chip with I/O pads (together with 2 power supply pads). Table.5-3 is the detailed description for each I/O port.

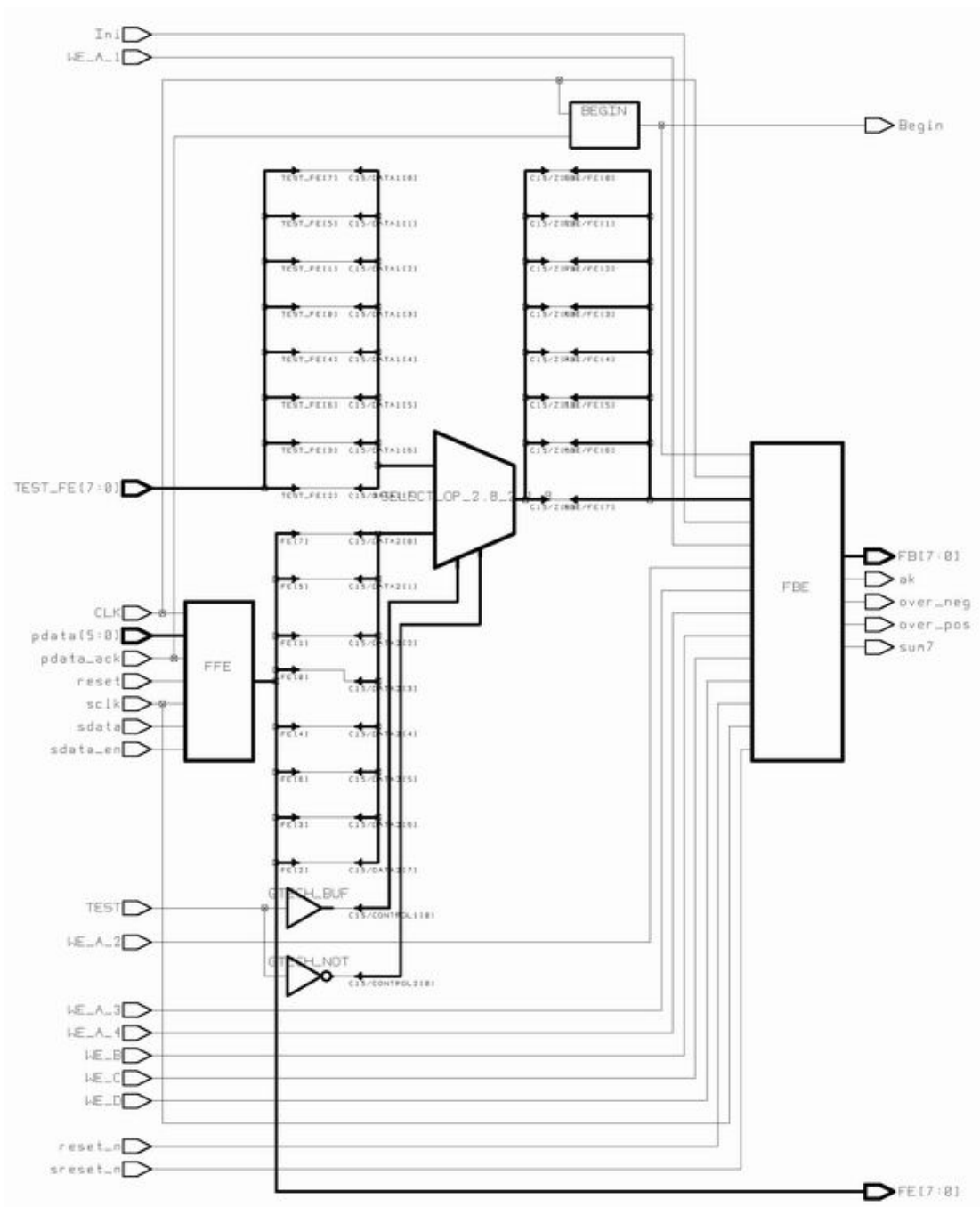


Figure.5-4 Schematic View of the combined system (partial ports)

Table.5-3 I/O Ports and Pads Description of the MDFE chip.

Input port	Width	Description	Pad Name
CLK	1	clock supply for the system	ICCK8P
Sclk	1	clock supply for SRAM's initialization	ICCK8P
reset	1	asynchronous reset for D flip-flops	ICUP
sdata	1	serial data for the initialization of the look-up-tables in SRAM's in FFE	ICUP
sdata_en	1	initialization enable	ICUP
pdata_ack	1	valid input data acknowledgement	ICUP
pdata	6	parallel input data	ICUP
reset_n	1	asynchronous reset for D flip-flops	ICUP
sreset_n	1	asynchronous reset for SRAM's initialization	ICUP
Ini	1	serial data for the initialization of the look-up-tables in SRAM's in FBE	ICUP
WE_A_1	1	write-enable to SRAM_A_1	ICUP
WE_A_2	1	write-enable to SRAM_A_2	ICUP
WE_A_3	1	write-enable to SRAM_A_3	ICUP
WE_A_4	1	write-enable to SRAM_A_4	ICUP
WE_B	1	write-enable to SRAM_B	ICUP
WE_C	1	write-enable to SRAM_C	ICUP
WE_D	1	write-enable to SRAM_D	ICUP
Test	1	test mode enable to FBE	ICUP
Test_FE	8	parallel test data as FE to FBE	ICUP
Vdd!	1	power supply (3.3V)	VDD3ALLP
Gnd!	1	ground	GND3ALLP
Output Port	Width	Description	Pad Name
FE	8	parallel output data from FFE	BU2P
FB	8	current feedback value	BU2P
sum_7	1	sign bit for the sum of FBE and FFE	BU2P
over_pos	1	sign bit for positive overflow	BU2P
over_neg	1	signal bit for negative overflow	BU2P
a _k	1	current decision bit	BU2P
Begin	1	valid data detection for FBE	BU2P

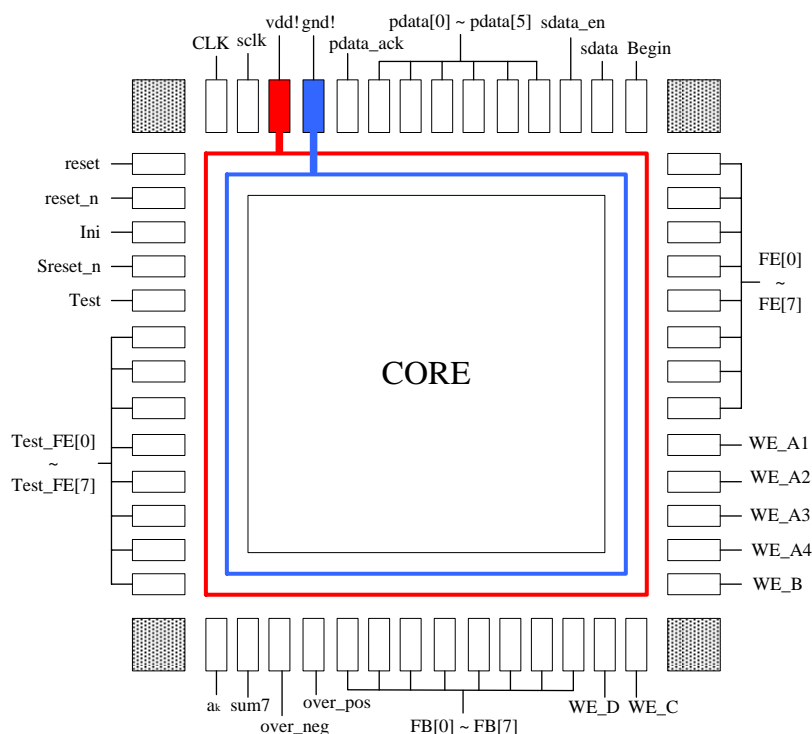


Figure.5-5 Diagram of the I/O pads of the chip

5.3.2 Constraints for the Synthesis

The constraints used for this design are described below. The *clock period* here is set as **5.8ns**, which aims to achieve the specific speed of **170MHz**. The *wire load model* is set as **30k** for the fanout is also increased. The detailed constraint script can be found in Appendix.B.1.

Synthesis Constraints for MDFE

• Clock Period:	5.8 ns
• Clock Uncertainty:	0.3 ns
• Input Delay (max):	2 ns
• Output Delay:	0
• Operating Conditions:	Typical (Library: csx_HRDLIB)
• Wire Load Model:	30k
• Output Load:	2 pf

5.3.3 Place and Route (LAYOUT)

The layout synthesis is done according to the design flow as Figure.5-6.

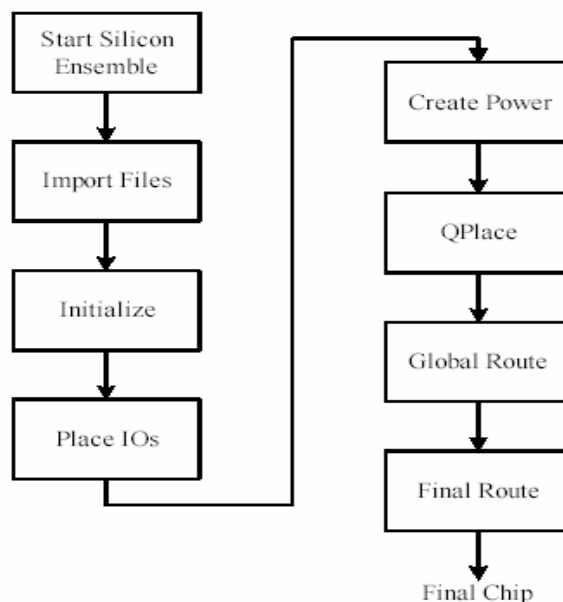


Figure.5-6 Flow chart of the layout process

The initialization step generates the floorplan for the chip. It is based on the given technology files and the netlist of the design. Beside these, the other parameters, such as the *IO-to-Core-Distance* and the *Row-Utilization(%)*, also need to be specified. These parameters will determine the size of the chip. In this design, the I/O-to-core-distance is set to **200** microns and the row utilization rate is **85%**.

For the placement of the I/O pads, it could either be done randomly around the all four edges by SE or by the user's specification. In this project, the latter is chosen.

The power lines are placed with the Core Ring Width set to **30** microns for MET1 and MET2, the Core Ring Space from core set to **10** microns, and the Block Ring offset set to **80** microns.

An important issue of the clock net design is buffering, which is necessary to control “clock skew” and delay. The clock skew is the maximum difference among the arrival times of the clock signals. The objective of clock net design is to select correct buffers in the *clock tree* so that the given constraint of the clock skew could be met and, at the same time, the clock delay (the maximum arrival time among clock signals) could be minimized.

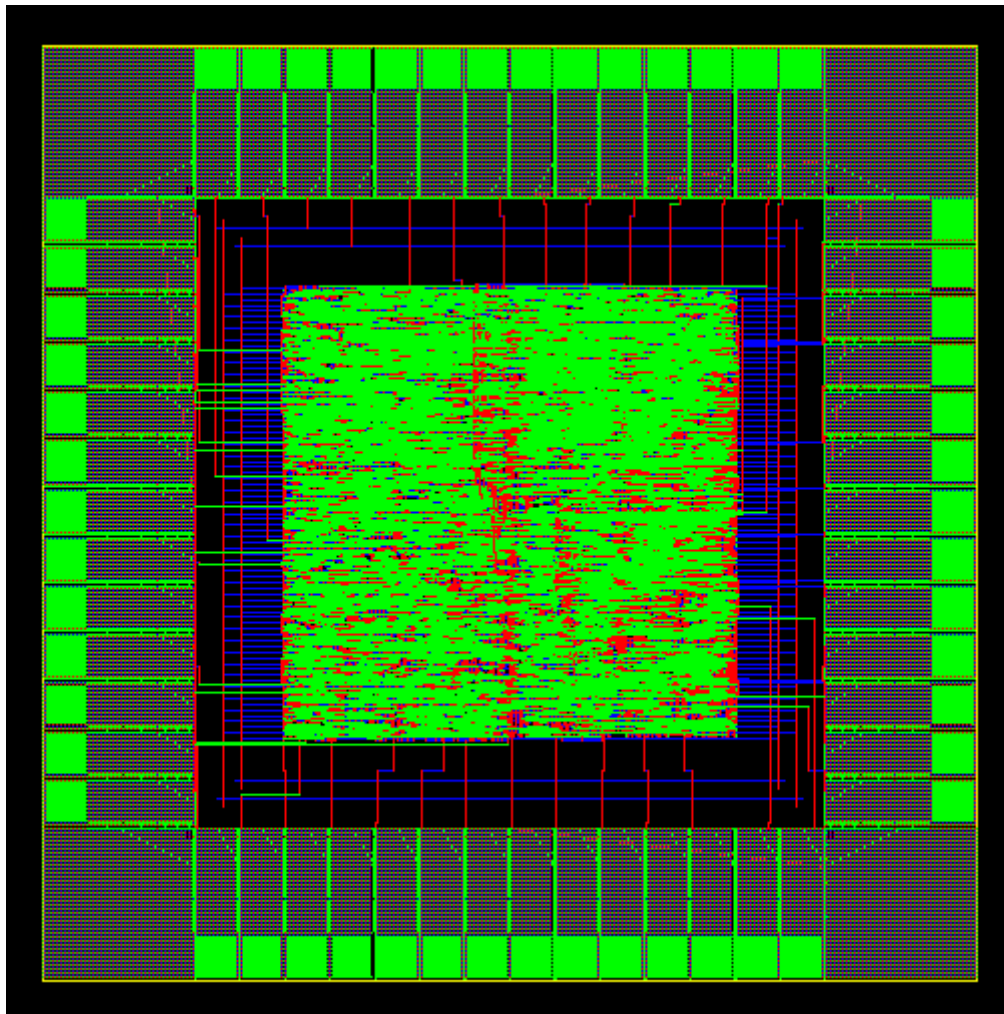


Figure.5-7 Layout View of the MDFE chip

After routing is completed, the layout of the MDFE chip is created in Figure.5-7.

5.4 Post–Layout Timing Analysis

With the parasitic extracted from the layout. The post-layout timing analysis is again carried out in PrimeTime. The delay information extracted from the layout is back-annotated in a **Standard Delay Format (SDF)** file.

An interior timing check verifies that the timing inside the block is correct. The Prime Time will use the **set_propagated_clock** command to include the insertion-delay of the clock-tree in its setup- and hold-time checks. This step will use the maximum transition time from the last step as clock-uncertainty to verify if the required safety margin is met. In addition, the insertion-delay from the last step will be used as the input-delay for off-chip inputs (otherwise, there will be a hold-time problem). This check will also record the delays and transition-times of on-chip outputs for the last step. The detailed script for pre-layout and post-layout timing analysis is in Appendix.B.2, B.3.

The network propagated delay is shown as a **latency** in the waveform, which is the case only in post-layout analysis with back-annotated information. The detailed waveforms for the critical path of both Pre-layout and Post-layout levels are given in Figure.5-8 and Figure.5-9. The clock periods are both constrained to **5.8 ns**.

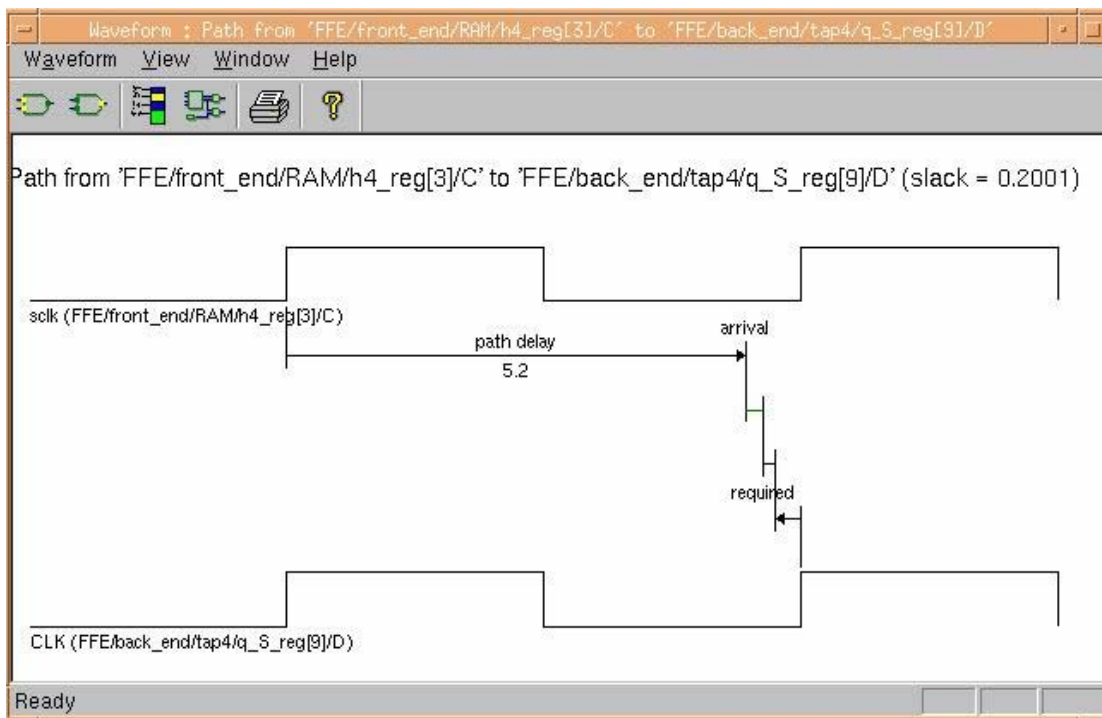


Figure.5-8 Time waveform of the critical path (Pre-Layout level)

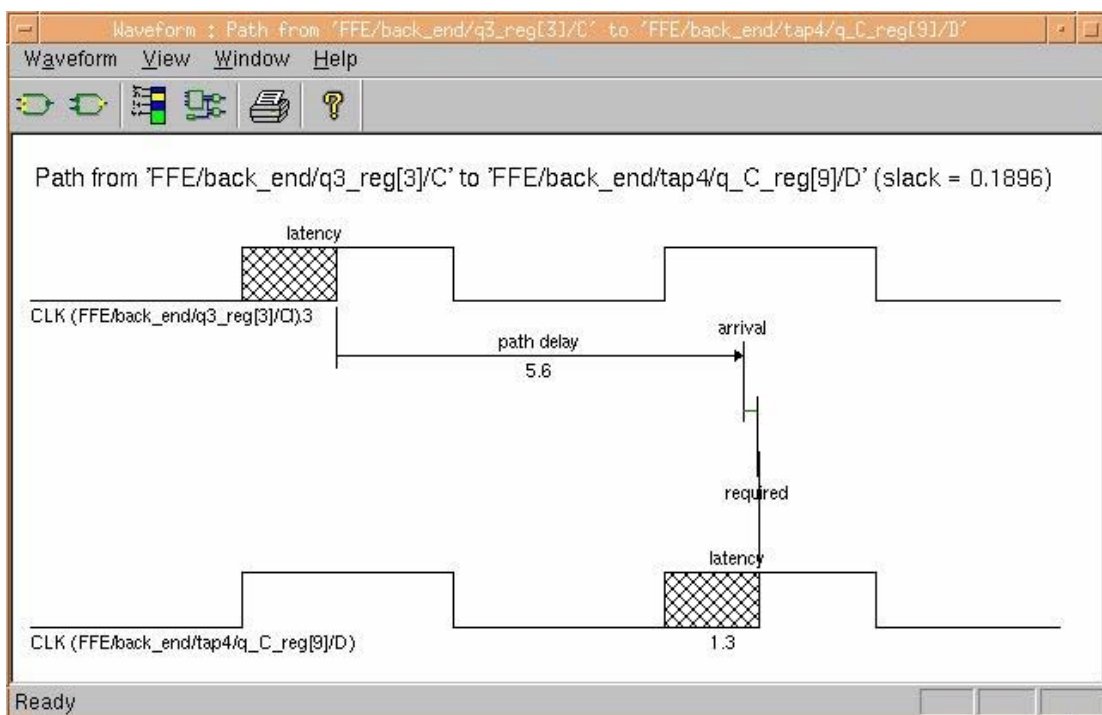


Figure.5-9 Time waveform of the critical path (Post-Layout level)

In Figure.5-8, it reports the longest path (critical path) in **Pre-Layout** level as:

Startpoint: FFE / front_end / RAM/h4_reg[3] / C
 Endpoint: FFE / back_end / tap4 / q_S_reg[9] / D
 Slack: 0.2001 ns (MET)

In Figure.5-7-(b), it reports the critical path in **Post-Layout** level as:

Startpoint: FFE / back_end / q3_reg[3] / C
 Endpoint: FFE / back_end / tap4 / q_C_reg[9] / D
 Slack: 0.1896 ns (MET)

Network propagated delay (Latency): 1.3 ns

From the comparison above, we could get that there is no obvious change on the clock rate even after layout process, though network propagated delay is added. This could be explained by the proper estimated constraints set in the synthesis process, such as *wire-load-model, clock-skew, and input-delay*.

Since the clock period is constrained to **5.8ns** and the slack is positive and thus meets the specification. The final MDFE at post-layout level could run at the speed of **170MHz**. The summary of the final specifications attained is given in Table.5-4, and the detailed reports of timing, area, and dynamic power could be found in Appendix.B4, B5, and B6.

Table.5-4 Performance of the MDFE chip at post-layout level

	MDFE (FBE & FFE)
Supply Voltage (V)	3.3
CMOS Technology (μm)	0.35
Input / Output Pins	54
Clock Rate in BEST case (MHz)	230
Clock Rate in TYPICAL case (MHz)	170
Clock Rate in WORST case (MHz)	125
Core Area (mm^2)	2.83
Chip Area (mm^2)	4.40
Dynamic Power (mW)	143.03
Number of Gate Cells	73,386

Chapter 6 Conclusion

A fully digital MDFE chip that consists of an 8-tap feedback equalizer (FBE) and a 10-tap feed-forward equalizer (FFE) has been successfully designed and implemented to the post-layout level. The FBE is implemented with the lookup-table based architecture that consists of five $2^2 \times 8$ -bit and three $2^3 \times 8$ -bit SRAMs as the LUTs. The past decisions are used to address the LUTs to form a decision feedback critical loop. A number of architectures for FBE have been investigated and compared, from which the final architecture is chosen. Three pipelined stages have been employed to relax the timing constraints. The chip area has been greatly reduced by splitting the large SRAM into small ones. The FFE has been implemented as a transposed filter. In its architecture, the multipliers are of parallel array type that uses radix-4 modified Booth encoding and a carry save partial product reduction scheme. An 8×8 -bit SRAM is used to store the 8-tap coefficients. Both the FBE and FFE are made programmable.

Based on a $0.35\mu\text{m}$ CMOS technology, the synthesized FBE and FFE at post layout level are capable of functioning up to 200MHz and 185MHz, respectively. For the integrated MDFE chip, the clock rate has achieved 170MHz in TYPICAL case, 230MHz in BEST case, and 125MHz in WORST case. Further improvement needs to be made to meet the specification of 150 MHz under the worst-case condition. The

physical layout with 54 I/O pads has the chip area of 4.4mm^2 and consumes a dynamic power of 143.03mW.

Table.6-1 gives out some previous published DFE/MDFE filters/detectors and the comparison with this MDFE chip.

Table.6-1 Published DFE/MDFE filters/detectors

Design	Architecture and Type	Technology	Speed (MHz)
[34] Kajley	4-Tap, Mixed-signal, Linear DFE	2 μm CMOS	50
[35] Mittal	4-Tap, Digital, Linear DFE	1.2 μm CMOS	67
[31] Brown	4-Tap, Mixed-signal, RAM-DFE	1 μm CMOS	80
[33] J. Hong	6-Tap, Mixed-signal, Linear DFE	0.35 μm CMOS	100
[32] Y.X. Lee	6-Tap, Analog , Linear DFE	0.5 μm CMOS	100
[16] L.Thon	6-Tap, Digital, RAM-MDFE	0.25 μm CMOS	360
This work	10-Tap, Digital, RAM-MDFE	0.35 μm CMOS	170

Suggested Future Work

The followings may be further pursued in the further research:

a). Optimization of the Booth Multiplier

Though the MDFE chip could run at 170MHz in the typical case, there is still a possibility to make further improvement since there is a performance gap between the FFE and FBE. The FFE is the speed bottleneck for the integrated MDFE chip. It has already found that the critical path in FFE is mainly caused by the booth multiplier, so

the optimization for the booth multiplier should be carried out. Furthermore, the investigation for the more proper multiplier can also be considered.

b) Improvement on the worst-case performance

To improve the speed on worst-case, a direct solution is adopting a more advanced CMOS technology such as 0.25 μm or 0.18 μm . By this means the speed could be improved significantly. However, when technology is specific, a possible solution that could be used to improve the speed is to “*set multiple constraints*” on the design. Once the critical path is found through timing analysis, it can be re-synthesized with a special “*worst-case constraint*”. Other means such as investigation of different architectures may also be considered.

REFERENCES

- [1] K. A. Schouhamer Immink, "Run-length limited sequences," Proceedings of the *IEEE*, pp. 1745-1759, Nov. 1990.

- [2] P.H. Seigel, "Recording codes for digital magnetic storage," *IEEE Trans. Magn.*, vol. MAG-21, no. 5, pp. 1344-1349, Sept. 1985.

- [3] R.W.Wood and D.A.Petersen, "Viterbi detection of Class-IV partial response on a magnetic recording channel," *IEEE Trans. Commun.*, vol. COM-34, pp. 454-461, May 1986.

- [4] R. D. Cideciyan, F. Dolivo, R. Hermann, W. Hirt, and W. Schott, "A PRML system for digital magnetic recording," *IEEE J. Select. Areas Commun.*, vol. 10, pp. 38-56, Jan. 1992.

- [5] A. M. Patel, "A new digital processing channel for data storage products," *IEEE Trans. Magn.*, vol. 27, pp. 4579-4584, Nov. 1991.

- [6] H. K. Thapar and A. M. Patel, "A class of partial response systems for increasing storage density in magnetic recording," *IEEE Trans. Magn.*, vol. 23, pp. 3666-3668, Sept. 1987.

- [7] J. J. Moon and L.R.Carley, "Performance comparison of detection methods in magnetic recording," *IEEE Trans. Magn.*, vol.26, pp.3155-3172, Nov.1990

- [8] K. D. Fisher, J. M. Cioffi, W. L. Abbot, P. S. Bednarz, and C. M. Melas, "An adaptive RAM-DFE for storage channels," *IEEE Trans. Commun.*, vol. 39, pp. 1559–1568, Nov. 1991.
- [9] J. G. Kenney, L. R. Carley, and R. W. Wood, "Multi-level decision feedback equalization for saturation recording," *IEEE Trans. Magn.*, vol.29, pp. 2160–2171, July 1993.
- [10] Brickner, B. and J. Moon, "A high dimensional signal space implementation of FDTS/DF," *IEEE Trans. on Magn*, vol. 32, no. 5, Sept., 1996
- [11] Brickner, B. and J. Moon, "A signal space representation of fixed delay tree search for use with d=0 codes," *Proc. of GLOBECOM '95*, pp. 577-581 Nov., 1995
- [12] C.A. Belifiore and J.H. Park, Jr., "Decision Feedback Equalization," *IEEE*, vol. 67, No. 8, pp. 1143-1155, Aug. 1979.
- [13] J.G. Kenney and R. Wood, " Multi-Level Decision Feedback Equalization: An Effective Realization of FDTS/DF", *IEEE Trans. Magn.*, vol 31, pp 1115-1120, March 1995.
- [14] P.S. Bednarz, S.C. Lin, C.S. Modlin and J.M. Cioffi, "Design, Performance, and Extensions of the RAM-DFE Architecture," *IEEE Trans. Magn.*, vol 31, pp 1196-1201, March, 1995.
- [15] J.G. Kenney and C.M. Melas, "A Parallel Architecture for Multilevel Decision Feedback Equalization," *IEEE Trans. Magn.*, vol 34, pp 588-595, March 1998.

- [16] L.Thon, “540MHz 21mW MDFE Equalizer and Detector in 0.25 μ m CMOS”, *ISSCC*, 1998.
- [17] George Mathew, B.Farhang-Boroujeny and R.W.Wood, “Design of multilevel decision feedback equalizer”, *IEEE Trans. Magn.*, Vol.33, No.6, pp.4528-4542, Nov.1997.
- [18] J. G. Kenney and M. Melas, “Pipelining for Speed Doubling in MDFE,” *IEEE Trans. Magn.*, pp 561-565, 1996.
- [19] L. P. Rubinfield, “A proof of the modified Booth’s algorithm for multiplication”, *IEEE Trans. Comput.*, Vol. C-24, pp. 1014-1015, October 1975.
- [20] A. Oppenheim and R. Schaffer, “Digital signal processing”, Eaglewood Cliffs, NJ: Prentice-Hall, pp. 153-155, 1975.
- [21] O. Salomon, J.-M. Green and H. Klar, “General algorithm for a simplified addition of 2’s complement numbers in multipliers”, *IEEE J. of Solid-state circuits*, Vol. 30, pp. 839-844, July 1995.
- [22] C. R. Baugh and B. A. Wooley, “A two’s complementary parallel array multiplication algorithm”, *IEEE Trans. Comput.*, Vol. C-22, pp. 1045-1047, December 1973.
- [23] Alan Y. Kwentus, Hing-Tsun Hung, and Alan N. Willson, “An Architecture for High-Performance/Small-Area Multipliers for Use in Digital Filtering Applications”, *IEEE Journal of solid-state circuits*, Vol. 29.No.2 Feb. 1994.
- [24] “Verilog-XL Reference Manual”, Cadence Design System.

- [25] “NC Verilog Reference Manual”, Cadence Design System.
- [26] “Design Compiler User Guide”, Synopsys Inc.
- [27] “Design Compiler Reference Manual:Constraints and Timing” Synopsys Inc.
- [29] “Design Compiler Reference Manual: Optimization and Timing Analysis” Synopsys Inc.
- [29] “PrimeTime User Guide”, Synopsys Inc.
- [30] “Silicon Ensemble Reference Manual”, Cadence Design System.
- [31] Brown, J., et al., “An 80Mb/s Adaptive DFE Detector in 1 μ m CMOS,” ISSCC Digest of Technical Papers, pp. 324-325, Feb., 1997.
- [32] Y. X. Lee, etc., “Design, implementation, and performance evaluations of an MDFE read channel” IEEE Trans. Magn., Vol.34, No.1, pp.166-171, Jan., 1998.
- [33] J. Hong, Y. X. Lee, H. Mutoh, “An Experimental MDFE Detector”, IEEE Trans. On Magn., Vol.33, No.5, pp.2776-2778, Sept. 1997.
- [34] Kajley, R., P. Hurst, J. Brown, “A Mixed-Signal Decision Feedback Equalizer that uses a Look-Ahead Architecture,” J. Solid-State Circuits, pp. 450-459, Mar., 1997.
- [35] Mittal, R., et al., “A Low-Power Backward Equalizer for DFE Read Channel Applications,” J. Solid-State Circuits, pp. 270-273, Feb., 1997.

APPENDIX.A HDL Codes of the Design

```

/*****/
// MODULE:      TOP (top module)
// FILE NAME:   TOP.v
// AUTHOR:      Xie Jiang
// DESCRIPTION: Top level description of MDFE
/*****/
module TOP(sdata,sdata_en,pdata,pdata_ack,sclk,CLK,reset,reset_n,Ini,sreset_n,WE_A_1,
          WE_A_2,WE_A_3,WE_A_4,WE_B,WE_C,WE_D,TEST,TEST_FE, FE,Begin,
          A_1,A_2,A_3,A_4,B,C,D, SUM_1,SUM_2, FB,SUM, over_pos, over_neg, ak);

// I/O PORTS DECLARATION
input      CLK,sclk;
input      reset, reset_n,sreset_n;
input      sdata, sdata_en, pdata_ack, Ini;
input [5:0] pdata;
input      WE_A_1,WE_A_2,WE_A_3,WE_A_4,WE_B,WE_C,WE_D;
input      TEST;
input [7:0] TEST_FE;
output     Begin;
output [7:0] FE, FB;
output [7:0] A_1,A_2,A_3,A_4,B,C,D;
output [7:0] SUM_1, SUM_2, SUM;
output     over_pos,over_neg, ak;

// INTERCONNECTIONS AND REGISTERS
wire [9:0] Q;
wire [7:0] FE_FBE;

// ASSIGN STATEMENTS
assign FE_FBE = (TEST==1) ? TEST_FE : FE;

//MODULE INSTANTIATION AND I/O CONNECTIONS
//=====//
FFE    FFE (sdata,sdata_en,pdata,pdata_ack,sclk,CLK,reset,FE);
FBE    FBE (CLK,reset_n,sclk,sreset_n,FE_FBE,Ini,WE_A_1,WE_A_2,WE_A_3,WE_A_4,
          WE_B,WE_C,WE_D,Begin,Q,A_1,A_2,A_3,A_4,B,C,D,FB,SUM_1,SUM_2,
          SUM,over_pos,over_neg,ak);
BEGIN  BEGIN(CLK,pdata_ack,Begin)
//=====//
endmodule

```

```

/*****/
// MODULE:      FBE
// FILE NAME:   FBE.v
// AUTHOR:      Xie Jiang
// DESCRIPTION: Top level description of FBE
/*****/
FBE      FBE (CLK,reset_n,sclk,sreset_n,FE,Ini,WE_A_1,WE_A_2,WE_A_3,WE_A_4,
          WE_B,WE_C,WE_D,Begin,Q,A_1,A_2,A_3,A_4,B,C,D,FB,SUM_1,SUM_2,
          SUM,over_pos,over_neg,ak);

// I/O PORTS DECLARATION
input      CLK,reset_n;
input      sclk,sreset_n;
input      Ini;
input      WE_A_1,WE_A_2,WE_A_3,WE_A_4,WE_B,WE_C,WE_D;
input [7:0] FE;
input      Begin;
output [9:0] Q;
output [7:0] A_1,A_2,A_3,A_4,B,C,D;
output [7:0] FB;
output [7:0] SUM_1,SUM_2,SUM;
output      over_pos,over_neg;
output      ak;

// INTERCONNECTIONS AND REGISTERS
wire [10:0] Initial_Data;
wire [7:0]  SUM_1,SUM_2,SUM_A,SUM_B,SUM_C,SUM_D,SUM_E;
wire [9:0]  Q;
wire       Q0;

// ASSIGN STATEMENTS
assign  Q0 = Q[0];

//MODULE INSTANTIATION AND I/O CONNECTIONS
//=====//
SFT_11      SFT_11      (sclk,sreset_n,Ini,Initial_Data);
LOOKUP      LOOKUP      (CLK,reset_n,sclk,ak,WE_A_1,WE_A_2,WE_A_3,WE_A_4,
                        WE_B,WE_C,WE_D,Initial_Data,Q,A_1,A_2,A_3,A_4,B,C,D);
PIPE        PIPE        (CLK,Q0,A_1,A_2,A_3,A_4,B,C,D,SUM_1,SUM_2);
FEEDBACK    FEEDBACK    (CLK,FE,SUM_1,SUM_2,Begin,Q0,FB,SUM,ak,over_pos,
                        over_neg);
//=====//
endmodule

```

```

/*****/
// MODULE:      LOOKUP
// FILE NAME:   lookup.v
// AUTHOR:      Xie Jiang
// DESCRIPTION: Function Module of Stage-1 in FBE
/*****/
Module LOOKUP (CLK,reset_n,sclk,ak,WE_A_1,WE_A_2,WE_A_3,WE_A_4,WE_B,WE_C,
              WE_D,Initial_Data,Q,A_1,A_2,A_3,A_4,B,C,D);

// I/O PORTS DECLARATION
input        CLK,reset_n;
input        sclk;
input        WE_A_1,WE_A_2,WE_A_3,WE_A_4,WE_B,WE_C,WE_D;
input  [10:0] Initial_Data;
input        ak;
output  [9:0] Q;
output  [7:0] A_1,A_2,A_3,A_4,B,C,D;

// INTERCONNECTIONS AND REGISTERS
wire  [1:0]  address_A,address_B;
wire  [2:0]  address_C,address_D;

// ASSIGN STATEMENTS
assign  address_A = (WE_A_1||WE_A_2||WE_A_3||WE_A_4) ? Initial_Data[9:8] : {Q[1:0]};
assign  address_B = WE_B ? Initial_Data[9:8] : {Q[3:2]};
assign  address_C = WE_C ? Initial_Data[10:8] : {Q[6:4]};
assign  address_D = WE_D ? Initial_Data[10:8] : {Q[9:7]};

//MODULE INSTANTIATION AND I/O CONNECTIONS
//=====//
DFF    DFF0( CLK, reset_n, ak,   Q[0]);
DFF    DFF1( CLK, reset_n, Q[0], Q[1]);
DFF    DFF2( CLK, reset_n, Q[1], Q[2]);
DFF    DFF3( CLK, reset_n, Q[2], Q[3]);
DFF    DFF4( CLK, reset_n, Q[3], Q[4]);
DFF    DFF5( CLK, reset_n, Q[4], Q[5]);
DFF    DFF6( CLK, reset_n, Q[5], Q[6]);
DFF    DFF7( CLK, reset_n, Q[6], Q[7]);
DFF    DFF8( CLK, reset_n, Q[7], Q[8]);
DFF    DFF9( CLK, reset_n, Q[8], Q[9]);
SRAM2  SRAM_A_1( sclk, WE_A_1, address_A, Initial_Data[7:0], A_1);
SRAM2  SRAM_A_2( sclk, WE_A_2, address_A, Initial_Data[7:0], A_2);
SRAM2  SRAM_A_3( sclk, WE_A_3, address_A, Initial_Data[7:0], A_3);
SRAM2  SRAM_A_4( sclk, WE_A_4, address_A, Initial_Data[7:0], A_4);

```

```

SRAM2 SRAM_B( sclk, WE_B, address_B, Initial_Data[7:0], B);
SRAM3 SRAM_C( sclk, WE_C, address_C, Initial_Data[7:0], C);
SRAM3 SRAM_D( sclk, WE_D, address_D, Initial_Data[7:0], D);
//=====================================================//
endmodule

/*****/
// MODULE:      PIPE
// FILE NAME:   pipe.v
// AUTHOR:      Xie Jiang
// DESCRIPTION: Function Module of Stage-2 in FBE
/*****/
module PIPE (CLK,Q0,A_1,A_2,A_3,A_4,B,C,D,SUM_1,SUM_2);

// I/O PORTS DECLARATION
input          CLK;
input  [7:0]   A_1,A_2,A_3,A_4,B,C,D;
input          Q0;
output [7:0]   SUM_1,SUM_2;

// INTERCONNECTIONS AND REGISTERS
wire  [7:0]   data_A_1_out,data_A_2_out,data_A_3_out,data_A_4_out,
              data_B_out,data_C_out,data_D_out;
wire  [7:0]   FB_1,FB_2;
reg    [7:0]   SUM_1,SUM_2,SUM_A,SUM_B,SUM_C,SUM_D,SUM_E;
reg    [7:0]   FB;

//MODULE INSTANTIATION AND I/O CONNECTIONS
//=====================================================//
REG8  REG8_1(CLK, A_1, data_A_1_out);
REG8  REG8_2(CLK, A_2, data_A_2_out);
REG8  REG8_3(CLK, A_3, data_A_3_out);
REG8  REG8_4(CLK, A_4, data_A_4_out);
REG8  REG8_5(CLK, B, data_B_out);
REG8  REG8_6(CLK, C, data_C_out);
REG8  REG8_7(CLK, D, data_D_out);
//=====================================================//

// MAIN CODE (PIPE STAGE 2)
always  @(data_A_1_out or data_A_2_out or data_A_3_out or data_A_4_out or data_B_out)
begin
    SUM_A <= data_A_1_out + data_B_out;
    SUM_B <= data_A_2_out + data_B_out;

```

```

        SUM_C <= data_A_3_out + data_B_out;
        SUM_D <= data_A_4_out + data_B_out;
    end

    always @(data_C_out or data_D_out) begin
        SUM_E <= data_C_out + data_D_out;
    end

    always @( Q0 or SUM_A or SUM_B or SUM_C or SUM_D or SUM_E) begin
        if (!Q0) begin
            SUM_1 <= (SUM_A + SUM_E);
            SUM_2 <= (SUM_B + SUM_E);
        end
        else begin
            SUM_1 <= (SUM_C + SUM_E);
            SUM_2 <= (SUM_D + SUM_E);
        end
    end

endmodule

/*****/
// MODULE:      FEEDBACK
// FILE NAME:   feedback.v
// AUTHOR:      Xie Jiang
// DESCRIPTION: Function Module of Stage-3 in FBE
/*****/
module FEEDBACK (CLK,FE,SUM_1,SUM_2,Begin,Q0,FB,SUM,ak,over_pos,over_neg);

// I/O PORTS DECLARATION
input          CLK;
input  [7:0]   SUM_1,SUM_2;
input          Begin;
input  [7:0]   FE;
input          Q0;
output [7:0]   FB;
output [7:0]   main_adder;
output        over_pos,over_neg;
output        ak;

// INTERCONNECTIONS AND REGISTERS
wire  [7:0]   FB_1,FB_2;
wire          bk;

```

```

reg    [7:0]    FB;
reg    [7:0]    SUM;

//MODULE INSTANTIATION AND I/O CONNECTIONS
//=====//
REG8   REG8_8(CLK, SUM_1, FB_1);
REG8   REG8_9(CLK, SUM_2, FB_2);
//=====//

// MAIN CODE (PIPE STAGE 3)
always @(Q0 or FB_1 or FB_2) begin
    if (!Q0) begin
        FB <= FB_1;
    end
    else begin
        FB <= FB_2;
    end
end

always @(FB or FE) begin
    SUM <= FE + FB;
end

// ASSIGN STATEMENTS
assign  over_pos = ((FE[7]==0) && (FB[7]==0) && (SUM[7]==1))? 1'b1:1'b0;
assign  over_neg = ((FE[7]==1) && (FB[7]==1) && (SUM[7]==0))? 1'b1:1'b0;
assign  bk = over_pos? 1'b0 : over_neg? 1'b1 : SUM[7];
assign  ak = (Begin==1)? bk : FE[7];

endmodule

/*****/
// MODULE:      BEGIN
// FILE NAME:   begin.v
// AUTHOR:      Xie Jiang
// DESCRIPTION: Delay Control Module in TOP
/*****/
module BEGIN(CLK,reset_n,D,Q);

// I/O PORTS DECLARATION
input    CLK;
input    D;
output   Q;

```

```

// INTERCONNECTIONS AND REGISTERS
wire [9:0]    q;

// ASSIGN STATEMENTS
assign Q = q[9];

//MODULE INSTANTIATION AND I/O CONNECTIONS
//=====================================================//
DFF    D0(CLK, reset_n, D, q[0]);
DFF    D1(CLK, reset_n, q[0], q[1]);
DFF    D2(CLK, reset_n, q[1], q[2]);
DFF    D3(CLK, reset_n, q[2], q[3]);
DFF    D4(CLK, reset_n, q[3], q[4]);
DFF    D5(CLK, reset_n, q[4], q[5]);
DFF    D6(CLK, reset_n, q[5], q[6]);
DFF    D7(CLK, reset_n, q[6], q[7]);
DFF    D8(CLK, reset_n, q[7], q[8]);
DFF    D9(CLK, reset_n, q[8], q[9]);
//=====================================================//
endmodule

/*****/
// MODULE:      SFT_11
// FILE NAME:   sft_11.v
// AUTHOR:      Xie Jiang
// DESCRIPTION: Serial to Parallel Converter
/*****/
module  SFT_11 (CLK,reset_n,Ini,Initial_Data);

// I/O PORTS DECLARATION
input      CLK;
input      reset_n;
input      Ini;
output [10:0] Initial_Data;

//MODULE INSTANTIATION AND I/O CONNECTIONS
//=====================================================//
DFF    D0(CLK, reset_n, Ini, Initial_Data[0]);
DFF    D1(CLK, reset_n, Initial_Data[0], Initial_Data[1]);
DFF    D2(CLK, reset_n, Initial_Data[1], Initial_Data[2]);
DFF    D3(CLK, reset_n, Initial_Data[2], Initial_Data[3]);
DFF    D4(CLK, reset_n, Initial_Data[3], Initial_Data[4]);
DFF    D5(CLK, reset_n, Initial_Data[4], Initial_Data[5]);

```

```

DFF    D6(CLK, reset_n, Initial_Data[5], Initial_Data[6]);
DFF    D7(CLK, reset_n, Initial_Data[6], Initial_Data[7]);
DFF    D8(CLK, reset_n, Initial_Data[7], Initial_Data[8]);
DFF    D9(CLK, reset_n, Initial_Data[8], Initial_Data[9]);
DFF    D10(CLK, reset_n, Initial_Data[9], Initial_Data[10]);
//=====//
endmodule

/*****/
// MODULE:      SRAM2
// FILE NAME:   sram2.v
// AUTHOR:      Xie Jiang
// DESCRIPTION: SRAM with 2-bit address
/*****/
module SRAM2 (CLK, WE, address,data_in, data_out);

// PARAMETERS
parameter width = 8;
parameter addr = 2;
parameter depth = 4;

// I/O PORTS DECLARATION
input  [width-1:0]  data_in;
input  [addr-1:0]  address;
input                    CLK, WE;
output [width-1:0] data_out;

// INTERCONNECTIONS AND REGISTERS
reg    [width-1:0]  mem    [depth-1:0];

// ASSIGN STATEMENTS
assign data_out = mem[address];

// MAIN CODE
always @(posedge CLK) begin
    if(WE)
        mem[address] = data_in;
end
endmodule

```



```

/*****/
// MODULE:      SRAM3
// FILE NAME:   sram3.v
// AUTHOR:      Xie Jiang
// DESCRIPTION: SRAM with 3-bit address
/*****/
module  SRAM3 (CLK, WE, address,data_in, data_out);

// PARAMETERS
parameter  width = 8;
parameter  addr  = 3;
parameter  depth = 8;

// I/O PORTS DECLARATION
input  [width-1:0]  data_in;
input  [addr-1:0]   address;
input                CLK, WE;
output [width-1:0]  data_out;

// INTERCONNECTIONS AND REGISTERS
reg    [width-1:0]  mem    [depth-1:0];

// ASSIGN STATEMENTS
assign  data_out = mem[address];

// MAIN CODE
always  @(posedge CLK) begin
    if(WE)
        mem[address] = data_in;
end

endmodule

/*****/
// MODULE:      REG8
// FILE NAME:   reg8.v
// AUTHOR:      Xie Jiang
// DESCRIPTION: Pipeline
/*****/
module  REG8 (CLK,data_in,data_out);

// I/O PORTS DECLARATION
input                CLK;

```

```

input   [7:0]   data_in;
output  [7:0]   data_out;

//MODULE INSTANTIATION AND I/O CONNECTIONS
//=====//
DFF8    D1(CLK, data_in[0], data_out[0]);
DFF8    D2(CLK, data_in[1], data_out[1]);
DFF8    D3(CLK, data_in[2], data_out[2]);
DFF8    D4(CLK, data_in[3], data_out[3]);
DFF8    D5(CLK, data_in[4], data_out[4]);
DFF8    D6(CLK, data_in[5], data_out[5]);
DFF8    D7(CLK, data_in[6], data_out[6]);
DFF8    D8(CLK, data_in[7], data_out[7]);
//=====//
endmodule

/*****/
// MODULE:      DFF
// FILE NAME:   dff.v
// AUTHOR:      Xie Jiang
// DESCRIPTION: D-Flip-Flop with asynchronous reset
/*****/
module DFF(CLK,reset_n,D,Q);

// I/O PORTS DECLARATION
input  CLK;
input  reset_n;
input  D;
output Q;

// INTERCONNECTIONS AND REGISTERS
reg    Q;

// MAIN CODE
always @(posedge CLK or negedge reset_n) begin
    if(!reset_n) begin
        Q <= 1'b0;
    end
    else begin
        Q <= D;
    end
end
endmodule

```

```
/******  
// MODULE:      DFF8  
// FILE NAME:   dff8.v  
// AUTHOR:      Xie Jiang  
// DESCRIPTION: D-Flip-Flop without reset  
/******  
module DFF8 (CLK,D,Q);  
  
// I/O PORTS DECLARATION  
input  CLK;  
input  D;  
output Q;  
  
// INTERCONNECTIONS AND REGISTERS  
reg    Q;  
  
// MAIN CODE  
always @(posedge CLK ) begin  
    Q <= D;  
end  
  
endmodule
```

APPENDIX.B Scripts and Reports

B.1 Script of the Constraints for Synthesis

```

/*****/
current_design TOP;
reset_design;

#=====#
# Setting up the environment
#=====#
set_operating_conditions -library csx_HRDLIB -max TYPICAL;
set_wire_load_model -lib csx_HRLIB -name 30k
set_load 2 all_outputs();

#=====#
# Setting up the timing assertions
#=====#
create_clock -period 5.8 -name CLK find (port, CLK);
set_dont_touch_network find (port, CLK);
set_clock_uncertainty -setup 0.3 find (port, CLK);
set_clock_uncertainty -hold 0.3 find (port, CLK);

create_clock -period 5.8 -name sclk find (port, sclk);
set_dont_touch_network find (port, sclk);
set_clock_uncertainty -setup 0.3 find (port, sclk);
set_clock_uncertainty -hold 0.3 find (port, sclk);

#=====#
# Setting up the port delays
#=====#
set_input_delay -max 2 -clock CLK find (port,pdata);
set_input_delay -max 2 -clock CLK find (port,reset_n);
remove_input_delay find (port,CLK);

set_input_delay -max 2 -clock sclk find (port,sdata);
set_input_delay -max 2 -clock sclk find (port,sdata_en);
set_input_delay -max 2 -clock sclk find (port,pdata_ack);
set_input_delay -max 2 -clock sclk find (port,reset);
set_input_delay -max 2 -clock sclk find (port,lni);
set_input_delay -max 2 -clock sclk find (port,WE_A_1);

```

```

set_input_delay -max 2 -clock sclk find (port,WE_A_2);
set_input_delay -max 2 -clock sclk find (port,WE_A_3);
set_input_delay -max 2 -clock sclk find (port,WE_A_4);
set_input_delay -max 2 -clock sclk find (port,WE_B);
set_input_delay -max 2 -clock sclk find (port,WE_C);
set_input_delay -max 2 -clock sclk find (port,WE_D);
set_input_delay -max 2 -clock sclk find (port,sreset_n);
remove_input_delay find (port,sclk);set_

```

```
output_delay -max 0 -clock all_outputs();
```

```
/******
```

B.2 Script of the Constraints for Pre-layout STA:

```
/******
```

```
current_design TOP
```

```
reset_design
```

```
#=====
```

```
# Setting up the environment
```

```
#=====
```

```
set_operating_conditions -analysis_type single TYPICAL -library csx_HRDLIB
```

```
set_wire_load_model -lib csx_HRDLIB -name 30k
```

```
set_load 2 [all_outputs]
```

```
#=====
```

```
# Setting up the timing assertions
```

```
#=====
```

```
create_clock -period 5.8 -name CLK [get_ports CLK]
```

```
set_dont_touch_network [get_ports CLK]
```

```
set_clock_uncertainty -setup 0.3 [get_ports CLK]
```

```
set_clock_uncertainty -hold 0.3 [get_ports CLK]
```

```
create_clock -period 5.8 -name sclk [get_ports sclk]
```

```
set_dont_touch_network [get_ports sclk]
```

```
set_clock_uncertainty -setup 0.3 [get_ports sclk]
```

```
set_clock_uncertainty -hold 0.3 [get_ports sclk]
```

```
#=====
```

```
# Setting up the port delays
```

```
#=====
```

```
set_input_delay -max 2 -clock CLK [get_ports pdata]
set_input_delay -max 2 -clock CLK [get_ports reset_n]
remove_input_delay [get_ports CLK]
```

```
set_input_delay -max 2 -clock sclk [get_ports sdata]
set_input_delay -max 2 -clock sclk [get_ports sdata_en]
set_input_delay -max 2 -clock sclk [get_ports pdata_ack]
set_input_delay -max 2 -clock sclk [get_ports reset]
set_input_delay -max 2 -clock sclk [get_ports Ini]
set_input_delay -max 2 -clock sclk [get_ports WE_A_1]
set_input_delay -max 2 -clock sclk [get_ports WE_A_2]
set_input_delay -max 2 -clock sclk [get_ports WE_A_3]
set_input_delay -max 2 -clock sclk [get_ports WE_A_4]
set_input_delay -max 2 -clock sclk [get_ports WE_B]
set_input_delay -max 2 -clock sclk [get_ports WE_C]
set_input_delay -max 2 -clock sclk [get_ports WE_D]
set_input_delay -max 2 -clock sclk [get_ports sreset_n]
remove_input_delay [get_ports sclk]
```

```
set_output_delay -max 0 [all_outputs]
```

```
/******
```

B.3 Script of the Constraints for Post-Layout STA

```
/******
```

```
current_design TOP
reset_design
```

```
#=====
```

```
# Setting up the environment
```

```
#=====
```

```
set_operating_conditions -analysis_type single TYPICAL -library csx_HRDLIB
set_wire_load_model -lib csx_HRDLIB -name 30k;
set_load 2 [all_outputs]
```

```
#=====
```

```
# Setting up the timing assertions
```

```
#=====
```

```
create_clock -period 5.8 -name CLK [get_ports CLK]
set_propagated_clock [get_clocks CLK]
create_clock -period 5.8 -name sclk [get_ports sclk]
set_propagated_clock [get_clocks CLK]
```

```
read_sdf ./latest/TOP.sdf
```

```
#=====#
# Setting up the port delays
#=====#
set_input_delay -max 2 -clock CLK [get_ports pdata]
set_input_delay -max 2 -clock CLK [get_ports reset_n]
remove_input_delay [get_ports CLK]

set_input_delay -max 2 -clock sclk [get_ports sdata]
set_input_delay -max 2 -clock sclk [get_ports sdata_en]
set_input_delay -max 2 -clock sclk [get_ports pdata_ack]
set_input_delay -max 2 -clock sclk [get_ports reset]
set_input_delay -max 2 -clock sclk [get_ports Ini]
set_input_delay -max 2 -clock sclk [get_ports WE_A_1]
set_input_delay -max 2 -clock sclk [get_ports WE_A_2]
set_input_delay -max 2 -clock sclk [get_ports WE_A_3]
set_input_delay -max 2 -clock sclk [get_ports WE_A_4]
set_input_delay -max 2 -clock sclk [get_ports WE_B]
set_input_delay -max 2 -clock sclk [get_ports WE_C]
set_input_delay -max 2 -clock sclk [get_ports WE_D]
set_input_delay -max 2 -clock sclk [get_ports sreset_n]
remove_input_delay [get_ports sclk]

set_output_delay -max 0 [all_outputs]
```

```
/******
```

B.4 Area Reports

```
*****
```

Report : area

Design : FBE

Version: 2001.08-SP2

Date : Fri Jun 18 14:58:51 2004

```
*****
```

Library(s) Used:csx_HRDLIB

(File: /app23/AMS_3.40_CDS_F/synopsys/csx_3.3V/csx_HRDLIB.db)

Number of ports:	105
Number of nets:	192
Number of cells:	64
Number of references:	7

Combinational area:	95859.398438
Noncombinational area:	195013.015625
Net Interconnect area:	35514.000000
Total cell area:	290872.406250
Total area:	326386.406250

Report : area
 Design : FFE
 Version: 2001.08-SP2
 Date : Wed Jun 23 18:17:42 2004

Library(s) Used:csx_HRDLIB
 (File: /app23/AMS_3.40_CDS_F/synopsys/csx_3.3V/csx_HRDLIB.db)

Number of ports:	20
Number of nets:	84
Number of cells:	2
Number of references:	2
Combinational area:	426098.375000
Noncombinational area:	162908.187500
Net Interconnect area:	86283.000000
Total cell area:	589006.562500
Total area:	675289.562500

Report : area
 Design : TOP
 Version: 2001.08-SP2
 Date : Fri Jun 18 14:22:10 2004

Library(s) Used:
 csx_HRDLIB (File: /app23/AMS_3.40_CDS_F/synopsys/csx_3.3V/csx_HRDLIB.db)
 csx_IOLIB_3M (File: /app23/AMS_3.40_CDS_F/synopsys/csx_3.3V/csx_IOLIB_3M.db)

Number of ports:	52
Number of nets:	5974
Number of cells:	5942
Number of references:	79

Combinational area: 2254036.250000
 Noncombinational area: 433809.000000
 Net Interconnect area: 142873.203125

Total cell area: 2687845.250000
 Total area: 2830718.500000

B.5 Dynamic Power Reports

Report : power -analysis_effort low

Design : FBE

Version: 2001.08-SP2

Date : Fri Jun 18 14:59:50 2004

Library(s) Used:

csx_HRDLIB (File:/app23/AMS_3.40_CDS_F/synopsys/csx_3.3V/csx_HRDLIB.db)

Operating Conditions: TYPICAL Library: csx_HRDLIB

Wire Load Model Mode: enclosed

Global Operating Voltage = 3.3

Power-specific unit information :

Voltage Units = 1V

Capacitance Units = 1.000000pf

Time Units = 1ns

Dynamic Power Units = 1mW (derived from V,C,T units)

Leakage Power Units = Unitless

Cell Internal Power = 0.0000 mW (0%)

Net Switching Power = 43.8552 mW (100%)

Total Dynamic Power = 43.8552 mW (100%)

Cell Leakage Power = 0.0000

Report : power -analysis_effort low

Design : FFE

Version: 2001.08-SP2

Date : Wed Jun 23 18:17:47 2004

Library(s) Used: csx_HRDLIB

(File:/app23/AMS_3.40_CDS_F/synopsys/csx_3.3V/csx_HRDLIB.db)

Operating Conditions: TYPICAL Library: csx_HRDLIB

Wire Load Model Mode: enclosed

Global Operating Voltage = 3.3

Power-specific unit information :

Voltage Units = 1V

Capacitance Units = 1.000000pf

Time Units = 1ns

Dynamic Power Units = 1mW (derived from V,C,T units)

Leakage Power Units = Unitless

Cell Internal Power = 0.0000 mW (0%)

Net Switching Power = 45.1983 mW (100%)

Total Dynamic Power = 45.1983 mW (100%)

Cell Leakage Power = 0.0000

Report : power -analysis_effort low

Design : TOP

Version: 2001.08-SP2

Date : Wed Jun 23 20:41:53 2004

Library(s) Used:

csx_HRDLIB (File: /app23/AMS_3.40_CDS_F/synopsys/csx_3.3V/csx_HRDLIB.db)

csx_IOLIB_3M (File: /app23/AMS_3.40_CDS_F/synopsys/csx_3.3V/csx_IOLIB_3M.db)

Operating Conditions: TYPICAL Library: csx_HRDLIB

Wire Load Model Mode: enclosed

Design	Wire Load Model	Library
TOP	30k	csx_HRDLIB

Global Operating Voltage = 3.3

Power-specific unit information :

Voltage Units = 1V

Capacitance Units = 1.000000pf

Time Units = 1ns

Dynamic Power Units = 1mW (derived from V,C,T units)

Leakage Power Units = Unitless

Cell Internal Power = 0.0000 mW (0%)

Net Switching Power = 143.0322 mW (100%)

Total Dynamic Power = 143.0322 mW (100%)

Cell Leakage Power = 0.0000

B.6 Timing Reports

Report : timing -path full -delay max -max_paths 1

Design : FBE

Version: 2001.08-SP2

Date : Wed Jun 23 20:01:54 2004

Operating Conditions: TYPICAL Library: csx_HRDLIB

Wire Load Model Mode: enclosed

Startpoint: PIPE/REG8_4/D2/Q_reg (rising edge-triggered flip-flop clocked by CLK)

Endpoint: FEEDBACK/REG8_9/D8/Q_reg (rising edge-triggered flip-flop clocked by CLK)

Path Group: CLK

Path Type: max

Des/Clust/Port	Wire Load Model	Library
FBE	10k	csx_HRDLIB
PIPE	10k	csx_HRDLIB
PIPE_DW01_add_8_3	10k	csx_HRDLIB
PIPE_DW01_add_8_0	10k	csx_HRDLIB

Point	Incr	Path
clock CLK (rise edge)	0.00	0.00
clock network delay (ideal)	0.00	0.00
PIPE/REG8_4/D2/Q_reg/C (DF82)	0.00	0.00 r
PIPE/REG8_4/D2/Q_reg/Q (DF82)	0.85	0.85 f
PIPE/REG8_4/D2/Q (DFF8_46)	0.00	0.85 f
PIPE/REG8_4/data_out[1] (REG8_5)	0.00	0.85 f
PIPE/add_41/A[1] (PIPE_DW01_add_8_3)	0.00	0.85 f
PIPE/add_41/U0_1_1/Q (NA22)	0.21	1.06 r
PIPE/add_41/U19/Q (IN4)	0.06	1.12 f
PIPE/add_41/U18/Q (AN21)	0.17	1.29 r
PIPE/add_41/U25/Q (ON21)	0.18	1.47 f
PIPE/add_41/U26/Q (IN4)	0.19	1.66 r
PIPE/add_41/U1_4_2_3/Q (ON21)	0.18	1.84 f

PIPE/add_41/U21/Q (EO1)	0.36	2.20 f
PIPE/add_41/SUM[4] (PIPE_DW01_add_8_3)	0.00	2.20 f
PIPE/U37/Q (IMU22)	0.22	2.42 r
PIPE/U59/Q (IN4)	0.07	2.49 f
PIPE/r570_0/A[4] (PIPE_DW01_add_8_0)	0.00	2.49 f
PIPE/r570_0/U12/Q (IN4)	0.10	2.59 r
PIPE/r570_0/U11/Q (IN3)	0.08	2.67 f
PIPE/r570_0/U0_1_4/Q (NA24)	0.12	2.78 r
PIPE/r570_0/U26/Q (ON21)	0.14	2.92 f
PIPE/r570_0/U1_4_1_6/Q (AN21)	0.22	3.14 r
PIPE/r570_0/U1_4_2_6/Q (ON21)	0.17	3.31 f
PIPE/r570_0/U27/Q (EN1)	0.44	3.75 f
PIPE/r570_0/SUM[7] (PIPE_DW01_add_8_0)	0.00	3.75 f
PIPE/U48/Q (IN3)	0.13	3.88 r
PIPE/U71/Q (IMU24)	0.38	4.26 f
PIPE/SUM_2[7] (PIPE)	0.00	4.26 f
FEEDBACK/SUM_2[7] (FEEDBACK)	0.00	4.26 f
FEEDBACK/REG8_9/data_in[7] (REG8_0)	0.00	4.26 f
FEEDBACK/REG8_9/D8/D (DFF8_0)	0.00	4.26 f
FEEDBACK/REG8_9/D8/Q_reg/D (DF8)	0.00	4.26 f
data arrival time		4.26
clock CLK (rise edge)	5.00	5.00
clock network delay (ideal)	0.00	5.00
clock uncertainty	-0.30	4.70
FEEDBACK/REG8_9/D8/Q_reg/C (DF8)	0.00	4.70 r
library setup time	-0.04	4.66
data required time		4.66

data required time		4.66
data arrival time		-4.26

slack (MET)		0.40

Report : timing -path full -delay max -max_paths 1

Design : FFE

Version: 2001.08-SP2

Date : Wed Jun 23 18:17:49 2004

Operating Conditions: TYPICAL Library: csx_HRDLIB

Wire Load Model Mode: enclosed

Startpoint: front_end/RAM/h0_reg[1] (rising edge-triggered flip-flop clocked by sclk)
 Endpoint: back_end/tap0/q_S_reg[7] (rising edge-triggered flip-flop clocked by CLK)
 Path Group: CLK
 Path Type: max

Des/Clust/Port	Wire Load Model	Library
FFE	10k	csx_HRDLIB
bc_2	10k	csx_HRDLIB
booth_0	10k	csx_HRDLIB
fa_38	10k	csx_HRDLIB
fa_6	10k	csx_HRDLIB
bm_13	10k	csx_HRDLIB
tap_0	10k	csx_HRDLIB
fa_20	10k	csx_HRDLIB

Point	Incr	Path
clock sclk (rise edge)	0.00	0.00
clock network delay (ideal)	0.00	0.00
front_end/RAM/h0_reg[1]/C (DFS84)	0.00	0.00 r
front_end/RAM/h0_reg[1]/Q (DFS84)	0.68	0.68 f
front_end/RAM/H0[1] (ram)	0.00	0.68 f
front_end/h_0[1] (front	0.00	0.68 f
back_end/h0[1] (fir)	0.00	0.68 f
back_end/tap0/h[1] (tap_0)	0.00	0.68 f
back_end/tap0/tap_booth/X[1] (booth_0)	0.00	0.68 f
back_end/tap0/tap_booth/bc2/X_i (bc_2)	0.00	0.68 f
back_end/tap0/tap_booth/bc2/U4/Q (EO1)	0.36	1.04 f
back_end/tap0/tap_booth/bc2/U3/Q (IN4)	0.13	1.17 r
back_end/tap0/tap_booth/bc2/U19/Q (INO22)	0.12	1.29 f
back_end/tap0/tap_booth/bc2/One_N (bc_2)	0.00	1.29 f
back_end/tap0/tap_booth/U11/Q (IN4)	0.14	1.43 r
back_end/tap0/tap_booth/U20/Q (IN4)	0.06	1.49 f
back_end/tap0/tap_booth/bm2_5/One_N (bm_13)	0.00	1.49 f
back_end/tap0/tap_booth/bm2_5/U7/Q (IMU2)	0.25	1.74 f
back_end/tap0/tap_booth/bm2_5/U2/Q (IMU2)	0.22	1.96 r
back_end/tap0/tap_booth/bm2_5/U8/Q (INO22)	0.18	2.14 f
back_end/tap0/tap_booth/bm2_5/out (bm_13)	0.00	2.14 f
back_end/tap0/tap_booth/fa2_5/Cin (fa_38)	0.00	2.14 f
back_end/tap0/tap_booth/fa2_5/U5/Q (IN4)	0.11	2.24 r
back_end/tap0/tap_booth/fa2_5/U7/Q (AN22)	0.25	2.50 f
back_end/tap0/tap_booth/fa2_5/Cout (fa_38)	0.00	2.50 f
back_end/tap0/tap_booth/fa3_4/Cin (fa_34)	0.00	2.50 f

back_end/tap0/tap_booth/fa3_4/U3/Q (EO3)	0.73	3.23 f
back_end/tap0/tap_booth/fa3_4/S (fa_34)	0.00	3.23 f
back_end/tap0/tap_booth/fa4_2/B (fa_31)	0.00	3.23 f
back_end/tap0/tap_booth/fa4_2/U1/Q (EO3)	0.71	3.94 f
back_end/tap0/tap_booth/fa4_2/S (fa_31)	0.00	3.94 f
back_end/tap0/tap_booth/S[7] (booth_0)	0.00	3.94 f
back_end/tap0/CSA1/I1[7] (csa_1)	0.00	3.94 f
back_end/tap0/CSA1/csa_fa8/A (fa_20)	0.00	3.94 f
back_end/tap0/CSA1/csa_fa8/U2/Q (IN2)	0.16	4.10 r
back_end/tap0/CSA1/csa_fa8/U1/Q (EN3)	0.34	4.44 r
back_end/tap0/CSA1/csa_fa8/S (fa_20)	0.00	4.44 r
back_end/tap0/CSA1/O1[7] (csa_1)	0.00	4.44 r
back_end/tap0/CSA2/I2[7] (csa_0)	0.00	4.44 r
back_end/tap0/CSA2/csa_fa8/B (fa_6)	0.00	4.44 r
back_end/tap0/CSA2/csa_fa8/U7/Q (IN4)	0.12	4.56 f
back_end/tap0/CSA2/csa_fa8/U3/Q (IN4)	0.09	4.65 r
back_end/tap0/CSA2/csa_fa8/U8/Q (EO3)	0.27	4.93 r
back_end/tap0/CSA2/csa_fa8/S (fa_6)	0.00	4.93 r
back_end/tap0/CSA2/O1[7] (csa_0)	0.00	4.93 r
back_end/tap0/q_S_reg[7]/D (DF8)	0.00	4.93 r
data arrival time		4.93
clock CLK (rise edge)	5.40	5.40
clock network delay (ideal)	0.00	5.40
clock uncertainty	-0.30	5.10
back_end/tap0/q_S_reg[7]/C (DF8)	0.00	5.10 r
library setup time	-0.13	4.97
data required time		4.97

data required time		4.97
data arrival time		-4.93

slack (MET)		0.05

Report : timing -path full -delay max -max_paths 1

Design : TOP

Version: 2001.08-SP2

Date : Wed Jun 23 20:15:19 2004

Operating Conditions: TYPICAL Library: csx_HRDLIB

Wire Load Model Mode: enclosed

Startpoint: FFE/front_end/RAM/h4_reg[3] (rising edge-triggered flip-flop clocked by sclk)
 Endpoint: FFE/back_end/tap4/q_S_reg[9] (rising edge-triggered flip-flop clocked by CLK)
 Path Group: CLK
 Path Type: max

Des/Clust/Port	Wire Load Model	Library
TOP	30k	csx_HRDLIB
FFE	10k	csx_HRDLIB
booth_4	10k	csx_HRDLIB
bc_18	10k	csx_HRDLIB
bm_108	10k	csx_HRDLIB
fa_186	10k	csx_HRDLIB
tap_4	10k	csx_HRDLIB
ram	10k	csx_HRDLIB
fa_189	10k	csx_HRDLIB

Point	Incr	Path
clock sclk (rise edge)	0.00	0.00
clock network delay (ideal)	0.00	0.00
FFE/front_end/RAM/h4_reg[3]/C (JKS94)	0.00	0.00 r
FFE/front_end/RAM/h4_reg[3]/QN (JKS94)	0.75	0.75 r
FFE/front_end/RAM/U53/Q (IN8)	0.09	0.84 f
FFE/front_end/RAM/H4[3] (ram)	0.00	0.84 f
FFE/front_end/h_4[3] (front)	0.00	0.84 f
FFE/back_end/h4[3] (fir)	0.00	0.84 f
FFE/back_end/tap4/h[3] (tap_4)	0.00	0.84 f
FFE/back_end/tap4/tap_booth/X[3] (booth_4)	0.00	0.84 f
FFE/back_end/tap4/tap_booth/U15/Q (IN4)	0.10	0.94 r
FFE/back_end/tap4/tap_booth/U23/Q (IN8)	0.08	1.02 f
FFE/back_end/tap4/tap_booth/bc2/X_k (bc_18)	0.00	1.02 f
FFE/back_end/tap4/tap_booth/bc2/U19/Q (IN8)	0.08	1.10 r
FFE/back_end/tap4/tap_booth/bc2/U5/Q (NA24)	0.05	1.15 f
FFE/back_end/tap4/tap_booth/bc2/U16/Q (INO22)	0.11	1.26 r
FFE/back_end/tap4/tap_booth/bc2/Two_P (bc_18)	0.00	1.26 r
FFE/back_end/tap4/tap_booth/U26/Q (IN4)	0.09	1.35 f
FFE/back_end/tap4/tap_booth/U13/Q (IN4)	0.15	1.50 r
FFE/back_end/tap4/tap_booth/bm2_6/Two_P (bm_108)	0.00	1.50 r
FFE/back_end/tap4/tap_booth/bm2_6/U6/Q (EO14)	0.49	1.99 r
FFE/back_end/tap4/tap_booth/bm2_6/U4/Q (IMU2)	0.13	2.13 f
FFE/back_end/tap4/tap_booth/bm2_6/U3/Q (IMU2)	0.21	2.34 r
FFE/back_end/tap4/tap_booth/bm2_6/U5/Q (INO22)	0.19	2.53 f
FFE/back_end/tap4/tap_booth/bm2_6/out (bm_108)	0.00	2.53 f

FFE/back_end/tap4/tap_booth/fa3_5/Cin (fa_189)	0.00	2.53 f
FFE/back_end/tap4/tap_booth/fa3_5/U4/Q (IN1)	0.33	2.86 r
FFE/back_end/tap4/tap_booth/fa3_5/U9/Q (EO3)	0.72	3.58 r
FFE/back_end/tap4/tap_booth/fa3_5/S (fa_189)	0.00	3.58 r
FFE/back_end/tap4/tap_booth/fa4_3/B (fa_186)	0.00	3.58 r
FFE/back_end/tap4/tap_booth/fa4_3/U8/Q (IN3)	0.11	3.69 f
FFE/back_end/tap4/tap_booth/fa4_3/U7/Q (IN1)	0.23	3.92 r
FFE/back_end/tap4/tap_booth/fa4_3/U10/Q (IN1)	0.12	4.03 f
FFE/back_end/tap4/tap_booth/fa4_3/U2/Q (NA2)	0.17	4.21 r
FFE/back_end/tap4/tap_booth/fa4_3/U1/Q (NA2)	0.10	4.31 f
FFE/back_end/tap4/tap_booth/fa4_3/U4/Q (NA22)	0.25	4.55 r
FFE/back_end/tap4/tap_booth/fa4_3/Cout (fa_186)	0.00	4.55 r
FFE/back_end/tap4/tap_booth/C[9] (booth_4)	0.00	4.55 r
FFE/back_end/tap4/CSA2/l1[9] (csa_8)	0.00	4.55 r
FFE/back_end/tap4/CSA2/csa_fa10/A (fa_160)	0.00	4.55 r
FFE/back_end/tap4/CSA2/csa_fa10/U4/Q (EO3)	0.62	5.17 r
FFE/back_end/tap4/CSA2/csa_fa10/S (fa_160)	0.00	5.17 r
FFE/back_end/tap4/CSA2/O1[9] (csa_8)	0.00	5.17 r
FFE/back_end/tap4/q_S_reg[9]/D (DF8)	0.00	5.17 r
data arrival time		5.17

clock CLK (rise edge)	5.80	5.80
clock network delay (ideal)	0.00	5.80
clock uncertainty	-0.30	5.50
FFE/back_end/tap4/q_S_reg[9]/C (DF8)	0.00	5.50 r
library setup time	-0.13	5.37
data required time		5.37

data required time		5.37
data arrival time		-5.17

slack (MET)		0.20

1
design_analyzer>